UNIVERSIDADE FEDERAL DO CEARÁ
CENTRO DE TECNOLOGIA
DEPARTAMENTO DE ENGENHARIA DE TRANSPORTES
PROGRAMA DE PÓS-GRADUAÇÃO EM ENGENHARIA DE TRANSPORTES

SAMUEL JOSÉ CELESTINO DE OLIVEIRA

STABILIZATION OF PLASTIC SOILS FOR USE IN PAVEMENT LAYERS WITH WOOD ASH AT DIFFERENT TREATMENT STEPS

FORTALEZA - CE
2025

SAMUEL JOSÉ CELESTINO DE OLIVEIRA

STABILIZATION OF PLASTIC SOILS FOR USE IN PAVEMENT LAYERS WITH WOOD ASH AT DIFFERENT TREATMENT STEPS

M.Sc. thesis presented to the Post-Graduate Program in Transport Engineering, as a partial fulfillment of the requirements for the Master's degree in Transport Engineering at Universidade Federal do Ceará.
Area within the Graduate Program: Transport Infrastructure.

Advisor: Prof. DSc. Suelly Helena de Araújo Barroso.

Co-advisor: Prof. DSc. Lilian Medeiros Gondim.

FORTALEZA - CE
2025

Dados Internacionais de Catalogação na Publicação
Universidade Federal do Ceará
Sistema de Bibliotecas
Gerada automaticamente pelo módulo Catalog, mediante os dados fornecidos pelo(a) autor(a)

O51s Oliveira, Samuel José Celestino de.
Stabilization of plastic soils for use in pavement layers with wood ash at different treatment steps / Samuel José Celestino de Oliveira. – 2025.
168 f. : il. color.

Dissertação (mestrado) – Universidade Federal do Ceará, Centro de Tecnologia, Programa de Pós-Graduação em Engenharia de Transportes, Fortaleza, 2025.
Orientação: Profa. Dra. Suelly Helena de Araújo Barroso.
Coorientação: Profa. Dra. Lilian Medeiros Gondim.

1. Biomass Ash. 2. Soil stabilization. 3. Soil-lime. 4. Sustainable pavements. I. Título.
CDD 388

SAMUEL JOSÉ CELESTINO DE OLIVEIRA

STABILIZATION OF PLASTIC SOILS FOR USE IN PAVEMENT LAYERS WITH WOOD ASH AT DIFFERENT TREATMENT STEPS

M.Sc. thesis presented to the Post-Graduate Program in Transport Engineering, as a partial fulfillment of the requirements for the Master's degree in Transport Engineering at Universidade Federal do Ceará.
Area within the Graduate Program: Transport Infrastructure.

Advisor: Prof. DSc. Suelly Helena de Araújo Barroso.

Co-advisor: Prof. DSc. Lilian Medeiros Gondim.

Approved in: 22/09/2025.

COMMITTEE

Prof. Suelly Helena de Araújo Barroso, DSc. (Advisor)
Universidade Federal do Ceará (UFC)

Prof. Lilian Medeiros Gondim, DSc. (Co-advisor)
Universidade Federal do Cariri (UFCA)

Prof. Iuri Sidney Bessa, DSc.
Universidade Federal do Ceará (UFC)

Prof. Éric Lachance-Tremblay, Ph.D
École de Technologie Supérieure (ÉTS)

ACKNOWLEDGMENTS

I am grateful to the Renewing Source of all grace for granting me the strength of body and the resilience of spirit to withstand long hours of silence, in the quiet company of dust, ashes and bags of earth. For the alkalinity of the ashes and the sharpness of people in moments marked by sweat and weariness. For the two tons of clayey soil processed, the nearly one thousand specimens shaped by hand, and the almost twelve thousand blows of the compaction hammer, delivered with both resolve and patience.

To my family, for their quiet support and constant presence in my life, and to my partner, Larissa Menezes, for bringing beauty and lightness even in the hardest moments.

To my advisor, Prof. Dr. Suelly Helena de Araújo Barroso, and co-advisor, Prof. Dr. Lilian Medeiros Gondim, for encouraging me to explore new paths. To Prof. Éric Lachance-Treblay, Ph.D., for the enriching experience at ÉTS in Montreal. To Prof. Lucas Feitosa Babadopulos, Ph.D., for the trust; Prof. Dr. Iuri Sidnei Bessa, for valuable contributions; and Profs. Dr. Heber Lacerda, Dr. Antônio Júnior Ribeiro, and Dr. Juceline Bastos for their support.

To my friends and colleagues Madson Lucas, Karol Lemos, Laura Prévitáli, Levi Chaves, Júnior Sombra, Elias Lima, and Mauro Filho, for their company and encouragement. Special thanks to Boris and Igor Santos, whose help made everything easier. To João Paulo, Bennaffe, and Weiny, for their shared effort and long hours with the specimens.

To the institutions and partners who made this research possible: UFC and PETRAN, for a stimulating academic environment; UFCA, for the support of supervisors Maria Silvana and Ary Ferreira, and for the infrastructure, especially the labs of Materials Characterization, Soil Mechanics, Analytical Center, and Pavement, with essential contributions from Daniel Silva, Ana Patrícia, João Barbosa, Cícero, and Jorge Marcel. To the Sanitation and Soil Labs at IFCE, with special thanks to Prof. Dr. Yannice Tatiana da Costa Santos and her team. To DNIT and FUNCAP, for financial support; to Mitacs and ÉTS, for the international opportunity; to FARMACE LTDA. and Carbomil Química, for material donations; and to the Soil Laboratory of CT ASFALTO-NE and the Metallurgy Lab at UFC, especially Assis, Ricardo, and André, for their invaluable technical assistance.

ABSTRACT

The combustion of biomass, which is a renewable energy source, generates ashes with potential for reuse in pavement construction, particularly in the stabilization of soils for the development of more cost-effective and environmentally sustainable pavements. This research evaluated the potential use of calcium-rich wood ash, subjected to different treatment steps, as a stabilizing agent for plastic soils for use in pavement layers. The ash, produced by an industry located in the Metropolitan Region of Cariri (Ceará, Brazil), underwent a series of laboratory-scale treatments, such as sieving, washing with heated water, calcination, and hydration, each aimed at modifying its chemical and physical properties. The treated ashes were incorporated into two clayey soils in order to assess changes in plasticity, expansiveness, saturation behavior, mechanical performance, and environmental safety. The study also included the design of a hypothetical pavement section using the most promising mixture, followed by a comparative cost feasibility analysis between a alternative solution (Soil-ash) and a conventional pavement structure typically employed in the region. Laboratory analyses comprised compaction tests, unconfined compressive strength (UCS), mini-CBR, consistency limits, CBR, and resilient modulus (MR) tests, conducted at different curing times (0, 28, and 90 days). Indirect tensile strength and fatigue tests were also carried out, in addition to leaching tests and physicochemical characterization of the ashes through particle size analysis, X-ray fluorescence (XRF), and X-ray diffraction (XRD).Although the addition of ash, regardless of the processing level, reduced the plasticity and expansiveness of the mixtures, improved saturation stability and the highest mechanical strength gains were observed in mixtures incorporating calcined ashes and commercial lime. From an environmental standpoint, the ashes were classified as hazardous due to their corrosivity, except for the washed ash. However, the adopted treatment processes significantly reduced the leaching potential of toxic elements. It is concluded that calcium-rich wood ashes can be transformed into effective binders through simple treatment procedures, contributing to waste reuse and promoting the circular economy within the pavement sector.

Key-words: Biomass ash, Soil stabilization, Soil-lime and Sustainable pavements.

RESUMO

A combustão da biomassa, que é uma fonte de energia renovável, gera cinzas com potencial de reaproveitamento na construção de pavimentos, especialmente na estabilização de solos para o desenvolvimento de estruturas mais econômicas e ambientalmente sustentáveis. Esta pesquisa avaliou o potencial de utilização de cinza de madeira rica em cálcio, submetida a diferentes etapas de tratamento, como agente estabilizante de solos plásticos para uso em camadas de pavimento. A cinza, produzida por uma indústria localizada na Região Metropolitana do Cariri (Ceará, Brasil), passou por uma série de tratamentos em escala laboratorial, como peneiramento, lavagem com água aquecida, calcinação e hidratação, cada um visando modificar suas propriedades químicas e físicas. As cinzas tratadas foram incorporadas a dois solos argilosos com o objetivo de avaliar alterações na plasticidade, expansividade, comportamento de saturação, desempenho mecânico e segurança ambiental. O estudo incluiu ainda o dimensionamento de um trecho hipotético de pavimento utilizando a mistura mais promissora, seguido por uma análise comparativa de viabilidade de custos entre uma solução alternativa (solo-cinza) e uma estrutura de pavimento convencional tipicamente empregada na região. As análises laboratoriais compreenderam ensaios de compactação, resistência à compressão simples (RCS), mini-CBR, limites de consistência, CBR e módulo de resiliência (MR), realizados em diferentes idades de cura (0, 28 e 90 dias). Ensaios de resistência à tração indireta e fadiga também foram conduzidos, além de testes de lixiviação e caracterização físico-química das cinzas por análise granulométrica, fluorescência de raios X (FRX) e difração de raios X (DRX). Embora a adição das cinzas, independentemente do nível de processamento, tenha reduzido a plasticidade e a expansividade das misturas, melhorado a estabilidade à saturação e proporcionado os maiores ganhos de resistência mecânica em misturas com cinzas calcinadas e cal comercial, do ponto de vista ambiental as cinzas foram classificadas como perigosas devido à sua corrosividade, exceto a cinza lavada. Entretanto, os processos de tratamento adotados reduziram significativamente o potencial de lixiviação de elementos tóxicos. Conclui-se que cinzas de madeira ricas em cálcio podem ser transformadas em estabilizantes eficazes por meio de procedimentos simples de tratamento, contribuindo para o reaproveitamento de resíduos e promovendo a economia circular no setor de pavimentação.

Palavras-chave: Cinza de biomassa; Estabilização de solos; Solo-cal; Pavimentos sustentáveis

LIST OF FIGURES

LIST OF TABLES

LIST OF ABBREVIATIONS AND ACRONYMS

AASHTO	American Association of State Highways and Transportation Officials
ABA	Algaroba Bottom Ash
ABNT	Associação Brasileira de Normas Técnicas (Brazilian Technical Standards Association)
ASTM	American Society for Testing and Materials
BIR	Bearing Index Ratio
BSEN	British Standard European Norm
CASH	Hydrated Calcium Silico-Aluminates
CBR	California Bearing Ratio
CL	Comercial Lime
CMR	Cariri Metropolitan Region
CONAMA	Conselho Nacional do Meio Ambiente (Brazilian National Environment Council)
CRBA	Calcium-Rich Biomass Ash
ITS	Indirect Tensile Strength
	Department of Transport Infrastructure)
DNER	Departamento Nacional de Estradas e Rodagem (Brazilian National Department of Roads and Highways)
DNIT	Departamento Nacional de Infraestrutura de Transportes (Brazilian National Department of Transport Infrastructure)
DP	Permanent Deformation
EPA	Environmental Protection Agency
EPE	Empresa de Pesquisa Energética (Brazilian Energy Research Company)
FBC	Fluidized Bed Combustion
GDP	Gross Domestic Product
GI	Group Index
IBGE	Instituto Brasileiro de Geografia e Estatística (Brazilian Geography and Statistics Institute)
LL	Liquidity Limit

MCT	Miniatura, Compacted, Tropical
MR	Resilient Modulus
MSW	Municipal Solid Waste
NBR	Norma Brasileira Regulamentadora (Brazilian Regulatory Standard)
NEN	Netherlands Norm
NRA	National Roads Authority
PI	Plasticity Index
PL	Plasticity Limit
SA	Sieved Ash
SWCA	Sieved, Washed and Calcined Ash
TR	Tensile Strength
TS	Technical Specification
UCS	Unconfined Compression Strength
UFC	Universidade Federal do Ceará (Federal University of Ceará)
UFCA	Universidade Federal do Cariri (Federal University of Cariri)
USCS	Unified Soils Classification System
WA	Washed Ash
XDR	X-Ray Diffractonetry
XFR	X-Ray Fluorescence

SUMMARY

1 INTRODUCTION

The growing global demand for energy and the search for more renewable matrices position biomass energy as an important alternative in the direction of energy sustainability. However, burning biomass generates an amount of ash that needs to be disposed of or recovered in a more appropriate way (Agrela *et al.,* 2019).

Considering compliance with the European Renewable Energy Directive 2009/28/EC (European union, 2009), the annual production for 2020 of biomass ash in the European bloc was estimated to be 15.5 million tons (Zagvozda *et al.,* 2017). In Brazil, the national energy balance for the year 2023 (EPE, 2024), reports that 8.6% of gross energy was generated by firewood and charcoal. Another 16.8% was generated by burning sugarcane bagasse, indicating that more than 25% of the gross energy produced in the country comes from biomass sources that generate ash.

Currently, much of this ash is indiscriminately discarded, generating environmental impacts associated with its leaching potential and high alkalinity. Other common uses are as soil conditioners for agricultural purposes, or simply disposed of in landfills, generating high economic costs (Zagvozda *et al.,* 2017).

Several authors have pointed out that biomass ash is a complex material with great variability in its properties. Its behavior, therefore, cannot be generalized, thus constituting a barrier to the wider and safer use. However, Vassilev *et al.* (2013) produced a comprehensive characterization of various biomass ashes and proposed more rational uses for them by classifying them into groups. Among the various uses listed by these authors, the use of calcium-rich biomass ash stands out as promising in the production of bricks, binders for low-strength materials, cementitious matrices such as mortars and concretes, the synthesis of geopolymers and the construction of pavement bases and sub-bases.

In this context, some authors have evaluated the potential for stabilizing plastic soils with woody biomass ash. Okagbue (2007), for example, pointed out that the addition of wood ash to a clay soil produced improvements in its bearing capacity, increases in unconfined compressive strength in the short term, improvements in workability and a reduction in expansion. However, the author mentions that wood ash is unlikely to replace lime in soil stabilization, as after 7 and 14 days of curing, large reductions in the mechanical strength of the mixtures were observed. According to the author, this loss of resistance may be associated

with the low percentage of lime in the wood ash used and this may be the cause of the drop in pH below 10, making the matrix environment unfavorable for the reaction and the development of resistance.

Contrary to the results observed by Okagbue (2007), Medeiros (2023) reports that woody biomass ash has been successfully used to stabilize clayey soils, with increasing resistance gains for the levels evaluated and over different curing times, highlighting the complexity of behavior and the need for further research on the subject.

From environmental concerns point of view, authors such as Vamvuka and Kakaras (2011), Nordmark *et al.* (2014) and Oburger *et al.* (2016) have investigated the impacts of using these materials in granular layers in field or laboratory studies. In some cases the ash was considered safe, while in others it was considered dangerous due to the concentrations of hazardous leachate elements above the limits of local legislation. Nordmark *et al.* (2014) also pointed out that leaching assessment methodologies are not always representative of field conditions, which can lead to the disqualification of promising and safe materials for soil stabilization applications for paving. The criticism of these methodologies has also been corroborated by Vasconcelos (2018) and Silva *et al.* (2019), who emphasized that compacting granular layers reduces percolation and the potential for leaching hazardous materials. The authors observed that in Brazil the use of compaction with encapsulants for contaminating materials is not yet standardized and has been little investigated.

To address the issue and propose solutions, this work seeks to investigate the stabilization of plastic soils using woody biomass ash at different stages of processing, considering geotechnical properties of interest for paving.

1.1 Background

According to Agrela *et al.* (2019), biomass is an essential element for the implementation of a more renewable energy matrix. The authors report a significant increase in the global use of biomass as an energy source, with Brazil being a leading country in the incorporation of these resources into its energy matrix.

Although the wood-to-ash conversion rate is only about 3% after combustion (Borlini *et al.,* 2005), firewood consumption in Brazil generates approximately 2.3 million tons of ash annually. In addition to wood, the burning of sugarcane bagasse is also a massive source of energy and ash generation in the country, with an even higher conversion rate, around 11%, according to Seye et al. (2010). The substantial volumes of ash produced need to be better

utilized, as they are generated in large quantities, may be harmful to the environment, and often present potential for use in various industrial applications, especially in the construction industry.

From the perspective of their applicability in construction, the literature indicates that biomass ashes can be used in the production of geopolymers or as partial or total substitutes for hydraulic binders such as Portland cement or lime, as discussed in studies by Ramujee and PothaRaju (2017), Maschio *et al.* (2010), and Melo (2018).

In the geotechnical context and for pavement purposes, studies such as those by Okagbue (2007), Ureña *et al.* (2012), Cabrera et al. (2014), Emeh *et al.* (2016), and Medeiros (2023) report that ashes have acted as chemical soil stabilizers, while others indicate that the ashes behaved inertly, functioning only as a granulometric stabilizer and producing a "filler effect" in the studied soil. This variability in behavior may be related to the technological differences among the types of ash studied, as well as to the distinct properties of the soils evaluated, which ultimately compromises the acceptance of these materials for large-scale use. In other words, it is recommended that each type of ash and soil be investigated individually, since generalizations often lead to the dismissal of alternative materials that may be suitable for specific industrial purposes.

The processing of ashes can also be a decisive factor in the performance of these materials. Melo *et al.* (2018), for example, point out that hydrated lime can be produced from Calcium-Rich Biomass Ashes (CRBAs), provided that preliminary treatment steps are applied. In this context, Agrela et al. (2019) propose that biomass ash processing stages can represent an important strategy for adapting the technological properties of these materials, aiming at the safe use of the waste. The authors highlight the growing production of biomass ash from energy generation worldwide and suggest that recycling measures are needed, with the construction and infrastructure sector representing a promising production chain capable of absorbing this type of waste. Therefore, it is believed that deepening the study on wood ash processing is an essential strategy to expand the safer and more rational reuse of this residue in the stabilization of pavement soils.

1.2 Objectives

The general objective of this research is to enable the use of wood ash subjected to different treatment steps in the stabilization of plastic soils for application in pavement layers. To achieve the general objective, some specific objectives were defined:

a) To assess the effect of processing on the chemical and physical composition of the wood ash.
b) To investigate the influence of treated ash on the plasticity, expansiveness, and saturation susceptibility of soil–ash mixtures.
c) To evaluate the improvement in mechanical performance of soil–ash mixtures as a result of each processing.
d) To assess the environmental risk associated with leachable elements in wood ash, comparing their concentrations with the limits established by Brazilian environmental legislation.
e) To design a hypothetical pavement section using the best-performing soil–ash mixture and to perform a cost analysis against conventional alternatives.

1.3 Organization of the dissertation

This dissertation is structured into five chapters, as outlined below:

Chapter 1 (Introduction) provides an initial overview of the research topic, addressing elements such as the definition of the research problem, the main objective, and the specific objectives of the study.

Chapter 2 (Literature Review) presents the fundamental concepts necessary for understanding the subject under investigation. This chapter discusses the use of soils in engineering, the stabilization techniques applied to improve their mechanical properties, with emphasis on chemical stabilization methods, particularly those using hydrated lime and ashes, and the application of these materials in soil improvement.

Chapter 3 (Materials and Methods) describes the origin of the materials used (soils, ashes, and commercial lime), the ash processing procedures, and the experimental methods adopted in the study. It details the basic characterization of the soils, the ash processing steps, the chemical analysis carried out at each stage, and the preparation of the mixture specimens. The chapter also presents the tests conducted to evaluate the plastic, mechanical, and environmental properties of the mixtures.

Chapter 4 (Results and Discussion) presents the findings related to the efficiency of each ash processing stage and the chemical transformations observed throughout. It includes the basic characterization of the soils and mixtures through compaction tests, Atterberg limits, saturated unconfined compressive strength (UCS), saturated and unsaturated Mini-CBR, as well as expansion and shrinkage tests. It also covers the identification of the best-performing

mixtures, and the evaluation of CBR, Resilient Modulus (MR), Indirect Tensile Strength (ITS), fatigue performance, environmental assessment, the design of a hypothetical pavement section using the optimal mixture, and a cost analysis comparing the stabilized solution with conventional pavement alternatives.

Chapter 5 (Conclusions and Suggestions for Future Work) summarizes the main conclusions drawn from the analyses carried out and provides recommendations and directions for future research. Finally, the list of bibliographic references that supported the development of this work is presented.

2 LITERATURE REVIEW

The literature review is divided into three parts:

I. Soil Stabilization: Addresses concepts, definitions and criteria on the subject, conventional and alternative materials used, as well as the state-of- the-art on the subject.
II. Biomass Ash: covers the origin and definition, the processes that interfere with the technological characteristics of the different ashes investigated and the chemical composition and some properties of these materials.
III. Environmental Analysis: Addresses definitions, national and international legislation and their criteria for using waste in pavement layers.

2.1 *Soil stabilization*

Soils are widely used as building materials and are therefore of great importance in the context of engineering applications, especially for pavement construction. As they are highly heterogeneous materials, it is extremely important to carry out tests to classify and understand their behavior.

When soil is transported to a particular location for use in a construction project, it is in a loose state and thus has a low capacity to support loads without showing tolerable deformations. It is important to densify the soil in order to improve its load-bearing capacity and ensure that it remains sufficiently stable in the face of the stresses imposed and variations in humidity.

According to Villibor (1982), stabilizing a soil involves modifying any property in order to gain mechanical properties for use in engineering applications. In other words, stabilization applies physical, physicochemical or mechanical processes to create a new material with resistance and compressibility properties that are more suitable for use in a specific project (Ingles and Metcalf, 1972; Santana, 1983). According to Guimarães (2002), soil stabilization methods can be divided into two types: those that use mechanical means and those that use chemical means.

2.1.1*Mechanical stabilization*

Mechanical stability can be achieved through compaction or granulometric stabilization. The Brazilian paving manual (DNIT, 2006) considers compaction to be the

process resulting from an increase in the apparent specific mass of the soil, by means of pressure, impact or vibration, which brings the particles of the material closer together and forms a mineral skeleton of greater density. According to Das (2007), compaction consists of densifying the soil by removing air and applying mechanical energy. Thus, the compaction process can be considered a stabilization process, improving the behavior of the soil.

2.1.2 *Particle size stabilization*

Particle size stabilization is also a mechanical stabilization mechanism and consists of combining and manipulating soils in the right proportions in order to obtain a final product with greater stability than the original soils and suitable for application in each particular case (Villibor,1982).

In turn, DNIT 141/2022 - ES (DNIT, 2022) Standard defines granulometric stabilization as the process of improving the characteristics of natural soils through the addition of one or more materials, in order to obtain a final mixture with suitable stability and durability properties.

The main requirements of this standard, which deals with granulometrically stabilized bases, regarding the strength of the particles retained on the 2 mm sieve, are that they must be hard, resistant and free of soft, elongated or flat fragments, vegetable matter or other harmful substances. In addition, the material must not show wear of more than 55% in the Los Angeles abrasion test and particle size ranges are recommended according to the estimated road traffic levels, as shown in Table 1.

Table 1 : Particle size ranges reference

Sieves		**Ranges**						**Design range tolerances**
		For N > 5 × 10^6				**For N < 5 × 10^6**		
Inch/Number	**mm**	**A**	**B**	**C**	**D**	**E**	**F**	
2”	50,8	100	100	-	-	-	-	±7
1”	25,4	-	75-90	100	100	100	100	±7
3/8”	9,5	30-65	40-75	50-85	60-100	-	-	±7
N° 4	4,8	25-55	30-60	35-65	50-85	55-100	70-100	±7
N° 10	2,0	15-40	20-45	25-50	40-70	40-100	55-100	±7
N° 40	0,42	8-20	15-30	15-30	25-45	20-50	30-70	±7
N° 200	0,074	2-8	5-15	5-15	10-25	6-20	8-25	±7

Source: DNIT 141/2022

Although the DNIT 141/2022 standard suggests granulometric ranges according to traffic, the document itself points out that they are examples and do not have to be followed, as long as parameters such as expansion of less than 0.5%, Resilient Modulus (RM) and

Permanent Deformation (PD) are met as specified in the case of mechanistic design.

If an empirical design method is used, the standard mentions the criteria to be met: California Bearing Ratio (CBR) greater than 60 or 80% (depending on the level of traffic), Liquidity Limit (LL) ≤ 25%, Plasticity Index (PI) ≤ 6%. The percentage of material passing the Nº 200 sieve must not exceed 2/3 of the percentage passing the Nº 40 sieve.

2.1.3 *Chemical stabilization*

Chemical stabilization is the stabilization method in which one or more chemical compounds interact with the soil particles, developing stabilizing reactions (Winterkorn; Pamukcu, 1991). According to Zagvozda *et al.* (2017), hydrated lime is traditionally used to stabilize soils with low bearing capacity and high cohesion, while cement is more commonly used to stabilize medium and low cohesion materials.

Although the type of soil is an important variable in determining the most effective stabilizing agent, in general, what determines the ability of these materials to act as soil improvers is their ability to develop agglomerating reactions with the soil particles. Agglomerating processes include cation exchange reactions or flocculation, pozzolanic reactions and carbonation (Little,1999).

The phenomenon of cation exchange or flocculation is promoted above all, by the addition of hydrated lime to a plastic soil and occurring through the replacement of calcium and magnesium cations by exchangeable cations present in the constitution of clay minerals. This replacement brings the clay particles closer together as illustrated in Figure 1, generating greater agglomeration between the grains, which generally produces an increase in the Plasticity Limit (PL), a reduction in the Liquidity Limit (LL) and Plasticity Index (PI), an increase in the California Bearing Ratio (CBR), flattening of the compaction curve and a reduction in the maximum dry specific mass, according to Picchi *et al.* (1988).

Figure 1 - Cation exchange

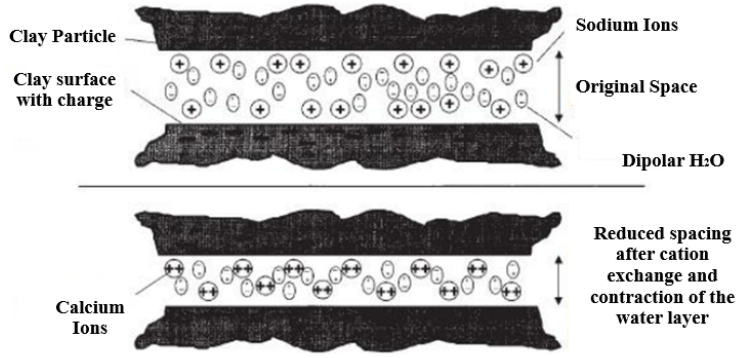

Sources: (Prusinski; Bhattacharja, 1999)

According to Little (1999), the saturation of calcium or the calcium hydroxide molecule on the clay surface drastically reduces the energy with which the clay surface attracts and retains water. As a result, physical changes occur in the lime-soil system as illustrated in Figure 2, due to the flocculation reaction which produces the agglomeration of particles into a larger effective particle size. This mechanism reduces plasticity and expansion potential, producing a drying effect, as the soil's water retention potential is reduced, improving workability and compactability and promoting greater shear strength due to the agglomeration of cations or molecules.

Figure 2 - Flocculation reaction mechanism

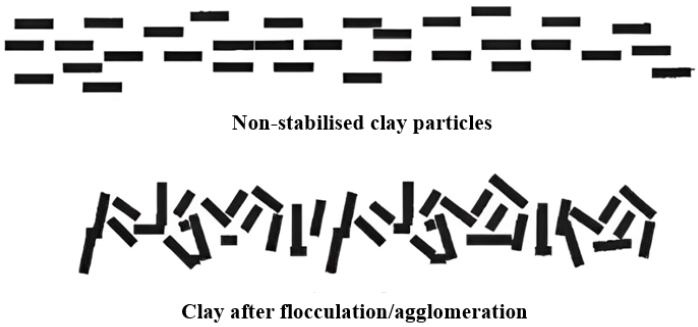

Source: (Prusinski; Bhattacharja, 1999)

Pozzolanic reactions, in turn, are mainly produced by the interaction between the calcium present in the lime and the amorphous silica and/or alumina present in the clay minerals of the soils, as illustrated in Figure 3. When enough hydrated lime is added to a soil, the pH of the mixture is raised to approximately 12.4 at 25 °C. At this pH, the alumina and silica present in the soil (pozzolans) become soluble and can combine with free calcium to form cementitious products such as Calcium Silicate Hydrate (CSH) and Calcium Silicate Alumina Hydrate (CASH), these compounds being the main agents responsible for the agglomeration process produced by cement (TRB, 1987; Little, 1999; Guimarães, 2002).

Figure 3: Mechanism of the pozzolanic reaction.

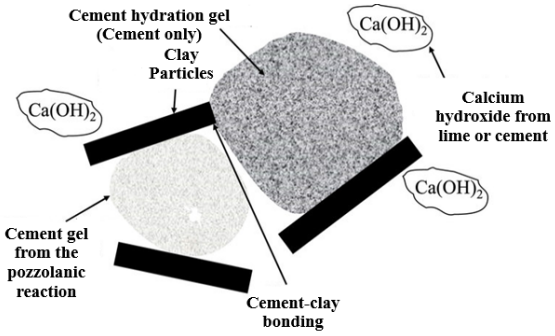

Source: Adapted from Prusinski; Bhattacharja, (1999)

The reversion of calcium to calcium carbonate occurs as the free lime reacts with carbon dioxide from the atmosphere, according to the lime cycle described in Figure 4. This reaction is considered deleterious in the stabilization process, as it depletes the free calcium system necessary for the flocculation mechanisms and the pozzolanic reaction (Little., 1999; Mallela; Quintus; Smith, 2004).

Figure 4: Lime cycle

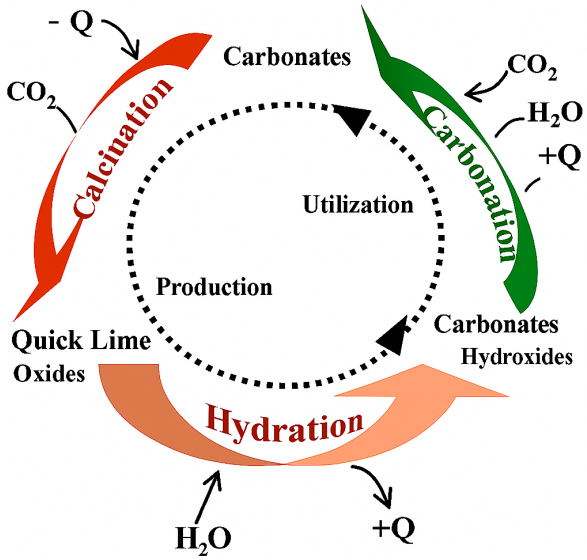

Source: (Freire *et al.*, 2014)

Although cement and hydrated lime are widely used in soil stabilization, various other materials have been used for this purpose. Medeiros, Ferreira and Belo (2023) point out the evolution of the chemical stabilization of expansive clay soils with works dating from the 1950s to the present day. The stabilizers mentioned by the authors in the literature survey were lime, ash, cement, asphalt emulsion, sodium derivatives, chlorides, scoria and powders, acids, sugar cane bagasse, carbonates, fibers, oxides and residues, polyvinyl acetate, brown sugar, seawater, polyvinyl alcohol, sand, calcium carbide, aluminate filler, hydrophobic polyurethane foam, gypsum, active silica and commercial nanomaterials. Table 2 lists studies that have investigated the use of some of the main chemical stabilizers, especially lime, in geotechnical and road applications.

In general, the studies showed especially in the 1950s and 1960s, that clayey soils were more compatible with lime, considering parameters such as the acquisition of resistance, a reduction in plasticity and expansion. On the other hand, granular soils tended to behave in a more promising way with cement additions, not developing good results when

stabilized with lime, and the mechanisms associated with these behaviors were not investigated in greater depth.

Since the works of Carrol (1959) and Diamond and Kinter (1965), the chemical interaction between soil clay minerals and stabilizing materials has been discussed in greater depth, explaining changes in the plastic and mechanical behavior of the materials. The long-term durability of these stabilized matrices became the subject of research, as in the works by Walker and Karabulut (1965) and Townsend and Klym (1966), investigating the mechanical behavior after freezing and thawing cycles, which indicated that mixtures with higher acquired mechanical strengths became more susceptible to the deleterious effects of the cycles.

Other materials were investigated in the light of available technical and scientific knowledge. The development of these investigations has become the basis for successful experiments in field situations in countries such as the United States, Bangladesh, India and Brazil, indicating a promising trend in the use of waste in the stabilization of paving layers, as reported in the works by Barroso and Santos (2006), Vasconcelos (2018), Ashraf *et al.* (2018) and Mahedi *et al.* (2018).

2.2 *Biomass ash*

Biomass, according to Agrela *et al.* (2019), is organic matter, of animal or vegetable origin, that can be used, among other applications, to generate energy. As a renewable energy source biomass is made up of organic matter from various plants, as well as agricultural, industrial and urban waste. Its main characteristic lies in its high energy potential, which can be used to generate heat, electricity and biofuels. In addition, this form of energy brings significant advantages, such as boosting economic and social aspects of the areas where it is used, along with a reduction in waste disposal and CO_2 emissions (Hernandez *et al.,* 2018).

Burning biomass can be considered to produce CO2 and other greenhouse gases. However, biomass is classified as neutral in the carbon cycle, not interfering with the carbon balance in the atmosphere, as illustrated in Figure 5. Unlike other solid fuels, CO_2 emissions from burning biomass are neutralized, since plants continuously emit and absorb this gas, which is a natural constituent of the atmosphere (Agrela *et al*., 2019).

Table 2 : Studies on the chemical stabilization of soils.

AUTHOR	ADDITIVE	LOCAL	RESEARCH RESULTS
Barshad (1950)	-	California (USA)	Effect of exchangeable cations on the expansion of clay minerals. How the degree o f hydration affects the expansion of these materials.
Chu *et al.* (1955)	Lime and Fly ash	Iowa (USA)	The best Unconfined Compression Strength (UCS) results at 28 days were in soil A-7-6 (clay), while in soil A-6 (silty) the results were lower. Use of miniature CPs (50 mm × 50 mm).
Jones (1958)	Lime and Cement	Denver (USA)	Both additives reduced the expansibility of the clay. The details of this reaction are not completely known. Cement reduced the drying shrinkage of the soil more than lime, but lime made the soil more resistant to deterioration by wetting and drying.
Carrol (1959)	Lime	Washington (USA)	The reactions are due to the chemical composition of the mineral and the chemical elements (ion exchange in clays).
Hilt and Davidson (1960)	Lime	Iowa (USA)	Kaolinitic and montmorillonitic soils gained in strength with lime alone, but chloritic and elliptic soils required the addition of cement together with lime to increase strength.
Ruff and Davidson (1961)	Lime and silicate sodium	Iowa (USA)	Field stabilization with sodium silicate and lime requires strict controls over the moisture content and the time elapsed between the final mix and the compaction required to obtain the desired strength.
Eades and Grim (1963)	Lime	Virginia (USA)	Field stabilization of 3 soils with different clay minerals and lime. Formation of new minerals (pozzolanic reactions) and calcium carbonate (carbonation).
Mateos (1964)	Fly ash from Coal	Iowa (USA)	5 types of fly ash were tested. Some have cementing materials such as lime and pozzolan. The best results were for granular soils such as dune sand.
Diamond and Kinter (1965)	Lime	Texas (USA)	In-depth understanding of the mechanism of how calcium hydroxide molecules interact on the surface of clay minerals to modify the surface and stabilize the clay. The need for the pozzolanic reaction to occur in order to increase strength and reduce plasticity.

Table 2: Studies on the chemical stabilization of soils (continued).

AUTHOR	ADDITIVE	LOCAL	RESEARCH RESULTS
Walker and Karabulut (1965)	Lime	Virginia USA	Two soils were stabilized with lime and evaluated in terms of freezing and thawing cycles. One was A-7-5 (clay) and the other A-5 (silty). The clay soil acquired greater resistance than the silty soil, but when subjected to freeze-thaw cycles it showed greater drops in resistance than silty.
Townsend and Klym (1966)	Lime	Canada	Durability of lime-stabilized soils.
Klemm (1980)	Kiln dust cement	Maryland (USA)	The chemical, mineralogical and physical composition of powders varies considerably from one plant to another, depending on the raw materials of origin, the type of furnace operation, the dust collection facility and the fuel used.
Baghdadi and Rahman (1990)	Kiln dust cement	Saudi Arabia	It was deduced that a mixing ratio of 30% cement kiln dust and 70% sand provided the best performance for application as base materials.
McCallister and Petry (1991)	Lime	Texas (USA)	They verified the changes in physical properties caused by leaching.
Lovato (2004)	Lime	Brazil	Stabilization of a lateritic soil with lime. High values of UCS (1519 kPa) and RT (216kPa0) were found for 28 days of curing. After 168 days the strengths decreased (carbonation).
Barroso and Santos (2006)	Lime	Ceará (Brazil)	Positive results of the laboratory study and the construction process of a 40 km highway length (melon highway) using the soil-lime technique.
Zhang e Tao (2008)	Cement	Louisiana (USA)	Investigation of 6 cement contents in an A-6 soil. The study confirms that durability tests and 7-day UCS are equivalent in predicting durability, and provisional graphs to guarantee the durability of low-grade soils. plasticity stabilized with cement were developed using the 7-day UCS or the maximum dielectric value values.
Gondim (2008)	Emulsion	Ceará (Brazil)	Stabilization of 3 different soils with slow-setting asphalt emulsion. Increases in resistance were observed in the mixtures. The amount of silica seems to have a negative influence on UCS.

Table 2: Studies on the chemical stabilization of soils (continued).

AUTHOR	ADDITIVE	LOCAL	RESEARCH RESULTS
Araújo (2009)	Lime	Ceará (Brazil)	Evaluation of two soils stabilized with lime powder and paste, at 3.5 and 7% and curing times of 0, 7, 14, 28 and 90 days. Inadequate pH dosage. Decrease in UCS for 90 days of curing.
Vizcarra (2010)	MSW ash	Rio de Janeiro (Brazil)	Decreased the material's expandability, showing a substantial increase in the CBR value with the insertion of fly ash and prior curing of the mixture doubled the Resilient Modulus (MR)value.
Vasconcelos (2018)	Fly Ashes and Lime	Ceará (Brazil)	The mixtures (50% soil + 50% ash), (95% ash + 5% lime) and (47.5% ash + 47.5% soil + 5% lime) showed compatible mechanical behavior for use in granular pavement layers.
Saksham *et al.* (2018)	Cement	India	As the cement content increases, the LL, PL and PI decrease, the cohesion values decrease, while the corresponding shear strength angle increases compared to the soil sample.
Obianigwe and Ngene (2018)	Cement	Nigeria	Cement contents of 2, 6, 10 and 14 % were investigated in a clayey sand (A-2-7). The optimum content found was 14%.
Ashraf *et al.* (2018)	Cement	Bangladesh	Dosage and durability analysis of soft soils treated with cement. The UCS was between 15 and 25 times higher with the addition of between 8 and 10% cement. The cement additions made the soils resistant to wetting and drying cycles, but increasing the cycles reduced the material's UCS.
Mahedi *et al.* (2018)	Cement and Slag	Texas (USA)	8, 12 and 16% cement content for stabilizing expansive soil. The expansion percentages of 12 and 18% were reduced to less than 1% for contents between 12 and 16%.

Figure 5: Carbon cycle

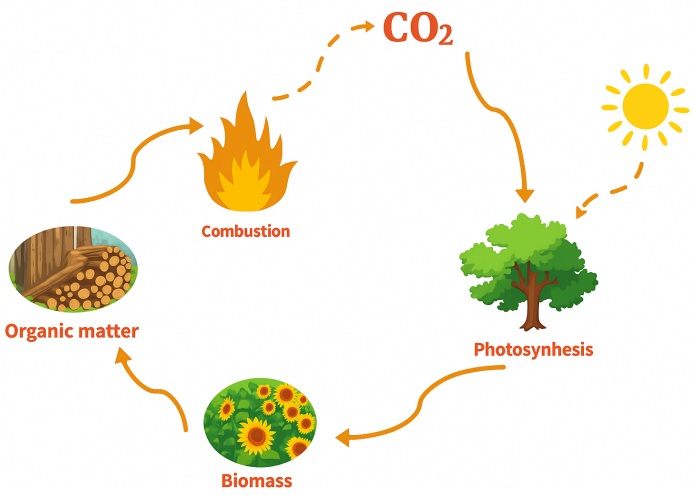

Source: (AGRELA *et al.,* 2019)

As well as being used in a variety of applications as a renewable energy source, biomass has been increasingly used in Brazil, making the country a pioneer on the international scene when it comes to the renewable energy matrix (Sales, 2012). When biomass is burned, ash is produced as a residue from the combustion of organic matter and the oxidation of inorganic constituents present in the fuel. The mineral fractions that do not volatilize easily during combustion typically react with oxygen, the oxidizing agent, to form oxides (Oburger *et al.,* 2016).

With the trend towards increased use of biomass as an energy source, there is also a need for proposals for the rational use of biomass ash. Recycling of large quantities of wood ash in an ecologically and environmentally acceptable way will benefit the bioenergy sector and society (Zhang *et al.,* 2022).

When wood or agro-industrial waste is burned, the organic carbon present in the plant tissues is released mainly in the form of CO_2 into the atmosphere, leaving as a by-product the mineral elements that the biomass absorbed from the soil during its life cycle (Vaske, 2012). According to the author, 70 to 85% of all the calcium and potassium present in a tree is found in the wood and bark of a typical trunk.

These examples are important to mention, because in the composition of biomass ash, silicon and calcium compounds can play an important role in the applicability of ash as a building material. On the other hand, the sodium (Na) and potassium (K) compounds, also known as alkalis, if present, can generate undesirable reactions in ash composites, damaging binding properties of particular interest to engineering (Agrela *et al*., 2019).

2.2.1 *Combustion technology*

The type of biomass directly affects the chemical composition of the ash generated. Although this is one of the most important variables to observe, other variables influence the quantity, type and characteristics of the ash generated. It is therefore possible to mention the main variables that interfere with the quantity, quality, characteristics and type of ash produced. According to Agrela *et al.* (2019) these variables are: (i) the type of biomass burned; (ii) the combustion technology used; (iii) the operating temperature of the furnaces and boilers and operating conditions, (iv) storage and processes and (v) the conditions and characteristics of the soil in which the biomass was produced.

From the combustion technology point of view, which, after the type of biomass burned, is the factor that most affects the quality and characteristics of the ash, there are usually two direct combustion options for the largest scales: (i) combustion in grate-type furnaces or (ii) combustion in fluidized bed furnaces.

Grate-type furnaces, illustrated in Figure 6, are a simple and robust solution, used mainly for burning biomass with low humidity. Its advantage is the low cost of installation and operation, making it a good option for small and medium-sized industrial facilities. The main disadvantage is its lower efficiency compared to other technologies, as it has limited control over the combustion process and may not be suitable for biomass with high humidity (LOO; KOPPEJAN, 2008).

Figure 6: Combustion in a fixed grate furnace

Source: Alfa Laval Boilers

Combustion in grate furnaces can be improved by using movable grates, as shown in Figure 7. This modification allows the use of a greater variety of biomass types, generating better control of combustion and air distribution, as well as greater efficiency compared to fixed grates. The main drawback of using this technology is the higher installation and maintenance costs inherent in the greater mechanical complexity of the furnaces.

Figure 7: Mobile grill-type furnace

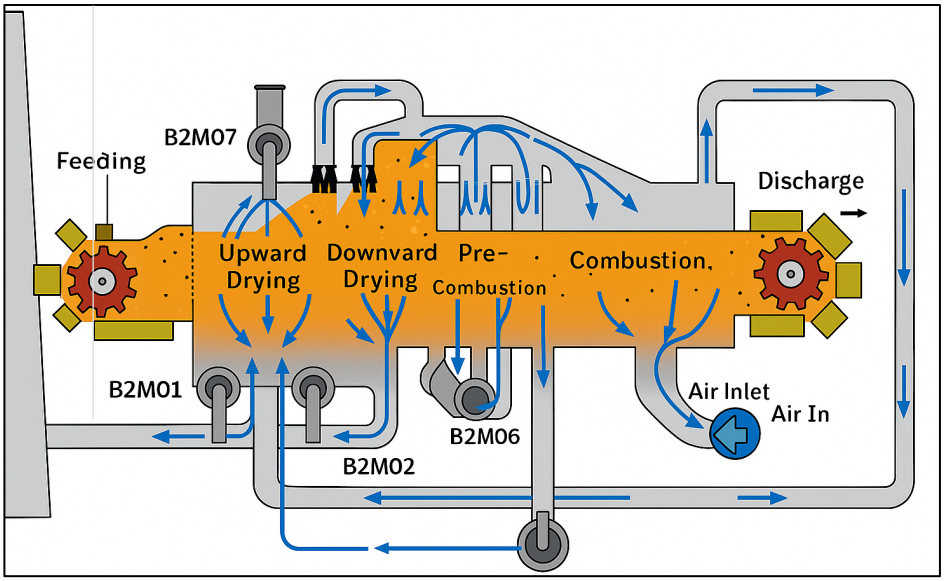

Source:(Fonseca, 2003)

Fluidized bed furnaces, illustrated in Figure 8, are a solution that allows for high combustion efficiency due to the greater uniformity in bed temperature, which leads to better capacity to burn biomass with high humidity and different particle sizes. The main weakness is linked to the high initial cost, greater operational complexity, the need for inert materials such as sand for the bed and stricter temperature control to avoid damaging the system (Loo; Koppejan, 2008).

Figure 8: Fluidized bed furnace

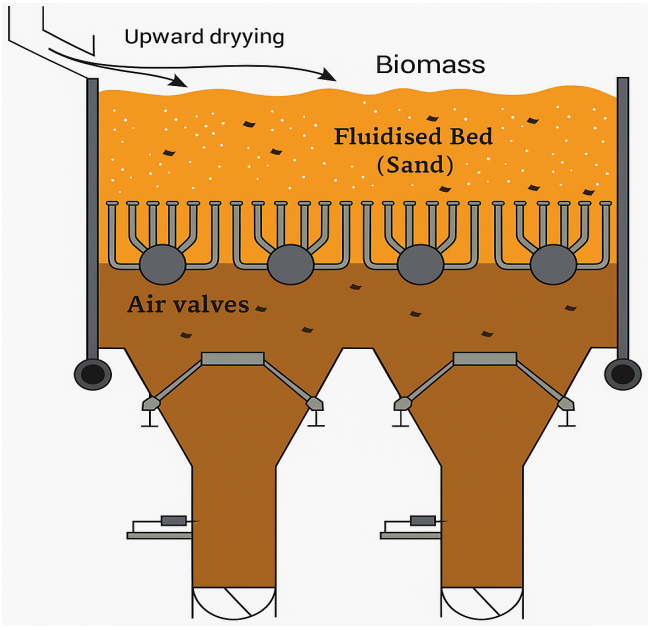

Source: (Basu, 2006)

Observing the combustion technology used is important because it directly influences the efficiency of biomass burning and the exposure of the ash to heat, resulting in a higher or lower coal content in the ash, different proportions of bottom ash or fly ash and interference in the reactions produced between the compounds that make up the ash. Figure 9 shows a schematic illustration of a biomass combustion plant.

Figure 9: Schematic representation of a biomass combustion plant

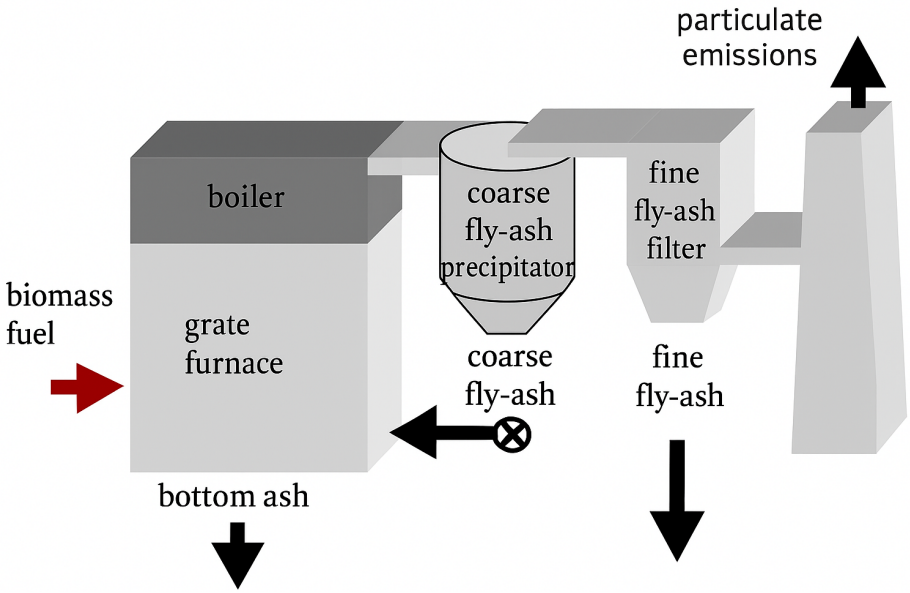

Source: (Dahl *et al*., 2002)

In these biomass combustion plants for energy and/or industrial purposes, two types of waste are generated from direct combustion*:* bottom ashes and fly ashes. Bottom ash is made up of material that has been completely or partially burnt. This ash fraction includes a coarser material with the presence of coal particles. *Fly* ash, on the other hand, is the finer fraction carried by the convection of combustion gases and is usually collected by appropriate filters that prevent the direct emission of these particles into the atmosphere. This portion of the ash is made up of a smaller fraction of unburned carbon and a larger inorganic fraction (Cruz *et al.,* 2017; Silva *et al*., 2019; Tarelho *et al*., 2015).

According to Supancic and Obernberger (2011), bottom ash corresponds to the largest share of ash generated in grate furnaces, ranging from 60 to 90% by mass of the total. With the use of Fluidized Bed Combustion (FBC) technology, for example, bottom ash becomes the smallest fraction corresponding to a generation in the range of 5 to 17% by weight (Dahl *et al.,* 2009).

The burning temperature of the biomass can be a decisive factor that interferes with the quality and characteristics of the ash. Etiégni and Campbell (1991) mention that for

operating temperatures below 500°C there is a predominance of carbonates and bicarbonates in the ash composition, while at temperatures above 1000°C there is a prevalence of oxides. These authors state that wood ashes are alkaline materials, and this alkalinity depends above all on the carbonates, bicarbonates and hydroxides present.

According to Caillat and Vakkilainen (2013) and Vassilev *et al.* (2013), biomass combustion temperatures in large-scale energy production plants vary between 500 and 1600 °C. On the other hand, Cruz *et al.* (2017) cite that more than 90% of the results found in the literature dealing with biomass ash report that it is produced at temperatures between 750 and 950 °C, which is therefore a typical temperature range for biomass combustion.

Pouey (2006) and Sales (2012) also highlight important points about the influence of temperature on the chemical reactivity of ash. One of these points is the phase transformation of the silica. As the temperature rises, the silica moves from an amorphous state to a crystalline state. Another relevant aspect is the action of the potassium compounds. These compounds act as fluxes, accelerating the crystallization process of amorphous silica.

These processes need to be considered, as one of the main agglomerating reactions responsible for increasing the strength of cemented materials is the pozzolanic reaction. For Cordeiro (2006), one of the main objectives of his work was to determine the optimum burning temperature for sugarcane bagasse, in order to achieve the highest pozzolanic activity index for the ashes studied. This index is directly associated with the percentage of silica present in the amorphous state.

2.2.2 *Yields and chemical composition*

According to Masiá *et al.* (2007), the percentage of ash generated varies according to the type of material burned. Agrela *et al.* (2019) mention that herbaceous biomass generates more ash than woody biomass. According to Borlini *et al.* (2005), burning wood produces around 3 % ash, while the percentage of ash generated from burning a type of fast-growing grass called elephant grass, or sugar cane bagasse, for example, can reach 10.9 % and 11.3 % respectively (Seye *et al*. *2000*). This data corroborates what Agrela *et al.* (2019) point out, citing that ash production from wood combustion is lower than the amount generated by burning herbaceous waste.

Table 3 summarizes some of the mass percentages of ash generated according to the type of material used while Xing *et al.* (2016) presents with Table 4 some chemical compositions of biomass ash according to the type of biomass burned.

Table 3: Percentage of ash depending on the type of fuel

Fuel	[%]
Wood bark	5-8
Wood chips with bark	1-2,5
Wood chips without bark	0,8- 1,4
Sawdust	0,5- 1,1
Demolition wood	3- 12
Straw and Grain	5- 14
Olive residue	4- 12
Miscanthus (Asian grass)	2-8

Source: (Zagvozda *et al.,* 2017)

Table 4: Chemical composition of biomass

Biomass	CaO	SiO_2	Al_2O_3	Fe_2O_3	K_2O	Na_2O	MgO	P_2O_5	TiO_2	MnO
Mixed Forest Pellets	21,24	26,4	4,47	2,78	6,42	2,31	4,27	1,84	0,68	2,08
Elephant grass	8,31	40,79	0,44	0,39	10,96	2,18	1,65	3,72	0,47	0,07
Oat straw	10,14	46,63	0,23	0,24	11,74	0,27	1,02	2,20	0,47	0,13
Wood Chips	26,26	19,32	2,78	2,48	5,67	1,48	2,75	2,78	0,65	4,06
Pine	39,15	2,49	0,41	0,37	11,13	1,39	4,78	9,74	0,48	0,12
Olive waste	8,36	5,19	0,58	0,45	33,03	2,17	2,41	3,52	0,47	0
Peanut shells	5,12	23,69	3,74	1,87	10,87	0,23	2,54	2,99	0,83	0,21

Source:(Xing *et al.,* 2016)

Cordeiro (2006), studying sugar cane bagasse ash, mentions that the silica present in sugar cane biomass ash comes from the process of plant transpiration, which generates an accumulation of silica in the form of silica gel between the cuticle and the wall of the plant's epidermal cells. This silicon accumulation mechanism acts as a barrier against pathogens and reduces water loss through transpiration. The occurrence of this natural process means that the presence of silica is notable in the composition of the ash generated by burning sugarcane bagasse.

Sales (2012) reports that several studies have evaluated the composition and use of agro-industrial waste ashes as pozzolanic materials. It can be inferred that, in general, ash from straw or similar waste tends to have high silica content in its composition and may therefore have the potential to act as a pozzolanic material. The author cites studies that have investigated rice husk ash, sugar cane bagasse, corn cobs, vetiver grass, elephant grass and wheat straw. The studies using these materials, most of which were incorporated as additions or substitutes in mortars and concretes, showed promising results. Table 5 shows the chemical composition of some of the ashes studied as possible pozzolanic materials, given the significant amount of silica (SiO_2) present.

Table 5: Chemical composition of silica-rich biomass

Biomass	CaO	MgO	SiO_2	Al_2O_3	K_2O	Na_2O	P_2O_5	TiO_2	MnO	Fe_2O_3	Authors
Corn cobs	13,19	2,05	27,65	2,49	35,49	-	2,49	-	-	1,55	Vassilev *et al.* (2013)
Elephant grass	8,31	1,65	40,79	40,79	10,96	2,19	8,31	0,47	0,074	0,397	Xing *et al.* (2016)
Panicum Virgatum	10,16	4,7	66,09	2,21	9,62	-	3,91	-	-	1,36	Vassilev *et al.* (2013)
Oat straw	10,15	1,02	46,63	0,23	11,74	0,27	2,20	0,471	0,129	0,239	Xing *et al.* (2016)
Rice husk	0,97	0,19	94,38	0,21	2,29	-	0,54	-	-	0,22	Vassilev *et al.* (2013)
Sunflower seed	15,18	7,27	23,46	8,67	28,29	-	7,07	-	-	7,27	Vassilev *et al.* (2013)
Sugarcane bagasse	5,97	8,65	60,96	0,09	9,02	0,70	8,34	-	0,48	0,09	Cordeiro *et al.* (2009)

Source: Elaborated by the author

Melo *et al.* (2018) report that Calcium-Rich Biomass Ash (CBRC) is different from other ashes, such as rice husk ash and sugarcane bagasse ash, because in addition to having a high concentration of calcium in its chemical composition, it has a lower concentration of silicon and aluminum, meaning that this ash does not have the necessary conditions to develop pozzolanic activity on its own. Although calcium-rich biomass ash (CRBA) does not meet the requirements to be considered a pozzolanic material, it can act as a calcareous filler in cementitious matrices and, if properly treated, serve as substitute for lime obtained from limestone mining and calcination.

ASTM C618 defines a pozzolanic material as one that, when combined with hydrated lime and water at room temperature, produces stable hydrated compounds with cementitious properties. This definition shows, in view of the results presented by Melo *et al.* (2018), that CRBAs may have the potential to act in conjunction with pozzolanic ash, creating the possibility of producing a bio-cementing material, a 'green cement'.

Table 6 shows the chemical composition of some ashes from burning wood. It can be seen the significant amount of Calcium Oxide (CaO) in relation to the other constituent compounds.

Table 6: Chemical composition of calcium-rich biomass

Biomass	CaO	MgO	SiO_2	Al_2O_3	K_2O	Na_2O	P_2O_5	TiO_2	MnO	Fe_2O_3	Authors
Eucalyptus	48,99	1,92	3,45	1,00	6,11	-	2,04	0,15	2,88	2,0	Vaske (2012)
Algaroba	78,66	3,06	1,41	0,53	9,73	0,72	2,35	-	-	0,51	Xing *et al.* (2016)
Mixed Forest	21,24	4,27	26,44	4,47	6,42	2,31	1,84	0,68	2,08	2,78	Vassilev *et al.* (2013)
Pine	39,15	4,78	2,49	0,41	11,13	1,39	9,74	0,47	0,12	0,37	Xing *et al.* (2016)
Olive tree pruning	31,41	2,45	6,84	2,73	12,31	-	-	-	-	1,39	Sklivaniti *et al.* (2017)
Wood Chips	26,26	2,75	19,32	2,78	5,67	1,48	2,78	0,65	4,06	2,48	Xing *et al.* (2016)
Beechwood	67,8	11,43	12,33	0,12	2,59	-	2,29	-	-	1,09	Vassilev *et al.* (2013)

Source: Elaborated by the author

Etiégni and Campbell (1991) mention the following elements found in wood ash: Ca,

K, Mg, Si, and P. The authors also report that wood combustion produces highly alkaline ash (pH = 9 - 13.5). The alkalinity of the material depends on the content of carbonates, bicarbonates and hydroxides. According to the authors, the possible compounds found in the ash studied are calcium oxide (CaO), calcite $CaCO_3$, portlandite $Ca(OH)_2$, calcium silicate (Ca_2SiO), among others.

2.2.3 *Ash classification*

As noted, the chemical composition of biomass ash is highly variable, as several authors such as Vassilev *et al.* (2013), Zagvozda *et al.* (2017) and Agrela *et al*. (2019) point out. In order to classify the types of ash into main groups with similar characteristics, Vassilev *et al.* (2013) propose 4 main groups of biomass ash which are type "S", "C", "K", and "CK" and six sub-groups ‘‘S-HA’’, ‘‘S-MA’’, ‘‘C-MA’’, ‘‘C-LA’’, ‘‘K-MA’’ e ‘‘K-LA’’.

Type "S" ashes are those with high SiO_2 contents, which normally contain significant levels of aluminum, iron, sodium and titanium oxides, with high concentrations of vitrified particles, silicates and oxyhydroxides. Since rice husk ash has a silica content of over 90%, it fits into this classification. According to Vassilev *et al.* (2013), type "S" ashes can be applied in various industrial segments, with emphasis on their use in cementitious matrices such as concrete, mortar or as additions to Portland cement, among countless other applications listed.

Type "C" ashes, on the other hand, are those with high CaO contents and which usually contain significant magnesium or manganese contents, with high concentrations of carbonates, oxyhydroxides, vitrified particles, phosphates and sulphates, with some silicate content being observed. Wood ash or woody biomass, with calcium contents above 30%, can be classified as such. The main uses cited by the author for this type of ash are the production of building blocks, use as a binder for low-strength materials and construction of granular pavement layers, as well as soil conditioning for agricultural purposes.

Type "K" ashes are those with high K_2O and low SiO_2 contents and which usually contain significant levels of phosphates, sulphates and chlorides. Ash from seaweed or agro-industrial waste such as corn cob ash, which has a high potassium content and low silicate content, can fall into this classification. "CK" type ashes, on the other hand, have balanced CaO and K_2O contents, and animal biomass ashes tend to fall into this classification region.

Vassilev *et al.* (2013) also mentions the subgroups HA (High Acid) or highly acidic,

MA (Medium Acid) or moderately acidic and LA (Low Acid) or slightly acidic respectively, indicating the tendency of behavior in chemical interactions. Figure 10 illustrates the trilinear ash classification diagram, showing a shaded region that corresponds to the one in which the biomass ash samples studied so far fall, demonstrating that biomass ashes are complex materials and cannot be classified into a single classification group.

Figure 10: Trilinear graph of biomass ash classification

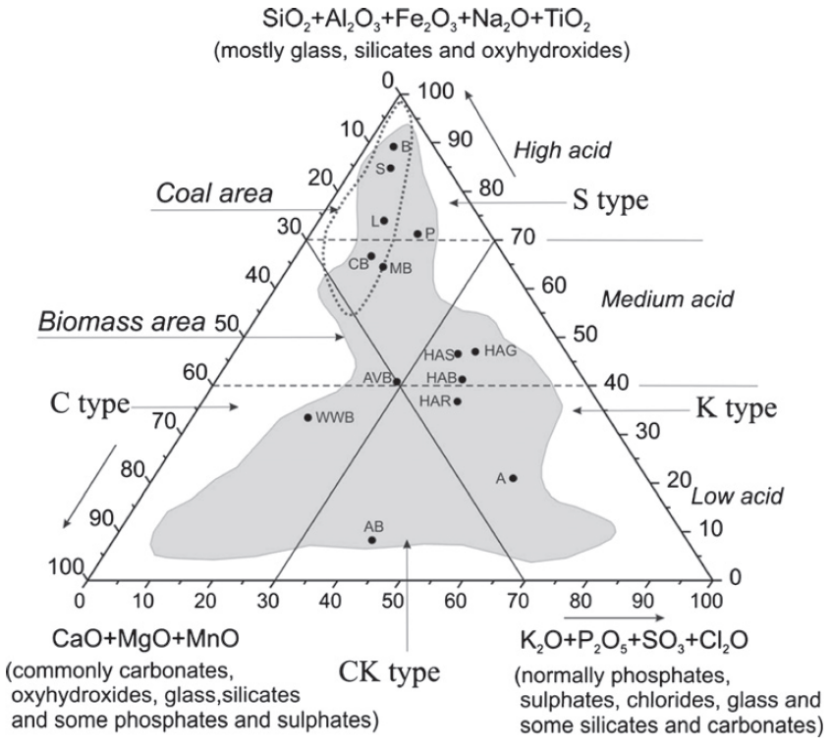

Source: (Vassilev *et al.,*2013)

The trilinear graph proposed by Vassilev *et al.* (2013) also points to a region where coal ash typically falls, demonstrating that it would fit into the S-HA", "S-MA" and "C-MA" regions. The author therefore proposes, based on the classification of ash into subgroups, the potential applications of these materials in various industrial production sectors.

2.2.4 *Geotechnical use of biomass ash in paving*

Among the sectors mentioned, those related to construction and the production of building materials include bricks and additions to Portland cement, ceramics, concrete, glass, the immobilization and solidification of hazardous waste, the synthesis of geopolymers, additions to asphalt mixtures and the construction of pavement bases and sub-bases. In this context, several studies, especially in northern European countries such as Sweden, Finland and Germany, have presented studies on the application of biomass ash in the construction of pavement bases and sub-bases.

Lahtinen (2001) used light biomass ash as a stabilizing component for granular materials and soft soils. The levels of biomass fly ash used were 80, 65 and 50% with Unconfined Compression Strength (UCS) values of 5 MPa, 3.2 MPa and 2.5 MPa, respectively. The author points out that the way fly ash is stored has a direct effect on the material's agglomerating properties, pointing out that if the ash is stored in silos without contact with moisture, there is no drop-in cementing capacity. However, ashes stored in stockpiles were studied and it was found that the UCS of fly ash samples dropped consistently for storage periods of 4 hours, 24 hours, 7 and 28 days, from around 1.5 MPa for ashes stored for 4 hours to less than 0.5 MPa for ashes stored for 28 days.

Macsik and Svedberg (2006) pointed out that fly ash had a positive effect on the stabilization of low-traffic-volume road bases made with gravel, with investigated proportions of 10%, 20% and 30%. The author concludes that the 30% fly ash content produced the highest resistance and the best behavior to freezing and thawing cycles. Areas where the stabilized base comes into contact with water should be avoided, as the material is highly leachable.

Okagbue (2007) evaluated the potential of wood ash in stabilizing clayey soils. The results showed that the geotechnical parameters of the clay soil improved substantially with the addition of wood ash; plasticity was reduced by 35% and CBR increased by 23 - 50% and 49 - 67%, respectively, for normal and modified energies. The highest CBR and strength values were achieved with 10% wood ash. The results also showed that curing improved the strength of the clay treated with ash. However, the gain in strength was short-lived, as the strength decreased rapidly after 7 to 14 days of curing. These results indicate that although ash provides some of the beneficial effects of lime in soil stabilization, such as reducing plasticity and expansion, improving workability and increasing strength, it is unlikely to be a substitute for lime, as the strength gain may be short-lived.

Nordmark *et al.* (2014) carried out an analysis of the leaching of fly ash from gravel roads in Sweden and concluded that the mobilization of hazardous compounds in the field was less than or almost equal to that obtained by leaching tests. It was found that standard leaching tests should not be used as a sole indicator of the mobility of hazardous elements and that the fly ash from the study in question was considered suitable for soil stabilization.

Cabrera *et al.* (2014) studied the application of heavy biomass ash from energy plants using olive industry waste as fuel in Spain. The authors found that the ash had CBR between 20 and 40% and could be used as filler material in road embankments.

Melo (2018) found that the use of algaroba bottom ash (ABA) and ABA lime are

viable for replacing commercial lime in the production of pressed soil-lime blocks. Melo (2018), also reported that it was possible to produce a hydrated lime from ABA through a simple process of sieving, washing and calcining the material.

Medeiros (2023) mixed A-4 soil with 4%, 6%, 8% and 10% ABA to evaluate the evolution of stabilization at different curing times (0, 7, 14 and 28 days). In the UCS test, the author pointed out that the increase in resistance was 228% for the soil with 10% ABA and 28 days of curing, while in the RT test the increase was 314%, while in the shear strength test was observed that cohesion increased as a result of the curing time and the increase in ash content.

The conclusions reported by Medeiros (2023) and Okagbue (2007), for example, point in opposite directions, casting uncertainty on the applicability of calcium-rich biomass ash in soil stabilization. Variables such as the type of ash, combustion technology and storage conditions can explain such different behaviors.

Another aspect worth taking into account when using biomass ash in road applications is the environmental impact that the use of this waste can have, especially when considering large-scale use and large volumes, as the paving industry usually demands. Related aspects, especially the leaching of hazardous compounds, must be considered, as well as evaluation methodologies.

2.3 *Enviromental analysis*

Improper disposal of biomass ash can have environmental impacts on soil and groundwater, harming plant and animal organisms or people who are exposed to contaminated soil, water or air. The main concerns regarding the use of these materials are their leaching capacity and high alkalinity. Handling these materials and excessive inhalation of volatile compounds and fine particles released are also potential risks to human health (Zagvozda *et al.,* 2017).

In an effort to reuse biomass ash, extensive research has been conducted in various fields, including soil amendment and fertilization for agricultural applications, as well as its incorporation into construction materials (Vassilev *et al.,* 2013). However, logistical challenges, variations in ash quality, lack of legislation and regulation in many countries, among other factors, result in most players opting to dispose of ash in landfills, generating a significant economic and environmental impact (Vamvuka and Kakaras, 2011). Biomass management is becoming an increasingly heavy burden from both an economic and environmental point of view.

One of the main uses of biomass ash has been as a fertilizer or soil conditioner for agricultural purposes. Several studies have investigated its benefits, challenges and concerns (Etiégni; Campbell, 1991; SteenarI *et al*., 1999; Bungart; Huttl, 2001; Demeyer *et al*., 2001; Zhang *et al.*, 2001; Dermibas, 2003; Tan; Lagerkvist, 2011; Vamvuka and Kakaras, 2011). There is no doubt that biomass ash contains nutrients that should be recycled back into the soil. However, some of the studies point to serious problems related to the ways in which these elements occur in different types of ash.

The main benefits of using this waste in agriculture is the supply of nutrients and essential elements to plants. In larger quantities, the main elements are (C, O, H, Ca, K, occasionally N), in smaller quantities (S, Mg, P, Cl, Na) and micronutrients (Mn, Zn, Fe, B, Cu, Mo, others) helping to improve the natural balance in the system. Another benefit is that it provides an alkaline character (liming effect), promoting advantages such as an increase in pH, improvements in electrical conductivity and nutrient exchange by soil roots and a reduction in Al, Mn and Fe toxicity. The addition of ash can reduce its exchangeable capacity and toxic metals in acidic soils, improve texture, aeration and water retention capacity and eventually improve biological activities by improving the environment for some microorganisms (Etiégni; Campbell, 1991; Vassilev *et al.,* 2013).

On the other hand, fundamental questions such as the amount of accessible or non-accessible nutrients, the absorption of contaminating elements and their long-term impacts on soils, plants and organisms, still require more detailed investigations with long-term monitoring to carefully clarify some important risks. High alkalinity can alter the soil's pH too much, negatively affecting local flora and fauna, as many soil plants and organisms are sensitive to changes in pH. The application of ash can change the structure of the soil, affecting its physical properties such as porosity and water retention capacity, which can negatively impact the local ecosystem. If ash cannot be used as a soil conditioner for agricultural purposes or fertilizer for these reasons, there are several other potential beneficial uses (Vassilev *et al.,* 2013; Zagvozda *et al.*, 2017; Agrela *et al.,* 2019).

Reference investigations such as those by Vassilev *et al*. (2013) indicate that significant proportions of nutrients are present as water-insoluble phases, while hazardous elements such as As, Bi, Br, Cd, Co, Cr, Cu, Hg, Mn, Mo, Ni, Pb, Sb, Se, V and Zn are in water-soluble phases in the ash. These hazardous elements often occur in water-soluble salts (chlorides, sulphates, carbonates) and hydroxides on the surface of ash particles. The presence of salts, heavy metals and other toxic compounds in biomass ash can lead to their accumulation in the soil, making it difficult for plants to absorb water and affecting their

growth and health.

Vassilev *et al.* (2013) describe the main leachable elements present in biomass ash, with maximum, average and minimum contents, as shown in Figure 11, and list these elements based on their occurrence and concentration in extracts leached from biomass ash. The authors also mention that the presence of elements such as Ca, Cd, Cl, Cr, Cu, K, Mg, Mn, Mo, Na, Ni, P, Pb, S, Si and Zn in biomass ash could have significant industrial potential due to their effectiveness and low-cost recovery, as well as for the synthesis of new materials.

Figure 11: Range of water-soluble elements leached from biomass ash, % by weight.

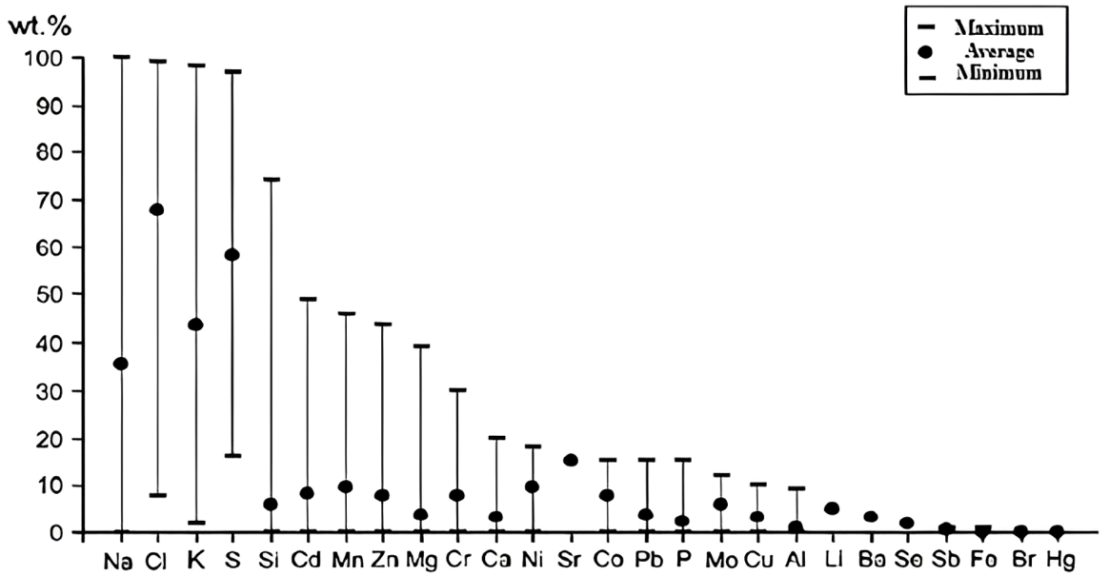

Source: (Vassilev *et al.,* 2013)

As shown in Figure 11, biomass ash has a wide range of chemical and mineralogical compositions and technological properties, which vary depending not only on the type of biomass burned and its elemental composition, but also on the combustion technology (Zagvozda *et al.,* 2017; Agrela *et al.,* 2019). Due to these factors, biomass ash should not be generalized in terms of its behavior and application, indicating the need for prior studies, especially in road construction (Zagvozda *et al.,* 2017).

Dermibas (2005) and Matalkah *et al.* (2016), for example, point out that the concentrations of heavy metals and chlorine are higher in wood ashes than herbaceous biomass ash. Supancic and Obernberger (2011) point out that fly ash produced in grate furnaces is not suitable for use as a soil stabilizer due to the high concentrations of heavy metals such as cadmium (Cd) and zinc (Zn).

In their work, Supancic and Obernberger (2011) investigated the use of different fractions of biomass ash from furnaces with different combustion technologies in soil

stabilization. According to the authors, due to the presence of heavy metals beyond the limits allowed by Austrian legislation, fly ash produced in grate furnaces is not suitable for use as a soil stabilizer. The authors also found that a mixture of bottom and fly ash from grate furnaces or light fly ash from fluidized bed furnaces can be used without exceeding the legal limits.

The environmental effects related to the use of biomass ash in civil projects vary according to different studies. Some studies have investigated the leaching of hazardous substances from ash, concluding that biomass ash does not pose significant risks to soil and groundwater quality (Kim; Kazonich, 1999; Oburger *et al.,* 2016; Papayianni; Tsimas; Moutsatsou, 2009).

Other research indicates that leaching is minimal when using biomass fly ash as part of cement-based materials (Berra *et al.,* 2015). However, recent studies highlight the diversity of high-quality biomass ash and its possible environmental impacts (Freire, Lopes; Tarelho, 2015). Some recommendations suggest that biomass ash should be primarily recycled as nutrients for forest soils, due to its fertilizing properties, and only secondarily employed in civil projects, such as road construction (Ribbing; Bjurström, 2011).

2.3.1 Environmental requirements and assessment procedures

Some regulations can be cited such as: the European Directive 2008/98/EC on waste, which includes specific guidelines for the use of waste in agricultural soils; EPA (*Environmental Protection Agency*) standards and criteria established by individual states in the US context; as well as in Brazil CONAMA Resolution No. 375/2006, which regulates the use of sewage sludge in agriculture, and can be used as a reference for biomass ash.

In Brazil, the environmental classification of soils and waste used in the road environment is carried out according to NBR 10004/2004 standard of the Brazilian Association of Technical Standards (ABNT). It is emphasized that although this standard is undergoing an updating process and a new revised version is expected to come into effect in December 2026, the waste classification criteria used in this research were based on the current version in force. According to this standard, waste is categorized into two types: Class I (Hazardous) and Class II (Non-Hazardous). Hazardous waste are those that has characteristics such as flammability, corrosivity, reactivity, toxicity or pathogenicity.

Class II (non-hazardous) waste is classified into two categories: Class II-A (Non-Inert) and Class II-B (Inert). Class II-B waste is waste that, when tested with distilled or deionized water, does not have a concentration of any component above the drinking water

standards. Waste that does not fall into Class I (Hazardous) or Class II-B (Inert) is classified as Class II-A (Non-Inert) and may have characteristics such as biodegradability, combustibility or solubility in water.

In order to properly classify solid waste, some laboratory tests can be carried out, such as the solubilization test (NBR 10006/2004) and the leaching test (NBR 10005/2004). The solubilization test measures the potential of the waste to release its components into pure water, comparing it with drinking water standards. The leaching test checks the waste's ability to release part of its components into the environment, assessing the potential impact on soils and groundwater.

As for leaching assessment methods, the most commonly used include the 10:1 liquid-to-solid ratio batch test, based on the Irish method of the *National Roads Authority* (*NRA*), the *British Standard European Norm* (*BSEN*) 12457 series, the Dutch tank leaching test of the *Netherlands Norm* (*NEN* 7375) particularly for monolithic materials and the upward percolation test based on the European *Technical Specification* (TS 14405:2004).

The 10:1 batch test consists of agitating the sample in deionized water at a 10:1 liquid-to-solid ratio for 24 hours, after which the extract is filtered and analyzed for contaminant concentrations. The British Standard European Norm (BS EN) 12457 series, in turn, specifies different ratios between residue and deionized water depending on the particle size of the material. The Dutch tank leaching test essentially involves the immersion of a monolithic piece of the material to be assessed, without fragmentation, with periodic renewal of the solution to measure the cumulative release of contaminants. The specimen must maintain a defined ratio between its exposed surface area and the volume of water, and the solution is replaced at 6 hours, 1 day, 2 days, 4 days, 8 days, 16 days, and 36 days, totaling seven leaching periods over 64 days. This test allows the evaluation of contaminant release by diffusion and serves as the basis for acceptance criteria in environmental regulations for waste disposal in landfills under European legislation (Decision 2003/33/EC).

Although the standard 10:1 method is perhaps the most common, it is an aggressive way of leaching components from a sample and therefore may not represent what occurs in the field. The tank test and the ascending percolation test, designed for monolithic and granular materials respectively, provide a more realistic way of determining leachability (Tiwari *et al.,*2015).

All this test to determine leaching are often carried out by solubilizing the material being assessed in a neutral liquid medium, which can be distilled or deionized water. In some cases, however, solubilization can be carried out in an acidic medium, usually in an acetic

acid solution, to simulate acidic conditions, which are common in landfills, for example. This method is described by the NBR 10005/2004 leaching test.

Basically, the sample is dried and ground or sieved to obtain a homogeneous particle size. The material is then solubilized in a neutral or acidic liquid in common proportions of 1:10 or 1:20, depending on the methodology used. The mixture is stirred for periods of time such as 18 or 24 hours to ensure interaction between the liquid and the solid being assessed, and then the solution is filtered for analysis of the extracted liquid and comparison with the limits established in the relevant regulatory standards.

These procedures do not simulate the specific conditions under which waste is used in compacted pavement layers, and this must be taken into account since the compaction and chemical stabilization techniques normally used reduce the permeability of the medium to percolating fluids.

Vasconcelos (2018) and Silva *et al.* (2019) mention that contaminant encapsulation technology, also known as the stabilization/solidification method, has become one of the alternatives for dealing with hazardous waste. The encapsulation process according to Wiles (1987) consists of adding a cementing agent, usually Portland cement or lime, to solidify waste. By cementing the mass of waste, the surface area of the mixture to be exposed to percolating liquids is reduced. This reduces the permeability of the material and therefore the solubility of hazardous compounds that could be released into the environment.

According to Consoli, Lopes Junior e Heineck (2009) the solubility of contaminants is inversely proportional to the increase in pH. This consideration is important because Baird (2002) mentions that the use of chemical stabilizers such as cement and lime, being alkalizing agents, reduce the solubility of hazardous substances, making it a promising alternative for dealing with contaminating materials.

In this context, Vasconcelos (2018) mentions that the ASTM D 4874 column leaching test has the advantage of simulating the conditions used in the paving sector in a more representative way, as it is an ascending percolation test that can use a treated and compacted sample in conditions similar to those in the field.

The main environmental regulatory requirements for the use of biomass ash in construction applications vary according to the region and local legislation, but generally include the following aspects: (i) Maximum limits for the concentration of heavy metals, such as arsenic (As), cadmium (Cd), lead (Pb), mercury (Hg), nickel (Ni), chromium (Cr), copper (Cu), zinc (Zn), among others; (ii) Appropriate pH range to prevent the use of biomass

ash. The considerations to be made regarding the environmental tests will be affected by the stabilization potential and results obtained for each processed ash sample. The materials to be used and the processes are described in section 3 Materials and methods.

2.4 Final considerations

Based on the literature review presented, it is highlighted that biomass ashes are renewable materials, highly diverse, and with different technological properties that directly influence their performance in construction applications. The main factors affecting the properties of ashes are related to the type of biomass, the combustion technology and temperature, as well as storage and the separation and beneficiation processes.

In general, ashes from wood and lignocellulosic materials tend to have higher calcium content, whereas ashes from straw, husks, and other agro-industrial residues tend to have higher silicon content. These components are precursors of binding materials such as lime, Portland cement, and geopolymers, highlighting the potential of using these materials for more sustainable infrastructure.

The literature indicates that ashes can improve relevant properties in mortars, concretes, and soils for geotechnical and pavement applications. However, the observed effects vary according to the technological properties of the ashes and their interaction with other components of the mixtures, such as aggregates, binders, and soils.

In pavement applications, studies show that ashes tend to reduce soil plasticity, decrease expansion and contraction, and improve mechanical properties. Nevertheless, in some cases, mechanical stability is not long-lasting, especially under moisture variations. Ash beneficiation is cited in the literature as a strategy to optimize their properties of interest. In addition, the presence of toxic components represents an additional challenge for the safe use of biomass ashes.

Therefore, this study comprehensively explores the potential of using wood ashes, subjected to different treatment stages, in soil layers for pavement construction, including physicochemical characterization of the ashes throughout the treatment steps, evaluation of mechanical properties under saturation conditions, assessment of environmental impact, and cost analysis of implementing this technology.

3 MATERIALS AND METHODS

3.1 Initial remarks

This chapter is divided into three parts: (i) general information about the study area; (ii) the materials selected (iii) the methods applied for the investigations and assessments. In the general information about the study area, the region selected for the collection of materials was characterized using geographic thematic maps, politics, the main road network, vegetation, relief, climate, geology and pedology.

In the section on materials, the soils, ash and hydrated lime were presented, with information on collection sites and general characteristics. The methods section presents the experimental program, describing and presenting the ash processing procedures, the material characterization tests, as well as the mechanical and environmental tests used to evaluate the idealized mixtures. Finally, some considerations on the design of hypothetical pavement sections and its cost feasibility.

3.2 General information about the study area

The materials collected in this study come from the *Cariri* Metropolitan Region (CMR). This region is located in northeastern Brazil, in the interior of the state of Ceará and its main economic hub is the municipality of *Juazeiro do Norte*, which is 507 km from the state capital, *Fortaleza*, as shown in Figure 12.

Figure 12: Location of the CMR in the state of Ceará and in Brazil.

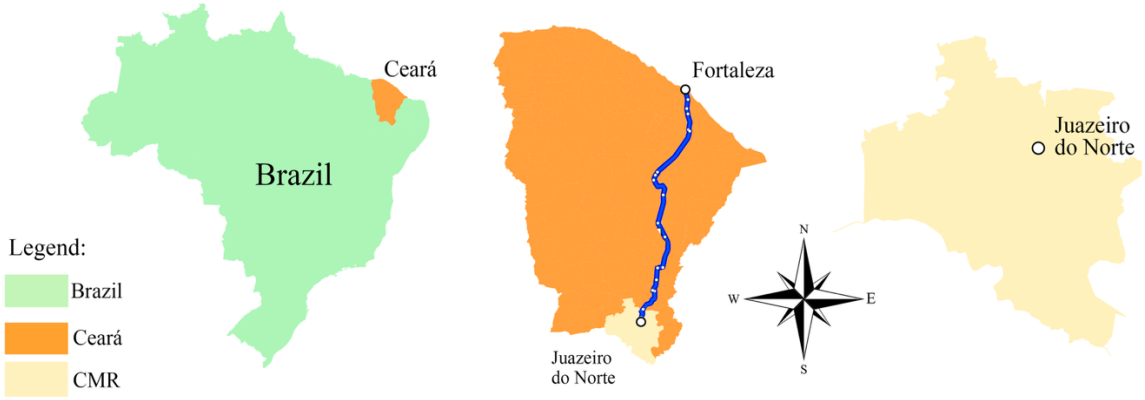

Source: Elaborated by the author

The CMR was created by State Complementary Law Nº 78 and is made up of 3 main municipalities: *Juazeiro do Norte, Crato and Barbalha* and another 6 bordering municipalities, *Santana do Cariri, Nova Olinda, Farias Brito, Caririaçu, Missão Velha* and *Jardim*, as shown in Figure 13.

Figure 13: Map of the Cariri Metropolitan Region (CMR)

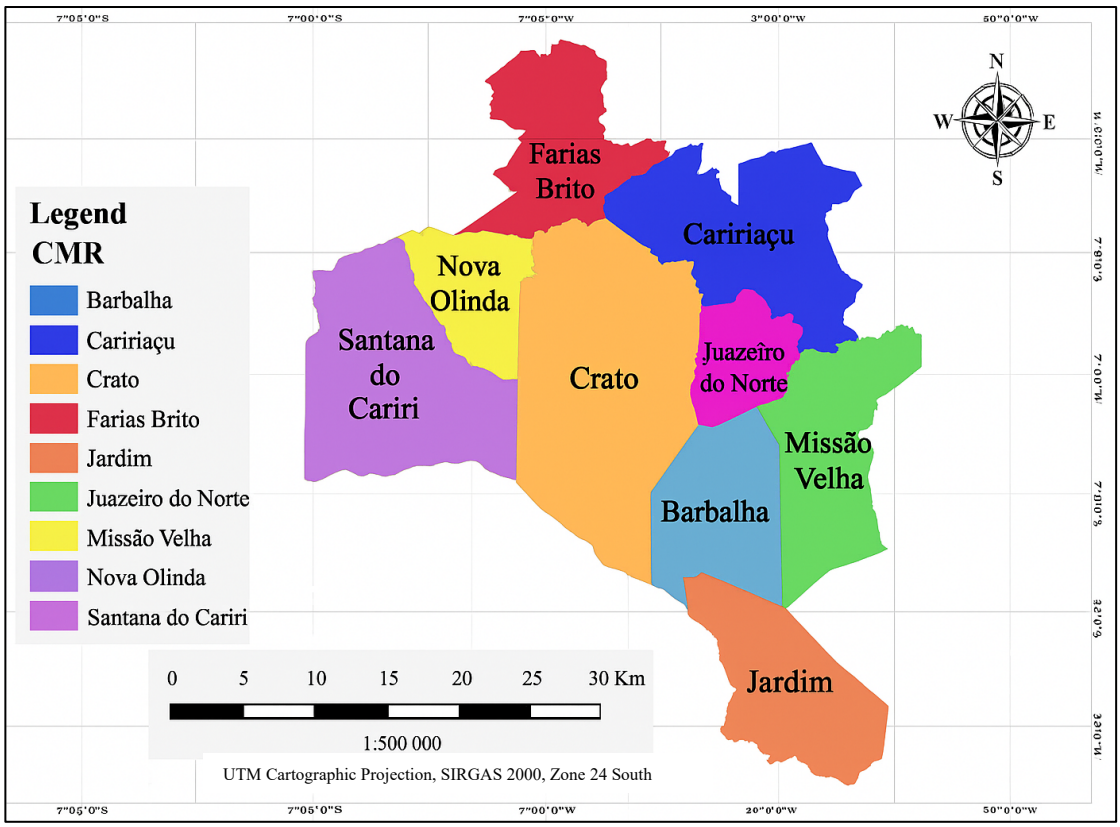

Source: Mascarenhas (2016)

Mendonça (2001) and Mascarenhas (2016) mention that the CMR is located in a privileged region of the state of *Ceará,* with considerable potential for water, mineral, soil resources and climate. The region has a population of 633,326, according to the IBGE (2021), which corresponds to 7.2% of the total population of the state of Ceará.

From an economic point of view, the region is a logistics hub, as it is practically equidistant from all the capitals of the northeast, and has a significant commerce and services sector, especially in the municipality of *Juazeiro do Norte*. The industrial park includes the footwear, medicine, clothing, veneer, ceramics and aluminum sectors, as well as public and private universities that together offer more than fifty undergraduate programs, making the region a university and medical center in the interior of the northeast, with reference hospitals and pharmaceutical industries in operation.

The Gross Domestic Product (GDP), which represents the total value of all final goods and services produced in CMR, is 5.01% in relation to the state of *Ceará* and it has a paved road network consisting of 14 highways, two of which are federal (BR-230 and BR-122) and twelve state roads (CE-060, CE-153, CE-166, CE-292, CE-293, CE-386, CE-388, CE-390, CE-492, CE-494, CE-530, CE-561) as shown in Figure 14.

Figure 14: Map of the road network in CMR

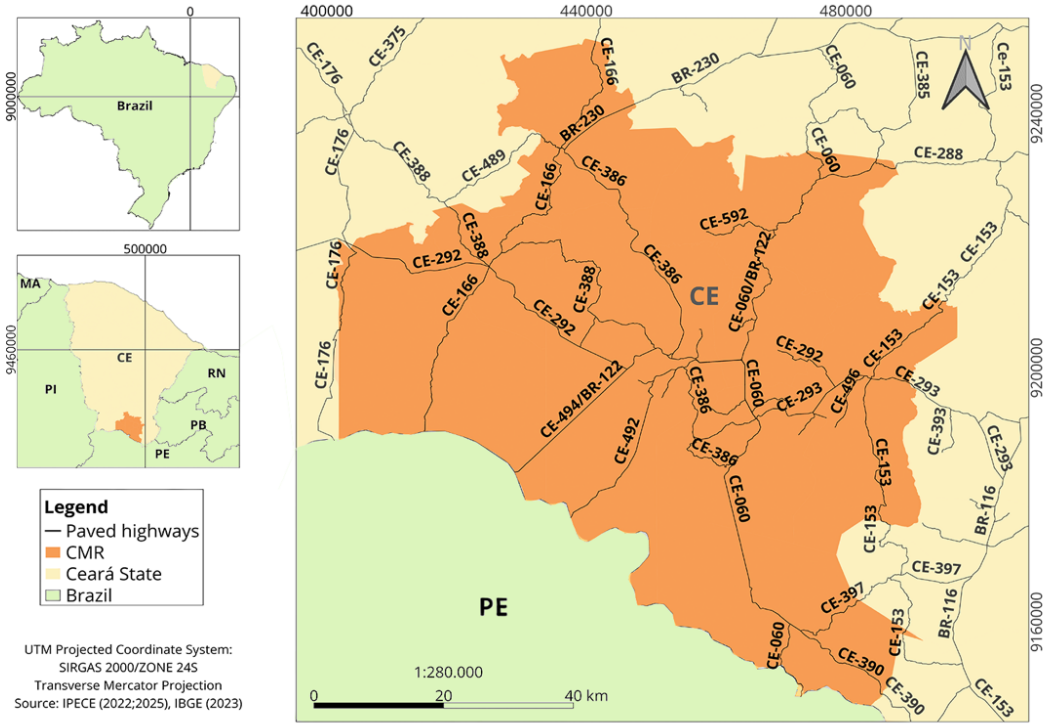

Source: Elaborated by the author

The region has an average annual rainfall of 1,033 mm, based on 74 years of observations at weather stations in the cities of *Barbalha, Crato*, *Juazeiro do Norte* and *Missão Velha*, with a rainy season between january and may, as shown in Figure 15, and temperatures between 13 and 35 °C (Mendonça, 2001). According to the rainfall map (Funceme, 2025), the municipalities in the *Cariri* region had rainfall between 800 mm and 1000 mm, such as the municipalities of *Farias Brito*, *Missão Velha* and *Juazeiro do Norte*, while municipalities such as *Crato* and *Nova Olinda* had between 1200 mm and 1780 mm.

Figure 15: Monthly historical rainfall in the CMR

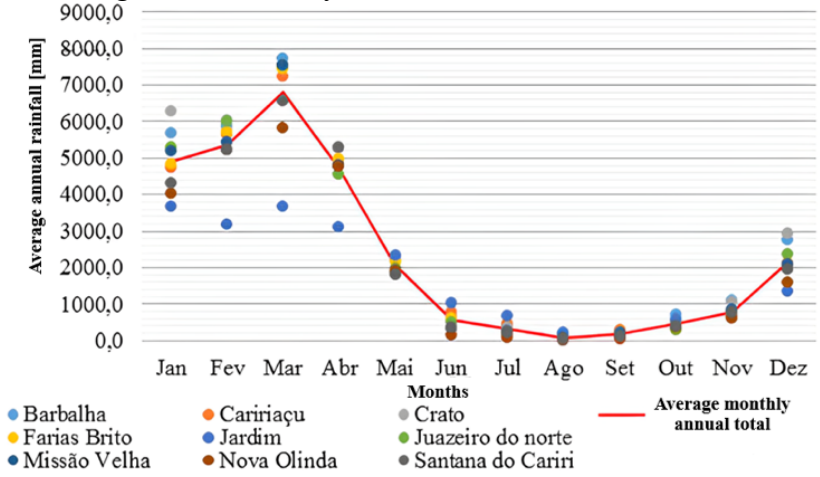

Source: Adapted form (SOUSA, 2018)

There are three predominant climates in the region: dry subhumid, tropical or subtropical; humid subhumid, tropical or subtropical; and semi-arid, tropical or subtropical. This variation in climatic types is associated with the 3 basic types of relief present in the region, which are the high plateaus, the *sertaneja* depression and the low massifs and mountains, described in Figure 16.

Figure 16: Landscape Map CMR

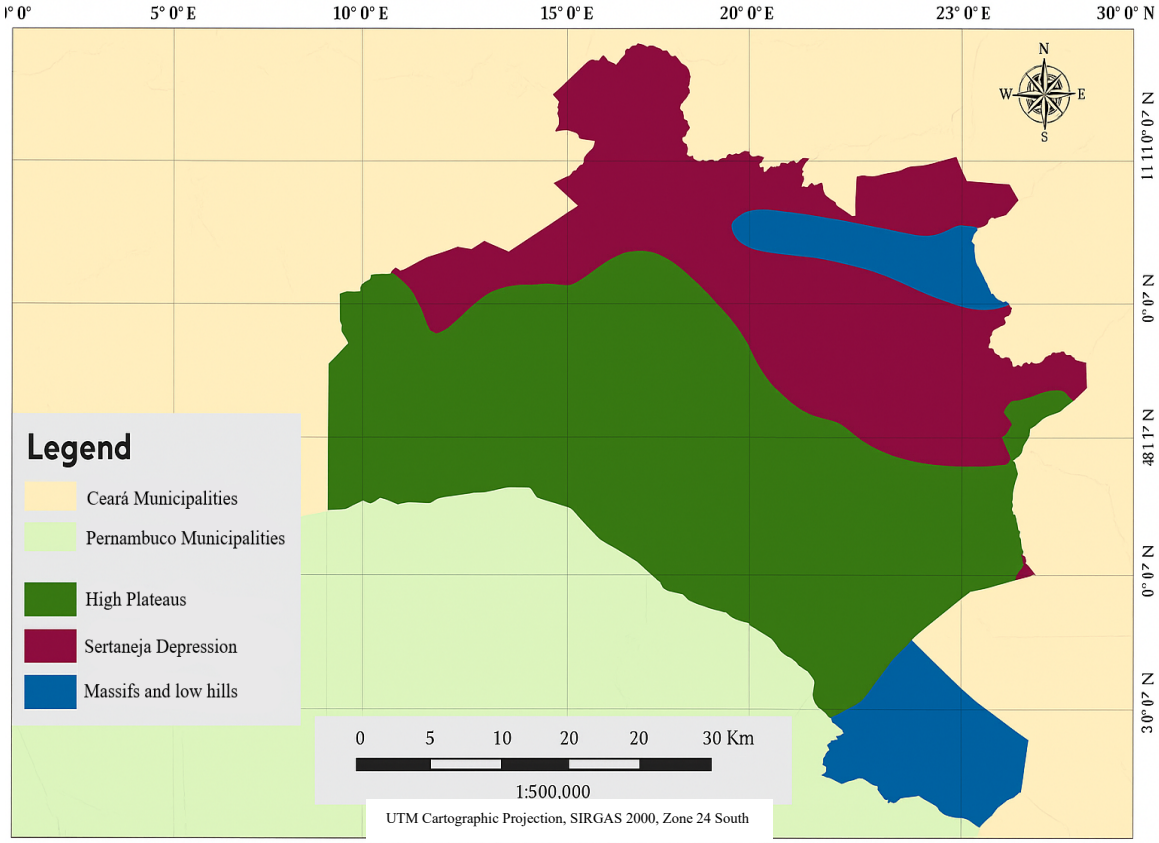

Source: Mascarenhas (2016)

The vegetation can be described in terms of the four types present in the region, which are the Subperennial Tropical Pluvial-Nebular Forest (humid forest), the Subcaducifolia Tropical Pluvial Forest (dry forest), the Deciduous Thorny Forest (arboreal caatinga) and the Subcaducifolia Tropical Xeromorphic Forest (cerrado).

The types of vegetation described in Figure 17 are related to the region's relief, climate and pedology. The humid forest is located on the slopes of the *Araripe* plateau, which due to the altitudes between 850 and 900 m above sea level, combined with the humid winds, produce favorable conditions for the development of this type of vegetation. The dry forest occurs in a transition zone below the slopes of the plateau, while the *cerrado* is on the *Araripe* plateau and the arboreal *caatinga* in the areas below the dry forest.

Figure 17: Vegetation map of the CMR

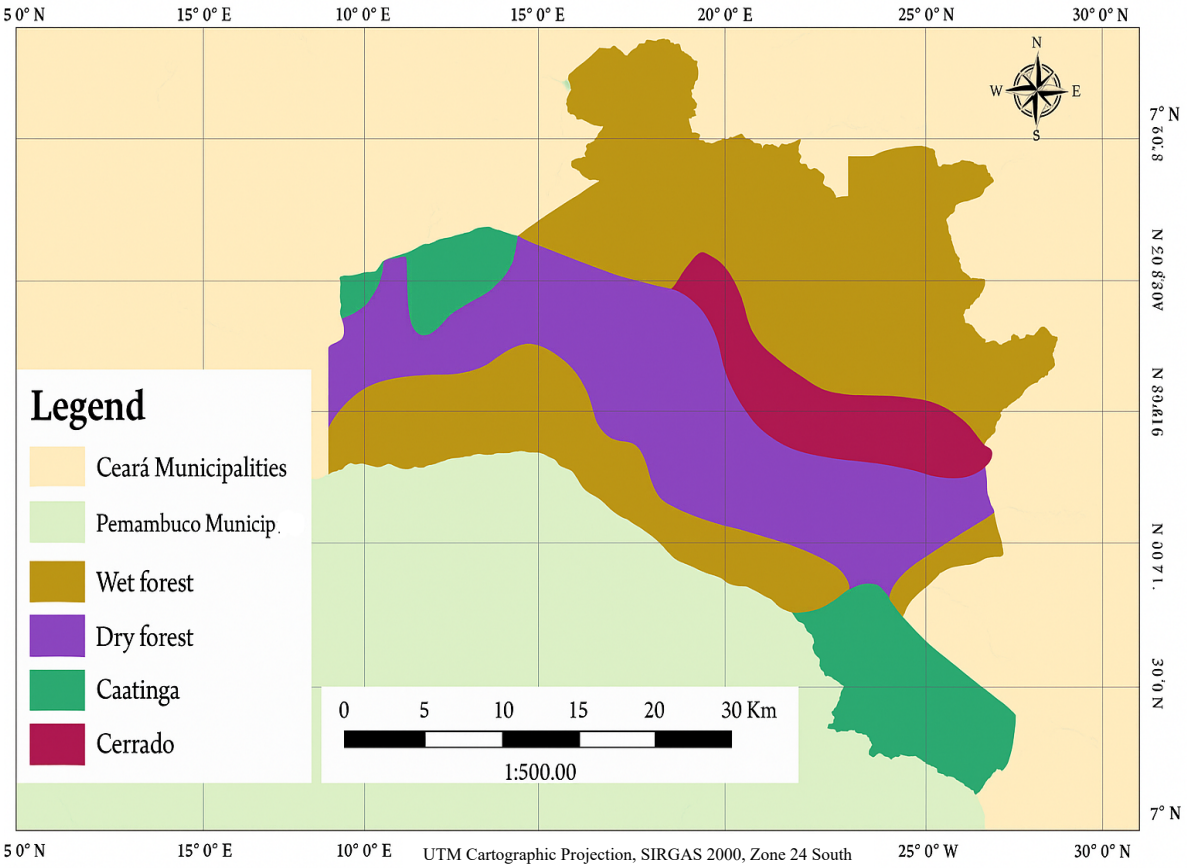

Source: Mascarenhas (2016)

From a geological point of view, Figure 18, the region is mainly made up of sedimentary formations, followed by metamorphic and igneous formations (Mascarenhas, 2016). Based on the geological characteristics described by Mendonça (2001), the samples are located in the geological formations corresponding to the *Brejo Santo* formation and the *Santana* formation, both inscribed in the Entisols range. It should be noted, however, that the classification adopted by the author is based on the Brazilian Soil Classification System (SiBCS). This classification has similarities with the USDA international classification and the soil classification described by the author was adapted to the international classification system.

The *Brejo Santo* formation is described by the author as composed of red or dark brown, silty, calciferous claystones and foliations, containing sporadic beds of green shales, between which there are layers of fine to medium sandstones and thin sheets of clayey limestone, rich in ostracodes, which makes them commonly calciferous.

Figure 18: Geology of the CMR

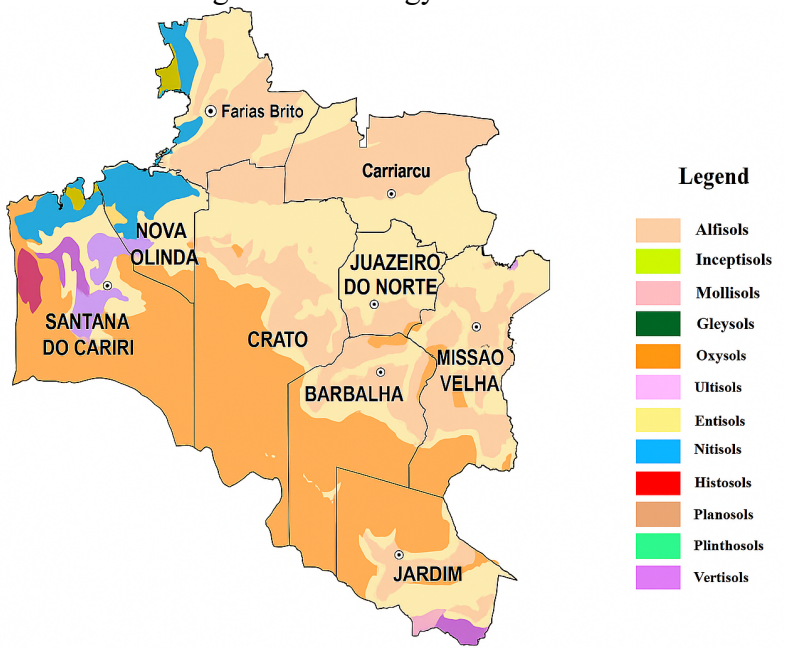

Source: Adapted from IPECE (2020)

The *Santana* Formation (*Crato* Member) is described as composed of gray, brown, calcareous, laminated shales and light gray and cream micritic limestones, clayey and finely laminated. From a pedological point of view, the soils collected are both located in the lithic Entisols zone, as illustrated in Figure 19.

Figure 19: Pedological map of the CMR

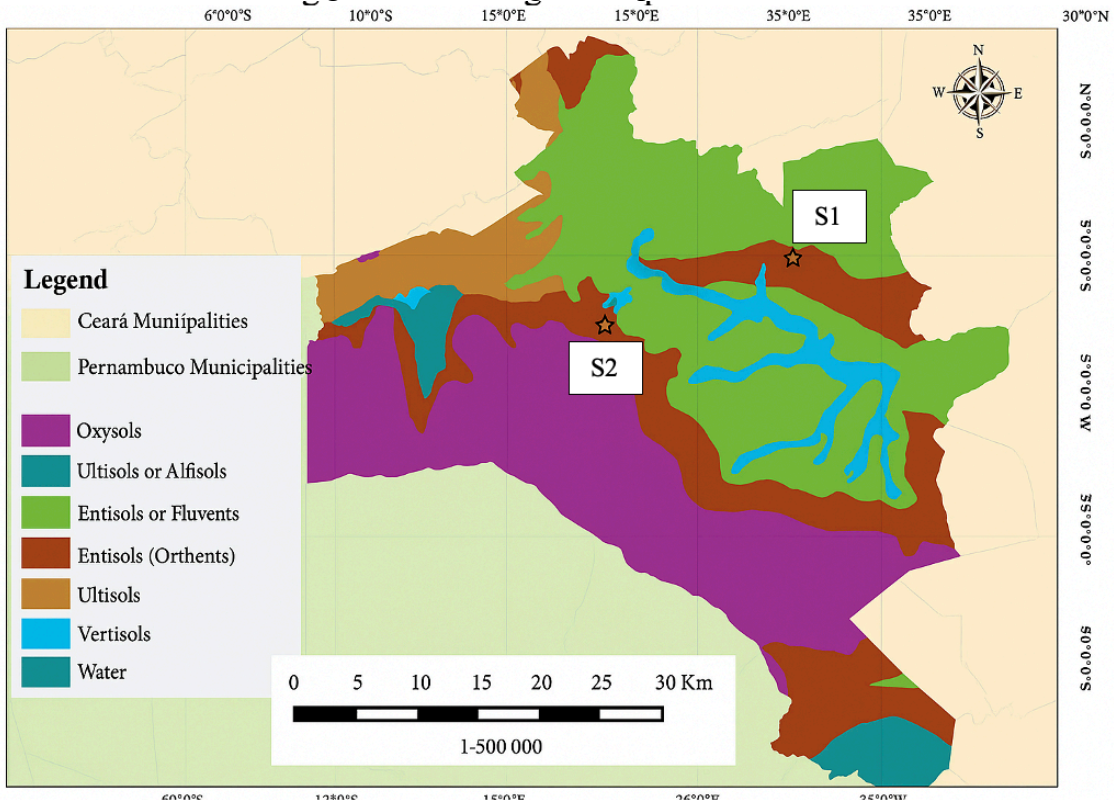

Source: Mascarenhas (2016)

3.3 Materials

The materials studied in this research were two soils collected in a region where Entisols predominate in the *Cariri* Metropolitan Region (CMR). Therefore, while soil 2 can be considered an Entisol, soil 1 exhibits characteristics of a Vertisol since it is located downstream from a small dam in an area where rainwater flows. Wood ash from an industry in the CMR and commercial hydrated lime classified by the Brazilian Association of Technical Standards (ABNT) as type CH I were also collected. The physical and chemical requirements for this classification are described further in the Table 8 and Table 9.

3.3.1 *Soils*

Soils from the CMR were investigated because it is where the ash studied in this work is generated. The first sample, called Soil 1 (S1), illustrated in Figure 20 (a), was collected on the banks of the beltway in *Juazeiro do Norte* - CE, in a lowland area near to the *Colina do Horto*. The second soil sample, called Soil 2 (S2), illustrated in Figure 20 (b), was collected from a slope of a housing development located in the municipality of *Crato*-CE, at the foot of the *Araripe* plateau. In this region there is a large presence of expansive soils, with great variability of soil textures in the same layer, and tactile-visual inspection showed the presence of reddish clay with veins of cream clay, indicating a variegated clay sample.

Figure 20: Soils collected in the CMR

a) Soil 1 (S1) b) Soil 2 (S2)

Source: Elaborated by the author

It should be noted that the coordinates of the soil collection points were marked using the smartphone application Mapnitude Version 8.0.3, as described in Figure 21 and Table 7.

Figure 21: Location of the soils collected at the CMR.

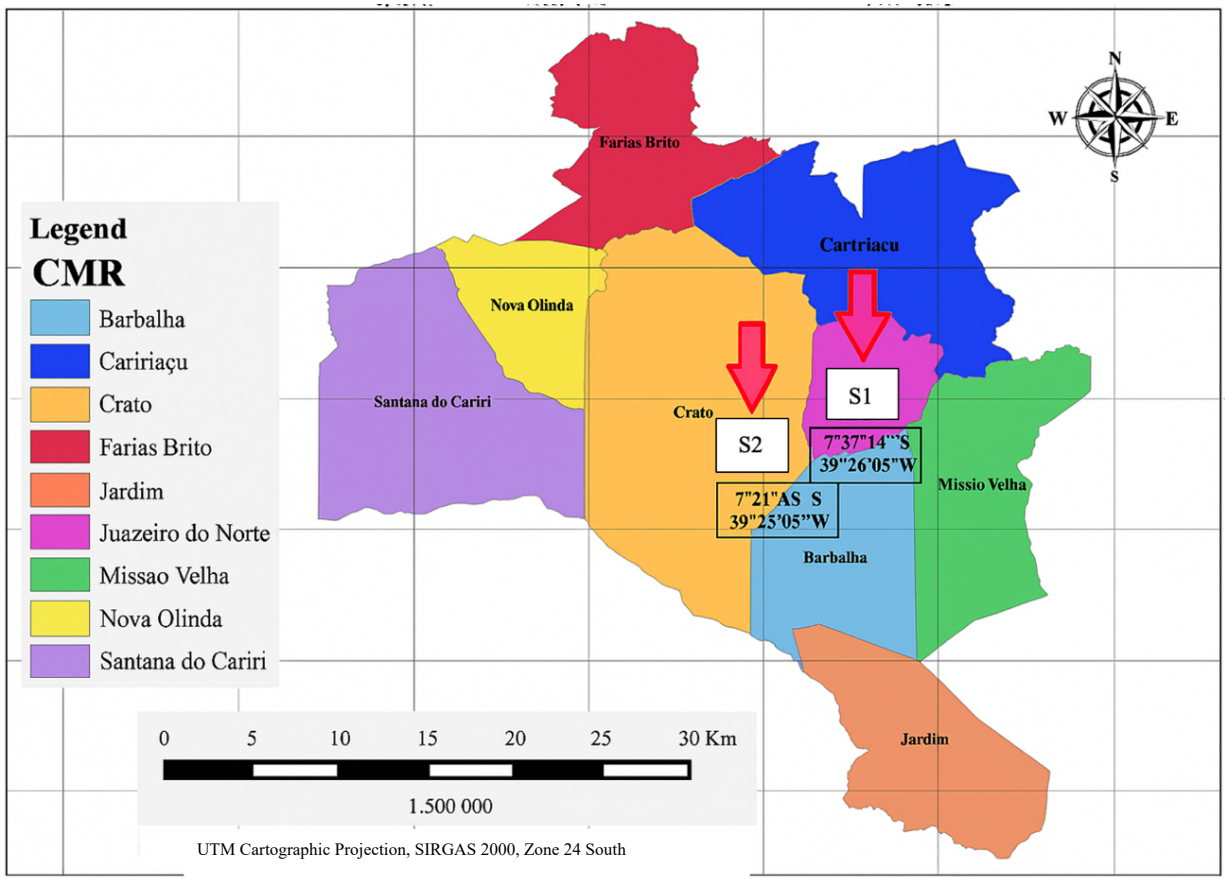

Source: Adapted from Mascarenhas (2016)

Table 7: Coordinates of the soil samples collected.

Sample	Latitude	Longitude
S1	7° 10’ 54” S	39° 18’ 09” W
S2	7° 13’ 15 S	39° 26’ 06” W

Source: Elaborated by the author

3.3.2 *Ashes*

Wood ash was collected from a boiler in a pharmaceutical industry located in the CMR. In the specific case of this industry, many of its industrial processes require the use of water vapor at high temperatures for specific applications in its production process. This water vapor is produced by burning wood that has been duly certified by environmental agencies. The boiler used in the pharmaceutical industry in question, illustrated in Figure 22, is an ambitubular fixed grate type for burning wood, chips, briquettes, bagasse and others solid fuels, with electronically controlled temperature, maintained at a maximum of 600 °C.

Figure 22: Ambitubular fixed grate boiler

Source: Elaborated by the author

The combustion of Algaroba wood and wooden pallets in this industry produces two types of ash. The first is fly ash collected by a multicyclone filter, while the second is bottom ash. According to Zagvozda *et al.* (2017), bottom ash has a higher concentration of free CaO and lower levels of heavy metals compared to fly ash. According to industry employees, bottom ash is produced in a volume of 3 tons per month and in a ratio of 5:1 of fly ash, corroborating the data reported by Melo (2018) on the production of algaroba ash in textile industries in the state of Pernambuco.

The ash collected for this work was from the lower compartment of the boiler, and is therefore bottom ash, with an observed amount of charcoal and a visually coarser grain size compared to fly ash, although with a significant amount of fines. Figure 23 a) shows the collection compartment under the boiler grate, while Figure 23 b) shows the aspect of the collected ash.

Figure 23: Ash collection

a) Collection compartment b) Visual appearance of collected ash

Source: Elaborated by the author

Currently, according to the employees, the base ash is stored in 200-liter metal drums while the fly ash is accumulated in cyclone filters. Both ashes are sold to a fruit farm in the region at low prices to be used as a fertilizer and soil pH corrector for agricultural purposes.

3.3.3 *Hydrated Lime*

The lime used in this research was type CH-I, as established by ABNT standard NBR 7175/2003. Table 6 and Table 9 set out the main chemical and physical requirements for classifying the types of hydrated lime. The material was provided by Carbomil Química S/A, located on the Baixa Grande farm, approximately 20 km from the municipality of Limoeiro do Norte - CE.

Table 8: Chemical requirements for classifying hydrated lime.

Compounds		Limits		
		CH-I	**CH-II**	**CH-III**
Carbonic anhydride (CO_2)	At factory	≤ 5 %	≤ 5 %	≤ 13 %
	Warehouse	≤ 7 %	≤ 7 %	≤ 15 %
Non-hydrated oxides (CaO + MgO)		≤ 10 %	≤ 15 %	≤ 15 %
Total oxides (CaO + MgO)		≥ 90%	≥ 88 %	≥ 88 %

Source: NBR 7175.

Table 9: Physical requirements for classifying hydrated lime.

Compounds		Limits		
		CH-I	**CH-II**	**CH-III**
Fineness (% Cumalative retained)	0,600 mm Sieve	≤ 0,5 %	≤ 0,5 %	≤ 0,5 %
	0,075 mm Sieve	≤ 10 %	≤ 15 %	≤ 15 %
Water retation		≥ 75 %	≥ 75 %	≥ 70 %
Sand incorporation		≥ 3,0	≥ 2,5	≥ 2,2
Stability		No cavities or lumps		
Plasticity		≥ 110	≥ 110	≥ 110

Source: NBR 7175.

3.4 Methods

The experimental program for this research is divided into five stages. The first stage describes the ash processing procedures and soil methods used for material characterization. It includes details of the sieving, washing, calcining, and hydrating steps for the ashes and other soil characterization procedures.

The second stage focuses on determining compaction parameters and selecting the optimum ash content for each processing condition, evaluating mixtures with ash contents of 3%, 5%, and 7%. The best contents are those that yield the highest Unconfined Compressive Strength (UCS) values after 28 days of curing, using miniature test specimens. This criterion follows an adaptation of the methodologies proposed by Thompson (1966), Núñes (1991), and Lovato (2004).

Since the specimens are submerged in water prior to the UCS test, as required by the Brazilian standard DNER-ME 180/94, it was observed mixture disintegration due to saturation, which may render the test unfeasible. In such cases, the selection of the optimum ash content considers the highest bearing capacity values under dry conditions (optimum moisture), as well as the lowest bearing capacities losses after saturation, along with expansion and shrinkage within acceptable limits. These parameters are determined using the Brazilian methodology for fine lateritic soils proposed by Nogami and Villibor (1995), through the Mini-CBR test. As this test is performed with a confining cylinder, it is suitable for granular (uncemented) materials and is used as a selection method for mixtures that eventually disintegrate. In this stage, it is also possible to observe the chemical reactivity of the soil-ash mixtures, indicated by increases in UCS, or their lack of reactivity, evidenced by the disintegration of the mixture.

The third stage investigates changes in the plastic behavior of the mixtures compared

to the untreated soil. For this purpose, consistency limit tests are conducted on the selected mixtures after 0, 28, and 90 days of reaction.

The fourth stage involved evaluating the mechanical strength of the mixtures through California Bearing Ratio (CBR), Resilient Modulus (MR), Indirect Tensile Strength (ITS), and fatigue tests, applied only to mixtures that did not disintegrate. Mixtures that disaggregated were assessed solely by the CBR test, as UCS and ITS cannot be performed in such cases.

Finally, the fifth stage comprises environmental tests related to the solubilization, leaching, and column leaching potential of chemical elements present in the ash, which may pose risks to the environment. Figure 24 presents a schematic overview of the experimental program, which is detailed in the following sections.

3.4.1 *Wood ash processing*

The wood ash undergoes processing stages in the laboratory to remove contaminating materials and promote chemical transformations. The process comprises three stages:

1. Sieving
2. Sieving and washing
3. Sieving, washing, calcination (and hydration)

The first stage, illustrated in Figure 25, consists of separating charcoal from the ash by sieving through 2 mm and 0.075 mm meshes. The 2 mm sieve removes excess residual charcoal from the ash, while the 0.075 mm sieve (No. 200) regularizes the particle size distribution, in accordance with the ABNT NBR 7175/2003 standard, which limits the percentage of material retained on the 0.075 mm sieve to 15% for hydrated lime.

The coarser fraction retained on the Nº 200 sieve is crushed and re-sieved. The material that remains retained is discarded, and the portion that passes through the mesh is collected to obtain a fine-grained ash sample. The physical, mechanical, and chemical characterization tests are conducted on this fine material, hereafter referred to as Sieved Ash (SA).

Figure 24: Experimental Program

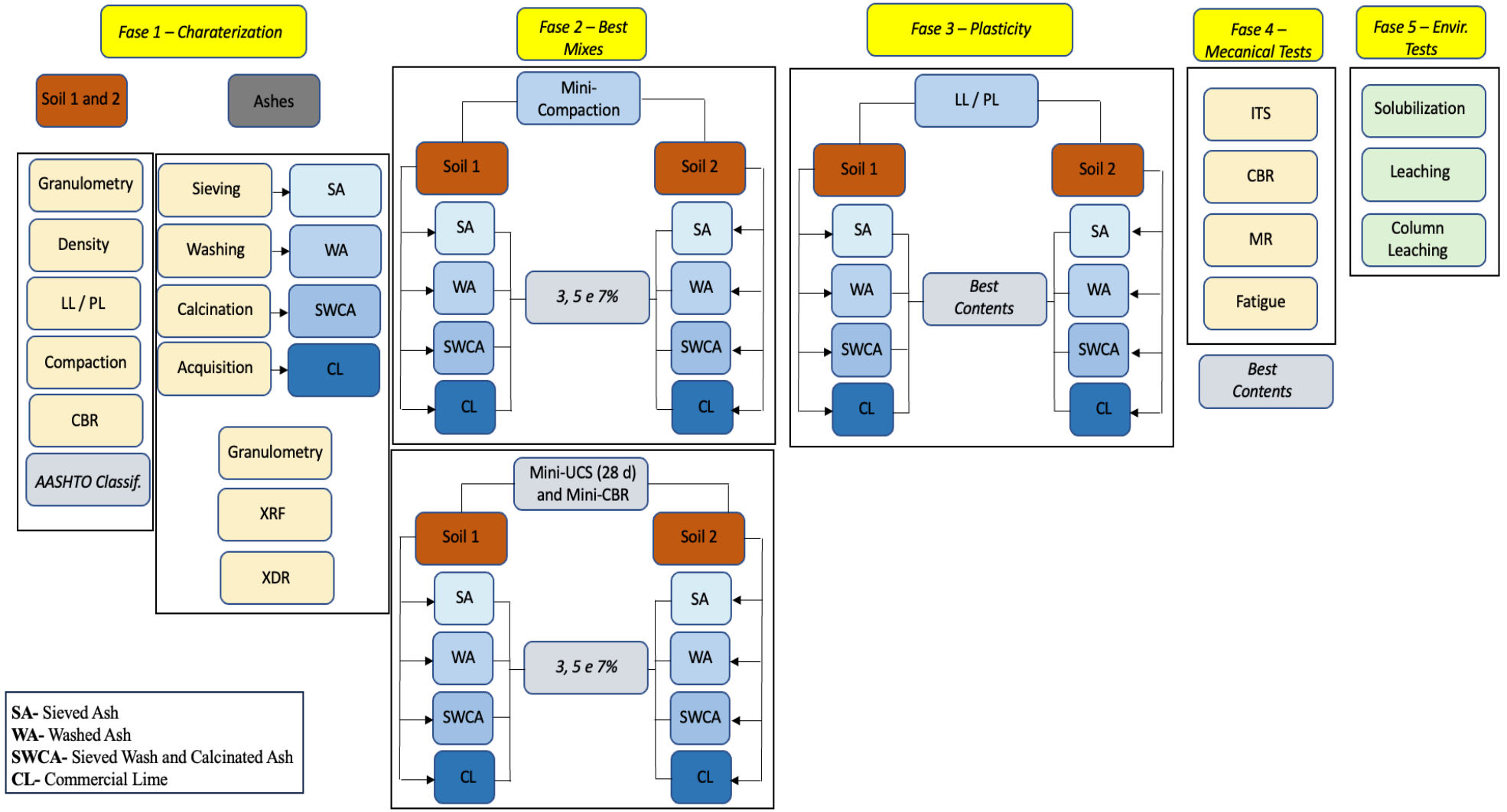

Source: Elaborated by the author

Figure 25: Separation of coal from ash.

a) Excess charcoal removed b) Sieved ash (SA)

Source: Elaborated by the author

The second stage, illustrated in Figure 26 and Figure 27, produces the sample referred to as Washed Ash (WA). After sieving, the material is washed twice in boiling water at 100 °C for 30 minutes, using a mass ratio of 1:8 (Ash:Water), following the methodology described by Melo *et al*. (2018). This washing step aims to reduce the concentrations of alkalis present in the ash, particularly sodium and potassium compounds, as reported by the author. After washing, the excess water is removed, and the ash is dried in an oven at 60 °C. Once dried, the material undergoes chemical, physical, and mechanical characterization tests.

Figure 26: Obtaining the WA sample (Washed Ash)

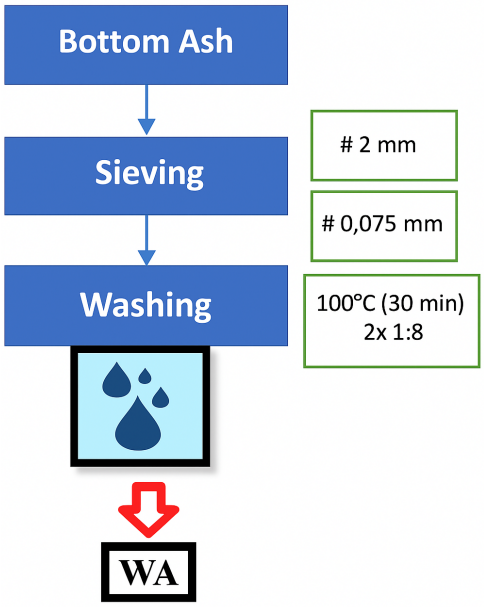

Source: Elaborated by the author

Figure 27: Stage 2 of processing - Washing the ash in boiling water.

a) Washing the ash in boiling water b) Removal of the washing water

Source: Elaborated by the author

The third processing stage, illustrated in Figure 28 and Figure 29, consists of calcining the sieved and washed sample at a temperature of 875 °C for 10 hours, with a heating rate of 10 °C per minute, in a laboratory oven, following the procedure described by Melo *et al.* (2018). After calcination, the ash sample is hydrated until the heat of hydration dissipates and the material becomes saturated. The water-saturated ash is then dried in an oven at 60 °C to remove excess water that is not chemically bound. From this point on, the material resulting from this processing stage is referred to as Sieved, Washed, Calcined, and Hydrated Ash (SWCA).

Figure 28: Obtaining the SWCA sample (Sieved, Washed and Calcined Ash)

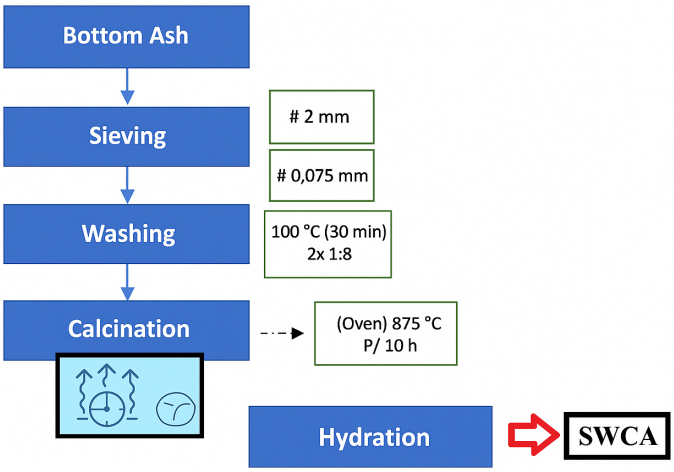

Source: Elaborated by the author

Figure 29: Calcination and hydration of ash.

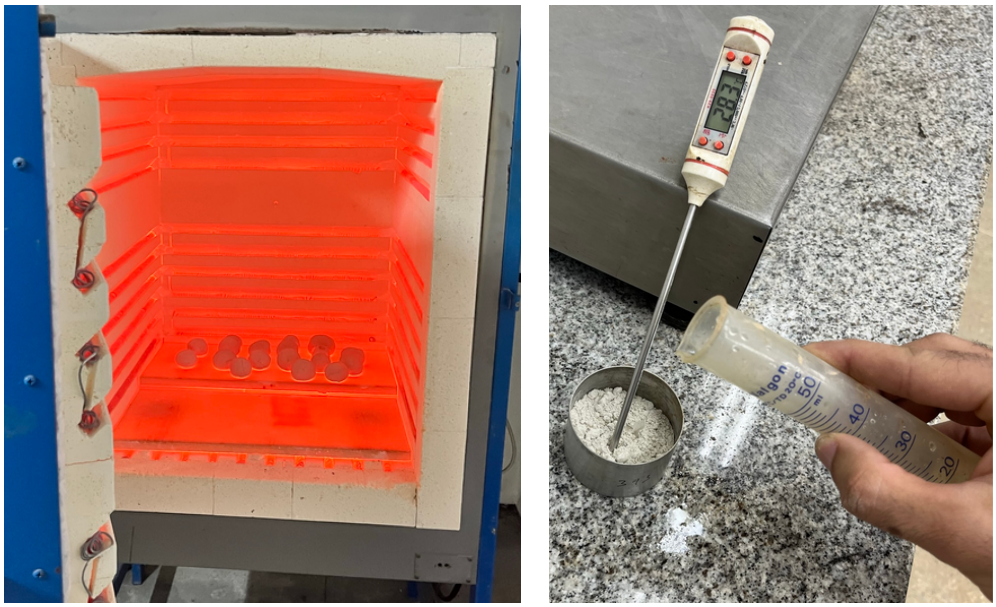

a) Calcination of the ash at 875 °C b) Hydration of the calcined ash

Source: Elaborated by the author

3.4.2 *Characterization of ash*

As previously mentioned, the ash is characterized from physical, chemical, and mineralogical perspectives. The physical characterization includes particle size distribution and determination of grains density. The chemical characterization consists of quantifying the oxide contents present in the ash throughout the processing stages, using X-ray fluorescence (XRF) analysis. The mineralogical composition is evaluated by identifying the main crystalline phases through X-ray diffractometry (XRD). Each procedure is detailed in the following subsections.

3.4.2.1 *Ash granulometry*

Particle size analyses are performed using dry laser diffraction on a Malvern Panalytical Mastersizer 2000, as shown in Figure 30. The method employed considers the specific light wavelength of the material as one of the main parameters for calculating the particle size distribution. Distinct methods are required for determining the particle size of ashes and soils, since ashes may exhibit reactivity with water, initiating pozzolanic reactions. For this reason, the particle size of reactive materials must not be determined by sedimentation in water.

Figure 30: Equipment for particle size analysis of ash.

Source: Malvern Panalytical

3.4.2.2 *Specific gravity of ash*

To establish relationships between mass and volume, it is essential to determine the specific gravity of a material. According to Freitas (2014), the density of a material allows for the identification of several properties, such as drainage capacity, porosity, and hydraulic conductivity. Furthermore, knowing the densities of the materials used in mixtures with granular soils is important, as this information enables the assessment of behavioral trends in compaction tests. The specific gravity test for finely pulverized materials is standardized by DNER-ME 085/94 (Finely Pulverized Material – Determination of Specific Gravity) and is conducted using a Le Chatelier flask, as illustrated in Figure 31.

Figure 31: Determination of the actual specific mass of the ash using Le Chatelier's flask.

Source: Elaborated by the author

3.4.2.3 X-*Ray Fluorescence de (XRF)*

The concentrations of the main oxides present in the soils and ashes are analyzed using the X-ray Fluorescence Spectroscopy (XRF) technique, a non-destructive method that enables the quantification and identification of the chemical elements in the sample. The equipment used for this analysis, shown in Figure 32, is the Epsilon1 model manufactured by Malvern Panalytical, and is part of the infrastructure of the LABCAM – Laboratory for Materials Characterization at the Federal University of *Cariri.*

Figure 32: X-ray Fluorescence Spectroscopy analysis equipment.

Source: Elaborated by the author

3.4.2.4 X-*Ray Diffratometry (XDR)*

X-ray diffractometry (XRD) tests are conducted to identify the crystalline phases present in the ash at its different processing stages. Unlike the XRF technique, which identifies and quantifies the elemental or oxide composition of the sample, XRD identifies the mineralogical composition, providing a more precise indication of the crystalline structures of the inorganic elements present, although without directly quantifying them. The equipment used for this analysis, shown in Figure 33, is the Empyrean model, manufactured by Malvern Panalytical, and is part of the infrastructure of the LABCAM – Laboratory for Materials Characterization at the Federal University of *Cariri*.

Figure 33: X-ray diffractometry analysis equipment.

Source: Elaborated by the author

3.4.3 Soil characterization

Conventional sieving and sedimentation grain size tests, consistency limits, and the determination of the actual specific gravity of the grains are performed to characterize the soils according to the standards of the Brazilian National Department of Transportation Infrastructure (DNIT).

3.4.3.1 *Specific gravity of soils*

Based on the specific gravity of the grains, it is possible to determine the settling velocity of soil particles in an aqueous medium using Stokes' law, which is essential for grain size determination by sedimentation. The actual soil density test is standardized by DNER-ME 093/94 (Soils – Determination of Specific Gravity) and is illustrated in Figure 34.

Figure 34: Determination of the actual specific mass of the soils.

Source: Elaborated by the author

3.4.3.2 Granulometry

Particle size analyses are performed on the soil samples, as shown in Figure 35. The granulometry of the soils is determined by sedimentation and sieving in accordance with the DNER-ME 051/94 standard.

Figure 35: Soil granulometry by sedimentation.

Source: Elaborated by the author

3.4.3.3 *Consistency limits*

The Liquid Limits (LL) and Plastic Limits (PL) of the soils and mixtures with added ash are determined at different processing stages, as shown in Figure 36. These tests serve as indicators of chemical changes in stabilized soils and are essential for classifying the materials according to the AASHTO system for granular materials suitable for pavement sublayers. The Liquid Limit (LL) test is performed in accordance with the DNER-ME 122/1994 standard, and the Plastic Limit (PL) test follows the DNER-ME 082/1994 standard.

3.4.4 *Mini Compac*tion

Miniature compaction integrates the MCT (Miniature, Compact, Tropical) methodology, proposed by Nogami and Vilibor (1994), for characterizing fine tropical soils. Given that the materials used in this study are predominantly fine-grained, compaction tests are conducted using the miniature equipment illustrated in Figure 39 a) following the sampling plan shown in Figure 36 b) with specimens measuring 50 mm in diameter and 50 mm in height.

Figure 36: Compaction of miniature specimens.

ı) Miniature compaction equipment

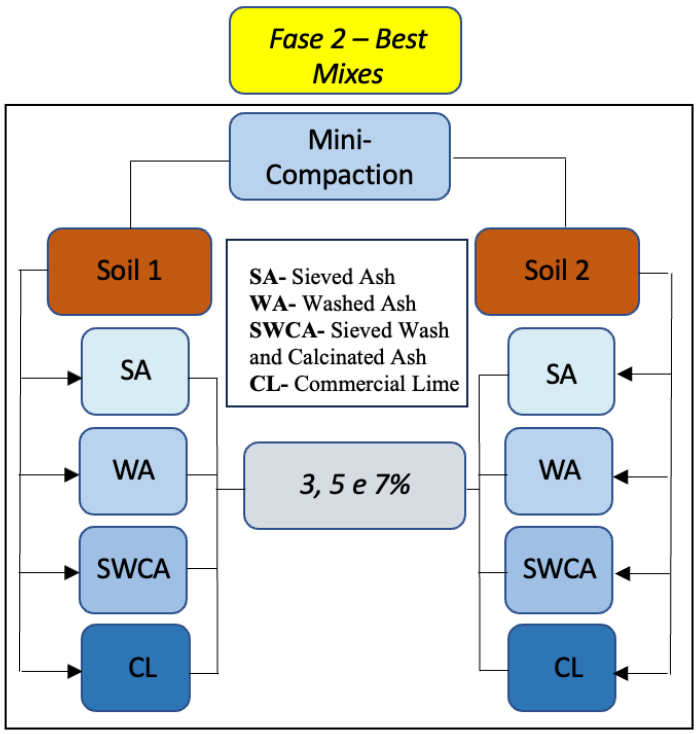

b) Mini-compaction sampling plan

Source: Elaborated by the author

Table 10 describes the 26 samples evaluated. Soils 1 and 2 are designated as S1 and S2, respectively, while the mixtures of these soils with each type of additive (SA, SWA, SWCA, and CL) are identified by the soil code followed by the additive abbreviation and the corresponding additive content. For example, the mixture of Soil 1 with 3% sieved ash (SA) is designated as S1SA3, as shown in Table 10.

Table 10: Number of miniature compaction tests

N	Miniature compaction test	[%] Additive	Code
1	Soil 1	-	S1
2	Soil 1 + Sieved Ash (SA)	(3)	S1SA3
3	Soil 1 + Sieved Ash (SA)	(5)	S1SA5
4	Soil 1 + Sieved Ash (SA)	(7)	S1SA7
5	Soil 1 + Sieved and Washed Ash (WA)	(3)	S1WA3
6	Soil 1 + Sieved and Washed Ash (WA)	(5)	S1WA5
7	Soil 1 + Sieved and Washed Ash (WA)	(7)	S1WA7
8	Soil 1 + Sieved, Washed, Calcined Ash (SWCA)	(3)	S1SWCA3
9	Soil 1 + Sieved, Washed, Calcined Ash (SWCA)	(5)	S1SWCA5
10	Soil 1 + Sieved, Washed, Calcined Ash (SWCA)	(7)	S1SWCA7
11	Soil 1 + Comercial Lime (CL)	(3)	S1CL3
12	Soil 1 + Comercial Lime (CL)	(5)	S1CL5
13	Soil 1 + Comercial Lime (CL)	(7)	S1CL7

14	Soil 2	-	S2
15	Soil 2 + Sieved Ash (SA)	(3)	S2SA3
16	Soil 2 + Sieved Ash (SA)	(5)	S2SA5
17	Soil 2 + Sieved Ash (SA)	(7)	S2SA7
18	Soil 2 + Sieved and Washed Ash (WA)	(3)	S2WA3
19	Soil 2 + Sieved and Washed Ash (WA)	(5)	S2WA5
20	Soil 2 + Sieved and Washed Ash (WA)	(7)	S2WA7
21	Soil 2 + Sieved, Washed, Calcined Ash (SWCA)	(3)	S2SWCA3
22	Soil 2 + Sieved, Washed, Calcined Ash (SWCA)	(5)	S2SWCA5
23	Soil 2 + Sieved, Washed, Calcined Ash (SWCA)	(7)	S2SWCA7
24	Soil 2 + Comercial Lime (CL)	(3)	S2CL3
25	Soil 2 + Comercial Lime (CL)	(5)	S2CL5
26	Soil 2 + Comercial Lime (CL)	(7)	S2CL7

Source: Elaborated by the author

3.4.5 *Selecting the best contents for each mixture*

To select the optimal contents for each mixture, specimens are molded for Unconfined Compression Strength (UCS) tests after 28 days of curing, as well as for Mini-CBR tests in both dry and saturated conditions to evaluate strength loss due to saturation.

The best content for a mixture is defined as the one that does not disintegrate during the submergence stage prior to testing and exhibits the highest UCS value after 28 days of curing. If all evaluated contents of a mixture disintegrate, the best content is determined based on the highest bearing capacity values in the dry condition (optimum moisture), the lowest bearing capacity loss after saturation, and expansion and contraction percentages within acceptable limits.

3.4.5.1 *Mini-UCS*

The same compaction apparatus is used to obtain specimens for UCS tests, however, instead of a 50 mm × 50 mm specimen, the molding process involved filling in three stages, with scarification performed between each layer totaling a 50 mm × 100 mm specimen. For each mixture and content, five specimens are molded following the optimum parameters for each material, totaling 130 specimens. Subsequently, the suitability of these samples was evaluated according to the acceptance criteria outlined in Table 11, aiming to validate the effectiveness of the obtained results.

Table 11: Number of miniature compaction tests

PARAMETERS	CRITERIA
Moisture content [%]	Value ± 2%
Degree of compaction	100% ± 3%
Dimensions [mm]	Diameter 50 ± 0.5; and high 100 ± 1

Source: Santos (2024)

The DNER-ME 180/94 standard—Soils stabilized with fly ash and hydrated lime—specifies that specimens must measure 100 mm in diameter by 200 mm in height and be tested after 24 hours of immersion in potable water. Conversely, the NBR 12770 standard (ABNT, 2022) specifies specimens of 50 mm in diameter by 100 mm in height, with no immersion stage mentioned.

Since chemically reactive mixtures must remain stable under saturation, the procedures of the DNER-ME 180/94 standard are followed using smaller specimens aiming at reducing the material consumption. Specimens are wrapped in plastic film and cured for 28 days. After curing, they are submerged in fresh water for 24 hours, as shown in Figure 37 (a). Specimens that do not disintegrate are then subjected to the UCS test, shown in Figure 37 (b), at a Matest triaxial press, model S301M, with 10 kN capacity with a loading rate of 1.0 mm/min.

Figure 37: UCS test with miniature specimens

a) Submerged for 24 hours b) Testing

Source: Elaborated by the author

Based on the UCS values at 28 days of curing, the contents with the highest UCS values are selected as the best for each processing stage (additive), and these are then

subjected to further evaluations of plasticity, expansion, and mechanical behavior. Specimens that disintegrate after submersion receive a zero-strength value in the UCS tests, being considered chemically unstabilized materials.

3.4.5.2 Mini-CBR

The bearing capacity of both cemented and uncemented materials was assessed using Mini-CBR tests**.** For each mixture, ten specimens (50 mm in diameter x 50 mm in height) were molded, totaling 260 specimens**.** The molding of all specimens followed the specific optimum parameters for each material. The procedure is carried out in accordance with the DNIT 254/2023-ME standard. Figure 38 (a) shows the specimens molding, Figure 38 (b) submersion and expansion measurements, Figure 38 (c) shows the specimens undergoing testing in the mini-CBR press.

Figure 38: Mini-CBR test

a) Molding b) Submersion/Expasion c) Testing

Source: Elaborated by the author

In addition to determining the mini-CBR, the Bearing Index Ratio (BIR) is measured during the test. This ratio indicates the loss of bearing capacity due to saturation by comparing the bearing capacity at optimum moisture with that after total saturation of the sample. As disintegration is observed in some mixtures, determining the BIR becomes important to indicate that some mixtures may perform adequately under non-saturated conditions. However, once saturated, these mixtures exhibit drastic reductions in mechanical capacity, indicating an inability to resist applied stresses. In addition, through these bearing capacity tests, the expansive behavior of paving materials is verified, which serves as an important indicator of stabilization reactions.

Once the best contents are determined for the chemically stable mixtures, consistency tests and other mechanical tests described in the following section are carried out. For the most promising mixtures that disintegrate, all proposed tests are performed except for UCS and ITS on specimens with conventional dimensions, since these materials do not withstand the saturation stage.

3.4.6 *Consistency limits of mixtures*

To assess the influence of ash and commercial lime on the consistency of the soils, Liquid Limit (LL) and Plasticity Limit (PL) tests are performed on the most promising mixtures after reacting periods of 0, 28, and 90 days. According to Araújo (2009), these analyses are related to the physicochemical interactions between the additives and the soils.

Picchi *et al*. (1988) associate the three main chemical reactions between lime and soil with their respective reaction times. Flocculation reactions are considered instantaneous and, therefore, are related in this study to changes in plasticity between the soil without additives and the soil with additives at 0 days of curing.

Since the authors report that pozzolanic reactions reach a certain equilibrium around 28 days, additional consistency determinations are carried out after this period. Finally, carbonation reactions are described as developing over the long term, particularly after 90 days. Within this context, the study evaluates whether the main chemical reactions between soils and lime influence the consistency of these materials.

3.4.7 *Mechanical tests*

Once the most promising mixtures and those that exhibit desintegration are identified, the mechanical tests listed in Figure 39 are performed.

Figure 39: Mechanical tests

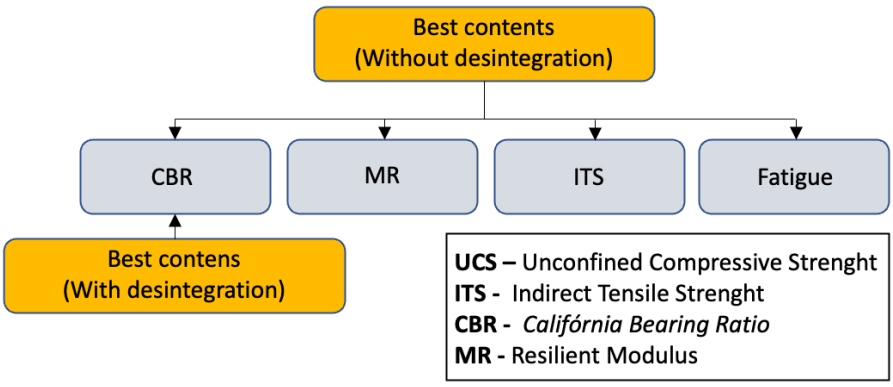

Source: Elaborated by the author

CBR, Resilient Modulus (MR), Indirect Tensile Strength (ITS), and Fatigue tests are conducted to evaluate the mechanical behavior of mixtures that do not exhibit disintegration. Although the CBR test is not the most appropriate for assessing chemically stabilized mixtures, its application is maintained to enable comparisons between mixtures, considering empirical pavement design methods. In contrast, the MR, ITS, and Fatigue tests are applied only to mixtures that show evidence of chemical stabilization.

3.4.7.2 Indirect *Tensile Strength (ITS)*

The determination of Indirect Tensile Strength (ITS), as illustrated in Figure 40 is carried out in accordance with the DNER-ME 181/94 test method, with samples produced in triplicate, and the ITS value corresponds to the arithmetic mean of the determinations. The specimens are wrapped in plastic film and kept in a temperature-controlled environment during curing periods of 0, 28, and 90 days, with testing preceded by immersion for 24 hours, following a procedure similar to that used for the UCS test.

Figure 40: Diametral compression rupture

Source: Elaborated by the author.

3.4.7.4 *California Bearing Ratio (CBR)*

The California Bearing Ratio (CBR), shown in Figure 41, is a geotechnical test used to determine the bearing capacity of granular materials for use in pavement layers, based on an empirical method for designing these structures.

Figure 41: California Bearing Ratio

a) Testing aparatus b) imersion

Source: Elaborated by the author

This methodology is normally used for non-chemically stabilized materials. However, for comparison purposes, CBR tests are carried out on both non-stabilized samples and those considered stabilized. The test follows the DNER-ME 049/1994 standard.

3.4.7.5 *Resilient Modulus (MR)*

The Resilient Modulus (MR) test is carried out according to two similar methodologies. The first, recommended by the DNIT 134/2018-ME standard, specifies the procedures for determining the MR of unstabilized granular materials, and is therefore used in this work to evaluate soils without ash addition and mixtures that do not show resistance to disintegration in the pre-UCS saturation stage. The second methodology is recommended by the DNIT 181/2018-ME standard and specifies procedures for chemically stabilized mixtures. This normative approach is used to assess the MR of soil mixtures with ash at different processing stages that resist disintegration and thus show non-zero UCS values.

Dynamic triaxial tests are performed using the MS 151 – Dynamic Triaxial apparatus from Owntest based on Soil Mechanics Lab from Federal Institute of Science and Technology of Ceara (IFCE), which consists of an electromechanical press with a servomotor, a triaxial cell compatible with specimens of Ø100 × 200 mm and a pneumatic pressure control system. This system enables the application of controlled cyclic loads for Resilient Modulus (MR) and Permanent Deformation tests, with loading frequencies of up to 5 Hz, and monitoring of test variables such as force, displacement, and pressure. In this study, a loading frequency of 1 Hz is adopted. The specimens are molded at intermediate compaction energy using a tripartite mold. The procedures for specimen compaction, coating, and MR testing are illustrated in Figure 42.

Figure 42: Preparation and Resilient Modulus (MR) test

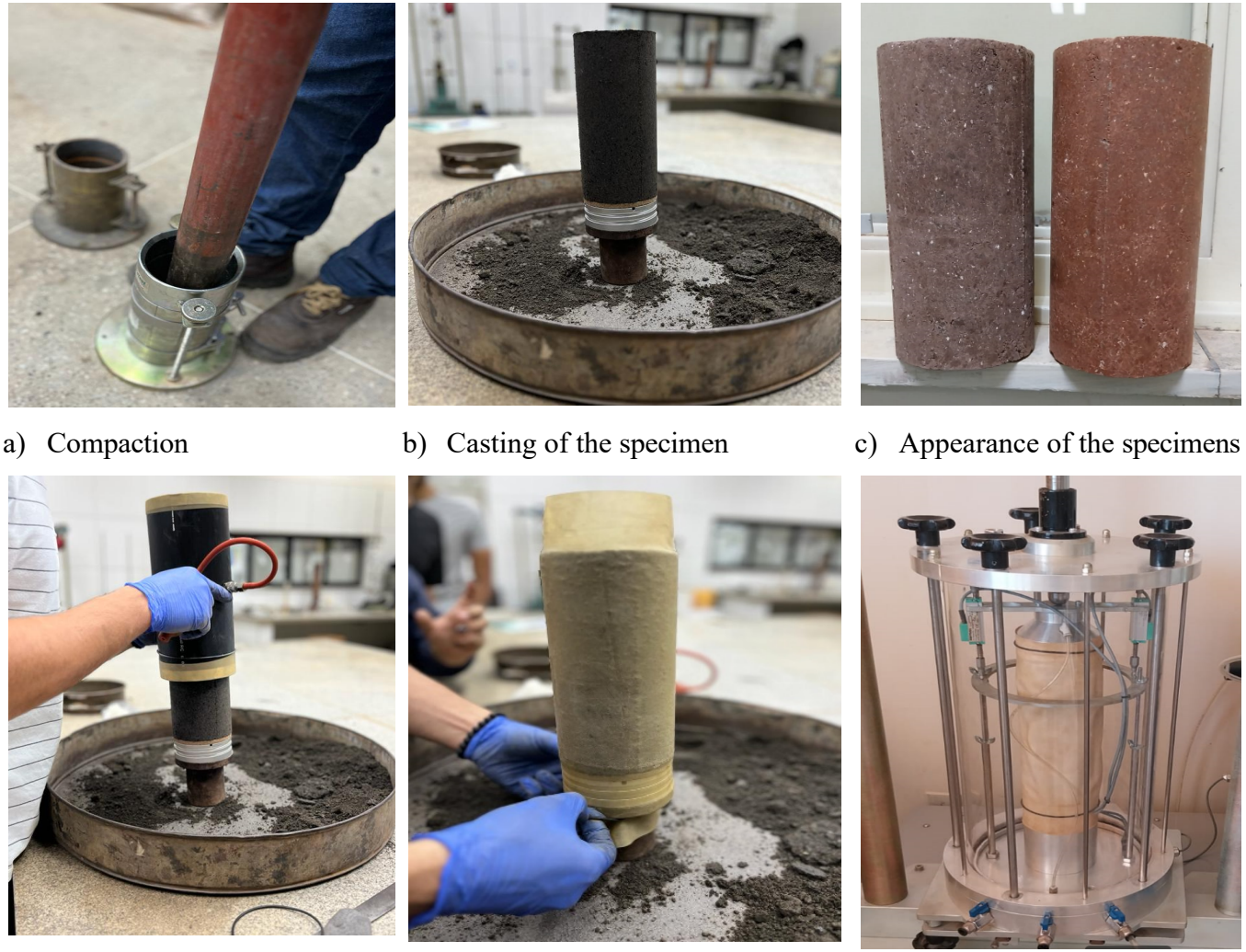

a) Compaction b) Casting of the specimen c) Appearance of the specimens

d) Placing the mebrane e) Adjustments f) Testing

Source: Elaborated by the author

The dynamic triaxial test, shown in Figure 42, is divided into two phases: the conditioning phase and the actual test. The specimen conditioning phase aims to reduce the influence of plastic deformations and minimize the effects of the specimen's stress history, while during the actual test, deformations are recorded.

At the end of the test, a modulus value is determined for each stress level. The results of the repeated load triaxial test consist of correlations between the Resilient Modulus and the applied stresses using mathematical models.

When a sandy, and therefore cohesionless, soil is subjected to increasing lateral confining stresses, the material tends to become less deformable, demonstrating a greater dependence on these confining stresses. This behavior is directly associated with the absence of cohesion between the granular particles. In contrast, clayey soils tend to be less susceptible to confining stresses because they exhibit cohesion and depend more significantly on deviatoric stresses.

This inherent behavior of each material leads to the formulation of distinct mathematical models to represent the Resilient Modulus (MR), which can be expressed as a function of confining stresses, deviatoric stresses, or both. Consequently, sandy soils are typically described by the model in Equation (1), clayey soils by the model in Equation (2), and the composite model is employed to represent the behavior of any material according to equation (3). Additionally, other mathematical models for describing the resilient modulus (MR) are also evaluated. In certain situations, as mentioned by Seed, Monismith and Chan (1967) and Uzan (1985), these models may be more suitable for representing the resilient behavior of stabilized materials, as they consider the stress invariant (θ), Octahedral tension (ƭ.oct) and atmospheric pressure ($P_{.atm}$) which is the total confining stress, the tension where the failures used to happen and the atmospheric components respectively and as described by Equations (4) and (5).

$$MR = k_1 \times \sigma_3^{k_2} \quad (1)$$

$$MR = k_1 \times \sigma_d^{k_2} \quad (2)$$

$$MR = k_1 \times \sigma_3^{k_2} \times \sigma_d^{k_3} \quad (3)$$

$$MR = k_1 \times \theta^{k_2} \quad (4)$$

$$MR = k1 \times (\theta/P_{atm})^{k2} \times (\tau_{oct}/P_{atm})^{k^3} \quad (5)$$

Although DNIT Standard 181/2018-ME, which describes the testing protocol for resilient modulus (MR) in stabilized mixtures, recommends that displacement measurements be taken at the mid-height of the specimens, due to technical limitations all measurements are performed at the top of the specimens. After carrying out the test protocol, the mathematical model that best represents the behavior of the tested material is chosen, based on the highest correlation coefficient (R^2) between the deflection and confining stresses as a function of the Resilient Modulus (MR).

3.4.7.6 *Fatigue tests*

The fatigue test for chemically stabilized layers is described in Brazil by standard DNIT 434/2022-ME and defines fatigue as a reduction in the resistance of a material under repeated loading, with a magnitude lower than its resistance under static loading. This test is fundamental for understanding the behavior of cemented materials under cyclic loading stresses, and from this procedure it is possible to predict the useful life of a chemically stabilized layer.

For granular layers without stabilization, assessing fatigue behavior is unnecessary since fatigue is directly linked to the progressive degradation of the material through crack propagation, an inherent characteristic of cohesive materials with brittle behavior, such as chemically stabilized mixtures. This consideration is important because, in this study, fatigue behavior is not evaluated for materials that do not exhibit signs of cementing reactions. For the most promising mixtures that demonstrate strength gain characteristics, this property can be investigated, and the feasibility of these evaluations is discussed in this work.

To determine the fatigue parameters of the mixtures, Indirect Tensile Strength (ITS) tests were carried out. Based on the ITS results, cylindrical specimens were subjected to cyclic loading at a frequency of 1 Hz until failure, in accordance with the DNIT 434/2022-ME standard. The applied stress levels were 85%, 75%, 65%, and 55% of the ITS value. The general expected behavior is that higher stress levels, closer to the static strength (ITS), result in a lower number of loading cycles until failure, while lower stress levels lead to a higher number of cycles to failure.

Based on the relationship between the ratio of cyclic tensile stress to the indirect tensile strength (ITS) and the number of cycles to failure, the material's fatigue curve can be expressed as described by Equation (6), In this equation, N is the number of cycles to failure, RF is the ratio of the applied tensile stress in the test (in MPa) to the ITS value, and k_1 and k_2 are coefficients to be determined through regression analysis.

$$N = 10^{(k1-k2\times\%RF)} \qquad (6)$$

3.4.8 *Environmental Analysis*

The assessments of the potential environmental impact of leaching should be carried out on the materials evaluated in this work. The procedures proposed for this can be those adopted in national standards, such as NBR 10.005 and NBR 10.006. However, it is proposed to evaluate the environmental behavior of the materials under specific conditions practiced in the paving sector, considering compaction and encapsulation by chemical stabilization of the granular layers.

Environmental tests are fundamentally important to verify the environmental viability of using ash as a soil stabilizer for granular paving layers. Since these materials may contain chemical elements that potentially contaminate the soil and groundwater, this study proposes to evaluate the environmental viability of mixtures using ashes with better mechanical performance. The proposed environmental tests include solubilization, leaching, and column leaching, as illustrated in Figure 43.

Figure 43: Tests for environmental analysis

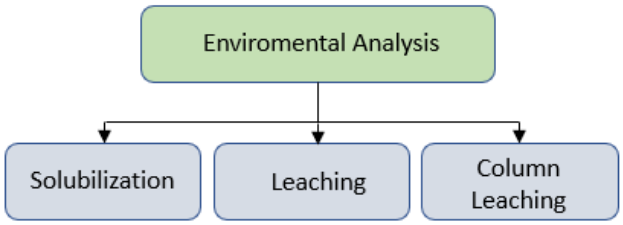

Source: Elaborated by the author

3.4.8.1 *Solubilization test*

The solubilization test evaluates the potential of the waste to release its constituent components into pure water, compared to the drinking water standard, according to the procedure established by NBR 10006/2004. The test consists of adding 250 g of each sample to a 1000 mL volumetric flask containing distilled water, followed by stirring for 5 minutes.

Due to limitations the quantity of material used in the test was reduced, while maintaining the concentration required by the standard. Instead of 250 g of ash in 1 L of water, 25 g were used in 100 mL as illustrated in Figure 44 (a). The flask is then covered with PVC film and left to rest for 7 days at a temperature of 25 °C. After this period, each sample is filtered, as illustrated in Figure 44 (b) to obtain the solubilized extract. The extracts

are analyzed using an Atomic Absorption Spectrophotometer, model SpectrAA 50B from Varian, as illustrated in Figure 45, which perform metal analysis in liquid samples through the absorption of radiation in a flame. The concentrations of metals and other hazardous compounds such as Cadmium (Cd), Lead (Pb), Chromium (Cr) and Silver (Ag).

Figure 44: Solubilization test

a) Solubilization samples

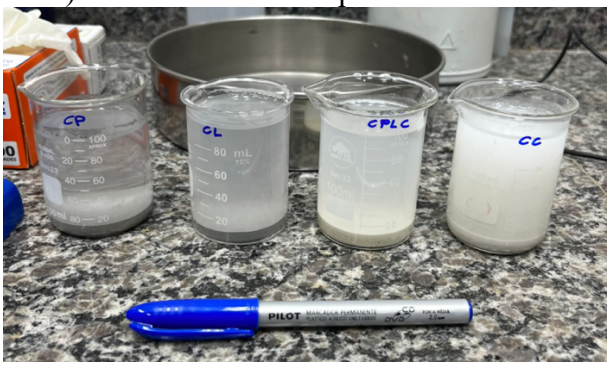

b) Samples Filtration

Source: Elaborated by the author

Figure 45 : Atomic Absorption Spectrophotometer

Source: Elaborated by the author

3.4.8.2 *Leaching*

The leaching test assesses the potential of the waste to release part of its components into the environment, evaluating its possible impact on soil and groundwater, and can be performed on samples in a loose state. The procedure follows the standard NBR 10005/2004.

The test consists of adding 2000 mL of a solution of acetic acid, as illustrated in Figure 46 (a) and water (5.7 mL of acetic acid per 1000 mL of solution) to 100 g of each analyzed sample as illustrated in Figure 46 (b). Due to limitations the quantity of material

used in the test was reduced, while maintaining the concentration required by the standard. Instead of 100 g of ash in 2 L of water, 50 g were used in 1 L. The solution and sample are transferred to the leaching flask and placed under agitation for 18 ± 2 hours at 25 °C on a rotary stirrer. After this stage, each sample is filtered to obtain the leached extract as illustrated in Figure 46 c).

Figure 46: Leaching test

a) Preparation of acid solution **b)** Sample after stirring

c) Samples Filtration

Source: Elaborated by the author

The extracts from all samples are analyzed using titrimetric methods for elements such as chloride (Cl^-) and sulfate (SO_4^{2-}). This method consists of adding a titrant solution of known concentration to the sample until the reaction reaches completion, which is indicated by a color change produced by specific indicators. For chloride determination, phenolphthalein (magenta color) is initially added, as illustrated in Figure 47 (a). Then, a 0.01N sulfuric acid solution is titrated to adjust the pH of the sample to between 7 and 10, causing the solution to return to a transparent state. After pH adjustment, potassium chromate

is added as an indicator, as shown by the characteristic yellow coloration in Figure 47 (b). Silver nitrate is then added as the titrant, forming a brick-red precipitate at the end point, as illustrated in Figure 47 (c). Knowing the concentration and volume of the titrant, the chloride concentration is calculated. A similar procedure is employed to determine sulfate concentrations, using a barium salt instead of silver nitrate.

Figure 47: Titration for chloride determination

a) Phenolphthalein as pH indicator b) Potassium Chromate addition

c) Brick-red color precipitate

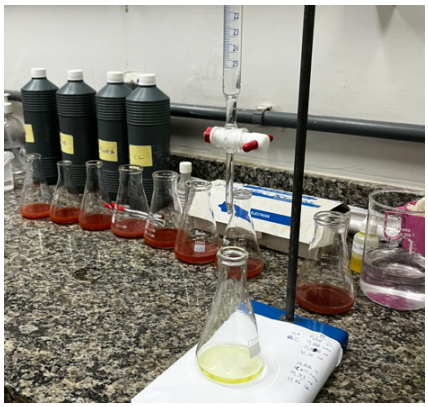

Source: Elaborated by the author

For the other elements such Cadmium (Cd), Lead (Pb), Copper (Cu), Chromium (Cr), Iron (Fe), Manganese (Mn), Silver (Ag) and Zinc (Zn), the Atomic Absorption Spectrophotometer method was used as illustrated previously in Figure 45.

3.4.8.3 *Column leaching*

The column leaching test is not standardized in Brazil, with procedures described in ASTM D 4874-95. Similar to the leaching test, it aims to assess the potential contaminants released by the sample that could impact soils and groundwater. However, the sample is

evaluated in a compacted state, which more closely simulates real percolation and leaching conditions in the field. In compacted samples, permeability is reduced, thus leaching processes are slower, promoting an encapsulation effect of the contaminants within the compacted solid mass.

The test apparatus consists of two connected cylinders: the first contains distilled water under pressure, and the second holds the compacted soil sample, which is percolated by upward flow through the liquid to be collected. This percolated liquid is collected and analyzed using an Atomic Absorption Spectrophotometer to determine the concentrations of metals and other hazardous substances, similarly to the previously mentioned tests. Illustrations of the test apparatus are not shown as the equipment used is under patent.

3.5. *Hypothetical design and economic assessment*

The CMR belt road Illustrated in Figure 69 is a strategic expressway designed to connect the region's main state highways (CE-060, CE-292, CE-487, and CE-516) and to divert heavy traffic away from the central urban areas of *Juazeiro do Norte*, *Crato*, and *Barbalha*. The completion of its sixth and still pending stage is essential to achieving the project's main goal: improving freight traffic flow and redirecting heavy vehicles away from urban centers, thereby enhancing safety in pedestrian-intensive areas.

Figure 48 : Belt Road around Juazeiro do Norte city

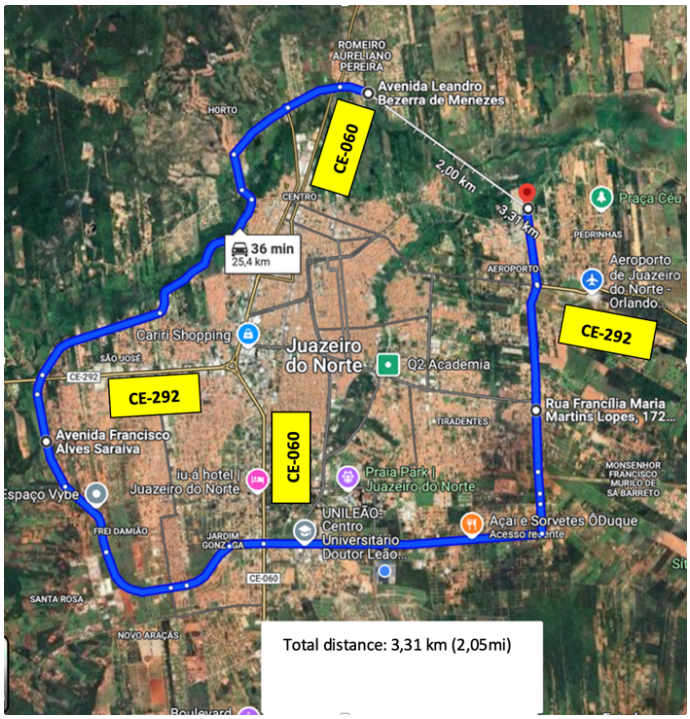

Source: Elaborated by the author

The segment corresponding to the sixth stage covers approximately 3.5 km required to complete the belt road perimeter, as illustrated in Figure 49. The implementation of this section faces technical constraints related to the geotechnical characteristics of the terrain, as it is located in a lowland area along the banks of the *Salgadinho* River. Studies conducted by Mascarenhas (2016) and Xavier (2018) highlight the significant soil diversity within the Cariri region, with both authors reporting the presence of reddish-orange sandy-silty soils. In the absence of a comprehensive geotechnical investigation, for the purpose of a hypothetical analysis, it is assumed that the subgrade of the section corresponding to the alignment along the ring road can be represented by a silty soil, as indicated by the aforementioned authors. Figure 49 (a) and (b) depict the interrupted pavement segment.

Figure 49: Unfinished road segment.

a) Interruption point of the section	b) Satellite view
	

Source: Elaborated by the author

To propose the pavement sections, some initial design assumptions were established regarding the road type, design period, and traffic data. As for the road type, it is classified as a primary arterial system, as it is a highway serving regional interconnection functions, characterized by medium traffic volumes, including heavy vehicles, and by facilitating the flow of goods between urban centers and rural areas. These roads play a key role in regional mobility and economic development.

The adopted design period was 10 years, as this time frame aligns with the average service life of flexible pavement layers without requiring major structural interventions. Furthermore, this period is frequently recommended and adopted in Brazil for flexible pavement layers according to Mello *et al*. (2016), for balancing economic factors, traffic forecasting, and long-term maintenance feasibility.

Traffic data were obtained from state agencies employees, and the traffic survey associated with this project dates back to 2013. These data are considered outdated, and the information received is of an average of 1,014 vehicles per day.

In the absence of updated data, a hypothetical annual growth rate of 1.5% was applied to the initial traffic volume of 1,014 vehicles per day in order to adjust outdated traffic data to present conditions. It is hypothetically estimated that, following the highway's inauguration, this annual traffic growth rate will double to 3%, which corresponds approximately to the rate of increase in the vehicle fleet reported by the Ceará State Institute for Economic Research (IPECE, 2024). Additionally, a representative vehicle distribution for the state of Ceará, based on traffic surveys from nearby highways, was proposed using the corrected hypothetical traffic. Table 12 presents the hypothetical traffic composition for the segment.

Table 12: Estimated traffic composition

Motorcycles/ Autos	888
Bus	133
Light truck	61
Heavy truck	39
Total	1200

Source: Elaborated by the author

Given these assumptions, Table 13 considers a volume of 1,200 vehicles per day, growing at an annual rate of 3%. This results in an annual number of equivalent single axle loads (N) of a $4{,}38\times10^5$ in the first year and a cumulative N of $5{,}02\times10^6$ by the end of the 10-year design period. In other words, the scenario assumes a gradual traffic increase of 3% per year, leading the pavement to experience a cumulative traffic level classified as medium to medium-heavy, according to Balbo (2007). At the end of this period, the pavement structure can be reassessed and potentially upgraded to meet future traffic demands.

Table 13: Design assumptions

Road Type	Primary Arterial System
AADT (1st Year)	1200
CV:	1.00
Anual ESALs (1st Year)	$4{,}38\times10^5$
% of vehicles in the design lane	100
Growth rate [%]	3.0
Design period [years]	10
Total ESALs	$5{,}02\times10^6$

Source: Elaborated by the author

Based on this hypothetical scenario, several pavement design sections were proposed for the studied segment. While some sections consider the use of chemically stabilized clayey soils with lime and calcined ashes, others consider borrow materials which are techniques conventionally used regionally as solutions in paving projects. The objective of proposing these alternatives is to compare the cost of each solution and assess the technical and cost feasibility of the materials investigated in this study.

Due to the limited availability of data on local mixtures and soils that combined permanent deformation properties and modulus of elasticity, some materials with the most similar characteristics were selected from the Medina software database, developed by the National Department of Transport Infrastructure (DNIT). The properties of the materials used are detailed in Table 14 to 17.

Table 14: Asphalt surfacing data

REF MIX (Barbosa *et al.,* 2025)	
Poisson's ratio	0.30
Resilient Modulus	5277 MPa
Density	2,463 g/cm^3
Asphalt Binder content	4,4 %
Permanent Deformation	
Modelo	k1. (et^{k2})
Regression Coefficient (k1)	1,0. 10-^{11}
Regression Coefficient (k2)	-3,381
Fatigue class	0
FFM (100μ a 250μ)	0,69

Source: Elaborated by the author

Table 15 : Chemically stabilized Base soils data

		S1CL 7	**S1SWCA 7**	**Clayey soil+ 7,5 % Lime type CH I (Medeiros, 2017)**
Poisson's ratio		0.25	0.25	0.25
Resilient Modulus			Nonlinear	
	k1	5530,3	5302,2	420,51
	k2	0,463	0,385	-0,091
	k3	0,123	0,140	-0,250
	k4	0,00	0,00	0,00
MCT group		-	-	LG'
MCT – Cohesion coefficient (c')		-	-	1,85
MCT – Effective friction angle (e')		-	-	1,08
Density [g/cm^3]		1,87	1,88	1,43
Optimum Moisture [%]		12	12,5	28,0
Compactiom Energy			Intermediate	
Standard or Specification			DNIT ES 420 / 421 /422	

Source: Elaborated by the author

Table 16: Granular base material data

		Soil-Crushed stone	**Graded aggregate base (GAB)**
Poisson's ratio		0.35	0.35
Resilient Modulus		Nonlinear	1149
	k1	501,80	0,4530
	k2	0,450	-0,180
	k3	-0,460	0,00
	k4	0,00	1149
Density		2,38 g/cm^3	2,22 g/cm^3
Optimum Moisture [%]		7,5	5
Compactiom Energy		Intermediate	Modified
Standard or Specification		DNIT ES 137	DNIT ES 139
Permanent deformation			
Model		$Ep = \Psi 1(\sigma 3^{\Psi 2})(\sigma d^{\Psi 3})(N^{\Psi 4})$	
Regression Coefficient (k1 ou Ψ 1)		0,27	0,0868
Regression Coefficient (k2 ou Ψ 2)		-0,14	-0,2801
Regression Coefficient (k3 ou Ψ 3)		1,33	0,8929
Regression Coefficient (k4 ou Ψ 4)		0,06	0,0961

Source: Elaborated by the author

Table 17: Subgrade soil data

		Silty soil NS'
Poisson's ratio		0.45
Resilient Modulus		Nonlinear
	k1	306,5
	k2	0,520
	k3	-0,309
	k4	0,00
MCT group		NS'
MCT – Cohesion coefficient (c')		1,00
MCT – Effective friction angle (e')		1,68
Density		1,8 g/cm^3
Optimum Moisture [%]		13,0
Compactiom Energy		Intermediate
Standard or Specification		DNIT ES 137
Permanent Deformation		
Model		$Ep = \Psi_1(\sigma 3^{\Psi 2})(\sigma d^{\Psi 3})(N^{\Psi 4})$
Regression Coefficient (k1 ou Ψ 1)		0,244
Regression Coefficient (k2 ou Ψ 2)		0,419
Regression Coefficient(k3 ou Ψ 3)		1,309
Regression Coefficient (k4 ou Ψ 4)		0,069

Source: Elaborated by the author

3.6. *Final considerations*

It is considered that, based on the descriptions presented in this section, the study area where the materials were collected has been adequately characterized, as well as the properties of the evaluated materials and their potential applications. The region of origin of the materials holds strategic economic and social importance for its surroundings. Although this work focuses on specific local materials, the solutions proposed, and the results obtained may be appliable to similar materials from other regions worldwide. The demand for alternatives in the use of industrial waste is a global concern, and the technical, economic, and environmental contributions towards the development of more sustainable infrastructure are within the scope of this study. The results of this work are presented in the following section.

4. RESULTS

This chapter is structured into five sections. Section 4.1 describes the processing yield and characterization of the additives used, namely the ashes and commercial lime. Section 4.2 covers the characterization of the soil, as well as the determination of compaction parameters for both the natural soil and the mixtures. Section 4.3 presents the best-performing mixtures, identified based on the different additive contents evaluated. Section 4.4 is dedicated to the analysis of consistency, volumetric changes, and the mechanical behavior of the previously selected mixtures. Section 4.5 addresses the environmental characterization of the analyzed ashes. Finally, Section 6.6 addresses the design of hypothetical sections with some of the mixtures evaluated in this study, presenting a comparative cost analysis among these sections.

4.1 Ash processing results

Preliminary sieving was performed using a 2 mm mesh to remove excess charcoal from the bottom ash. Since charcoal is an organic material subject to degradation, it was excluded from the sample, resulting in an 11.9% mass loss. After the removal of charcoal, laser granulometry was conducted on the remaining material, and the results are presented in Figure 50. The horizontal axis represents the average particle diameter, the vertical axis the cumulative volume percentage passing, while the histogram represents the accumulation of particles within each diameter range, while the red curve indicates the cumulative volume distribution.

Figure 50: Laser particle size distribution of bottom ash without coal.

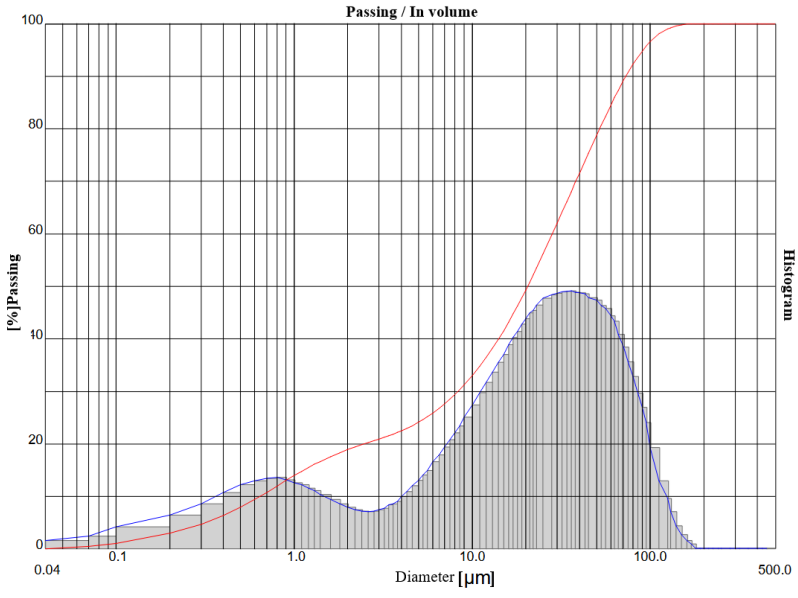

Source: Elaborated by the author

After the removal of residual charcoal, the base ash was found to contain approximately 25% of particles smaller than 0.005 mm (clay size) and 92% smaller than 0.075 mm, characterizing it as a silty material. The following ash processing stages consisted of sieving, washing and calcination (followed by hydration). At each stage, the losses inherent to the process were measured and representative samples of each material were taken, namely Sieved Ash (SA), Sieved and Washed Ash (WA) and Sieved, Washed, Calcined and Hydrated Ash (SWCA).

4.1.1 *Ash processing yield*

Next, following the procedure reported in Melo (2018), the ashes that passed through the 2 mm mesh (Bottom ash without coal) were subjected to the roughening stage and sieved again through the 0.075 mm mesh to make the material reach a granulometry similar to that of hydrated lime. The material retained on the 0.075 mm sieve amounted to 7.0 % by mass of the sample. Therefore, the sieving process and the constitution of the sieved ash sample (SA) showed losses of 11.9% and 7.0%, which together add up to a loss of 18.9% in relation to the initial mass.

After the sieving stage, the sample called Sieved Ash (SA) was washed in heated water as described in section 3.4.1. The washing stage consists of removing the heated water after sedimentation of the material. When the liquid phase is poured off, a certain amount of ash and a certain mass of soluble compounds are lost, in the order of 12.2% at this stage, and considering the initial mass, the accumulated losses are 31.1%.

During calcination, there was a loss of mass of around 34% in the WA sample, which after calcination was renamed SWCA. In relation to the mass of the initial sample, the losses amounted to 54.5%. Etiégni and Campbell (1991), Vaske (2012), Nakanishi (2013) and Zagvosda *et al.* (2017) point out that wood ash is rich in carbonates, especially calcium, potassium and magnesium, and that the calcination of ash generates a loss of mass associated with the degradation of these carbonates into oxides with the release of CO_2.

Figure 51: Ashes through steps

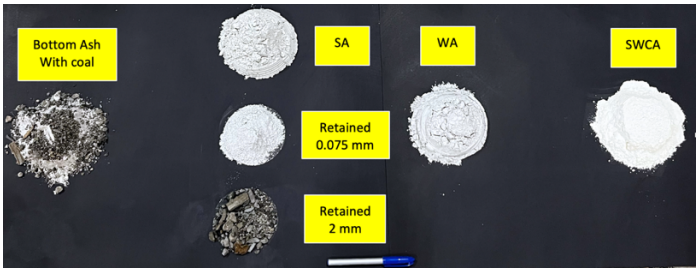

Source: Elaborated by the author

Melo *et al.* (2018) point out that calcined ashes have a high predominance of oxides, corroborating the aforementioned authors. According to Guimarães (2002), if these oxides are produced at controlled temperatures, they react with water through an exothermic reaction, releasing a great deal of heat. This process produces an increase in mass and generates physical-chemical changes in the material, as can it be seen in Figure 52 (a) and in Figure 52 (b). The first figure shows that the ashes occupy about half of the container and that they are at room temperature as measured by the thermometer, which reads 28 °C. After adding water, also at room temperature, a progressive increase in temperature was observed, reaching a peak of 141.3 °C, as shown in Figure 52 (b).

Figure 52: Hydration of calcined ash

(a): Before hydration **(b):** During hydration

Source: Elaborated by the author

It is therefore assumed that hydration was responsible for triggering exothermic reactions, typical of the process of transforming Quicklime (CaO) (calcium oxide) into Hydrated Lime (Ca(OH)2) (calcium hydroxide). The yield of calcined and hydrated ash (SWCA) is 1.22 in relation to the calcined sample. This value is obtained after hydration and drying to constant mass in an oven at 100 C°. Table 18 and Figure 53 show the variations in mass throughout the processes.

Table 18: Processing yield

Raw Ash	Sieving ABNT n° 10 (2 mm)	Sieving ABNT n° 200 (0,075 mm)	Washing	Calcination	Hydration
	Loss of 11,9%	Loss of 7,0%	Loss of 12,2%	Loss of 34,0%	Gain of 22,0%
5271 g	4645 g	4273 g	3632 g	2397 g	2925 g

Source: Elaborated by the author

After the addition of water, it was found that the ash had a significantly larger volume, with a change in the tactile-visual aspect of the particles, which previously had a certain granular aspect and after hydration acquired an aspect similar to talc, as shown in Figure 52 (b).

Considering all the processing, the total yield was 55.4% by mass from the ash obtained *in natura*. Progressive losses throughout the treatment stages can be reduced by optimizing processes, especially in the sieving and washing stages, which, due the artisanal method, ended up generating a certain amount of material waste. If these processes were replicated on an industrial scale, yields could be significantly increased.

Figure 53: Mass variation throughout the processing stages

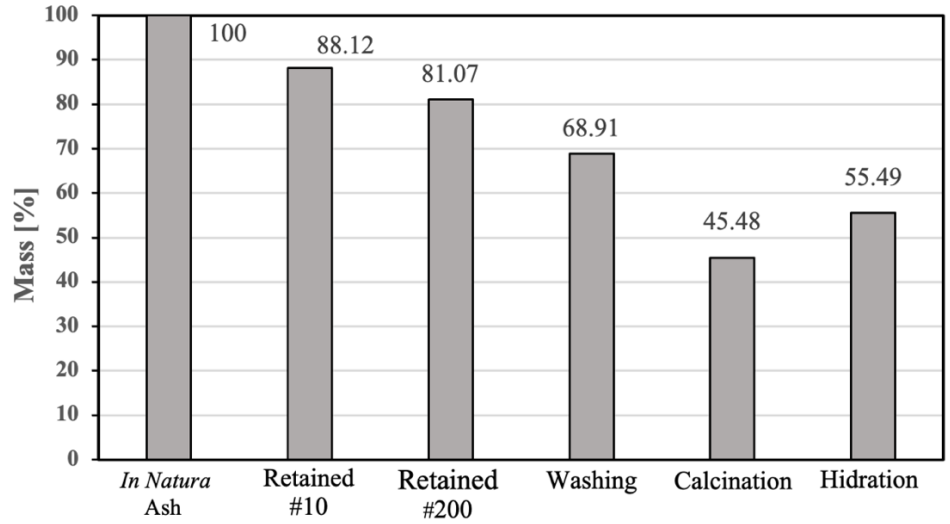

Source: Elaborated by the author

4.1.2 *Chemical characterization of ash and commercial lime*

To determine the chemical and mineralogical composition of the ash throughout the processing stages, X-ray fluorescence (XRF) and X-ray diffractometry (XRD) tests were carried out, respectively. Figure 54 shows the main oxides while Table 19 shows the full chemical composition in the form of oxides for each material.

Figure 54: Chemical analysis of the samples

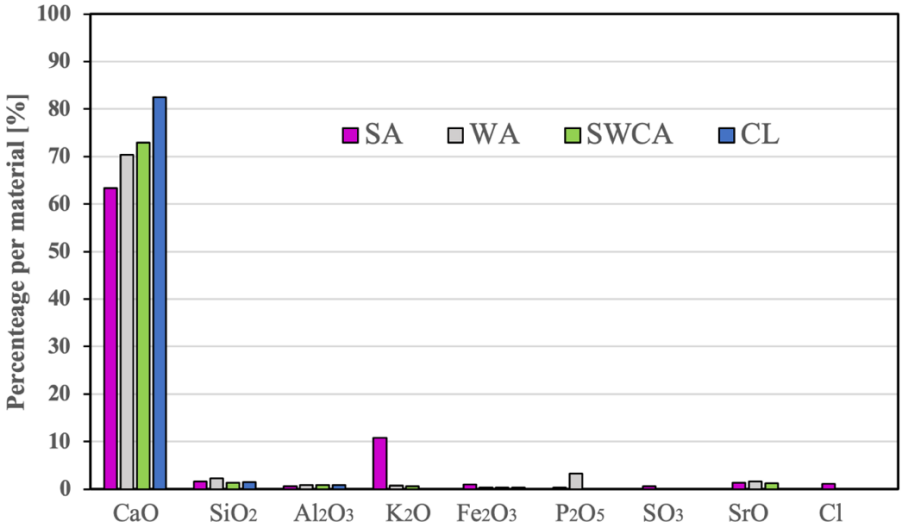

Source: Elaborated by the author

Table 19: Chemical composition of ash and commercial lime.

Compound	SA [%]	WA [%]	SWCA [%]	CL [%]
CaO	63,3090000	70,4060000	72,9090000	82,5090000
SiO_2	1,6090000	2,2160000	1,3430000	0,9100000
Al_20_3	-	0,8860000	0,8930000	1,4530000
P_2O_5	2,8020000	3,3440000	2,8140000	-
Fe_2O_3	0,3190000	0,3740000	0,3890000	0,3330000
SO_3	0,5690000	0,1350000	0,1320000	0,0490600
Cl	1,0710000	0,1510000	0,1320000	0,0331800
K_2O	10,820000	0,7070000	0,6500000	0,0276200
GeO_2	7,9550000	10,6920000	-	-
SrO	1,3790000	1,6370000	1,2710000	0,0289900
As_2O_2	-	-	-	0,3920000
TiO_2	0,0349400	0,0337900	0,0963500	0,0497500
V_2O_5	-	-	0,0129200	0,0055900
MnO	0,0656100	0,0769500	0,0835700	0,0213300
CuO	0,0136500	0,0129800	0,0142000	0,0036900
ZnO	0,0039200	0,0066600	0,0069000	0,0052100
Br	0,0000425	0,0003600	-	0,0000300
Rb_2O	0,0130200	0,0035900	-	-
Y_2O_3	0,0002200	0,0962700	-	0,2590000
ZrO_2	0,0100900	0,0135200	-	0,0673800
MoO_3	0,0029800	0,0022500	0,0030100	0,0006400
SnO_2	-	0,0058500	-	-
BaO	0,0749500	0,0888400	-	-
OsO_4	0,0237500	0,0219700	-	-
Re	0,0099800	0,0124400	-	0,0135400

Source: Elaborated by the author

From the data obtained, it was found that SA has a high content of calcium compounds (CaO) with 63.30%, a significant presence of potassium compounds (K_2O) with

10.82% and low amounts of silica-aluminum materials. This corroborates the data reported by Vaske (2012), Melo (2018) and Agrela *et al.* (2019), who report that wood ash does in fact tend to have high calcium contents and low levels of silica-aluminum materials.

The presence of various metallic and non-metallic elements is also noted, among which some are classified as toxic according to the ABNT NBR 10004 standard, which establishes criteria for the classification of solid waste based on its hazardousness. Elements such as manganese (Mn), zinc (Zn), copper (Cu), barium (Ba), and arsenic (As) must have their concentrations determined through solubilization and leaching tests. The potential environmental impacts associated with the presence of these elements are discussed in Section 4.2.7.

From the data described in the Table 19, it was found that, as reported by Melo *et al.* (2018), the washing step under heating proved to be efficient, as it reduced the concentration of K_2O in the system, changed from 10.82% to 0.70% and increased the concentration of calcium, from 63.30% to 70.40%. These results can be explained by the fact that potassium compounds become more soluble in water as the temperature rises, while calcium compounds become more insoluble, causing the material to precipitate and therefore have its concentration increased during the washing process.

The removal of potassium compounds from the system is important, because according to Melo *et al.* (2018), the direct calcination of wood ash at 850 °C, without prior washing, produced a compact and non-reactive material, similar to limes calcined at temperatures above 950 °C, as mentioned by Guimarães (2002). The latter author points out that excess calcination temperature can produce an unreactive lime due to changes in the crystalline structure of the material. Melo *et al.* (2018), in turn, reports that excess potassium in the ash can act as a reducer of the crystallization temperature of the lime, producing insoluble crystals, confirming the importance of the prior washing step to reduce the concentration of these elements that can act as inactivators of the chemical potential of the lime produced from wood ash.

Another point to mention about the removal of potassium is that according to Gibbs (1939), by cooking wood ash it is possible to extract potassium carbonate, which is a compound that is very soluble in water. According to the author, in the presence of water, K_2CO_3 undergoes a hydrolysis reaction, producing potassium hydroxide (KOH) according to Chemical Equation 1).

$$K_2CO_3\ (s) + H_2O\ (l) \rightarrow KHCO_3\ (aq) + KOH\ (aq) \qquad (1)$$

Potassium hydroxide extracted from wood ash is popularly known as potash (caustic potash) or lye and is one of the oldest ways of producing soap, through saponification reactions with vegetable or animal fats. The visual tactile aspect of handling wood ash with high moisture content soils in the laboratory is similar to the emollient aspect of handling soap powder and water as illustrated in Figure 55.

Figure 55: Emolient aspect of handling wood ashes

Source: Elaborated by the author

This empirical finding may suggest that the contact of potassium products present in wood ash with saturated soils may be detrimental to grain-soil contact because the emollient capacity of potassium hydroxide can contribute to the loss of mechanical stability of the soil matrix, which is one of the reasons why the washing stage was included in this work.

The purpose of the calcination stage, from a chemical point of view, is to transform the calcium compounds into active oxides by releasing CO_2 from the carbonate molecules present in the ash. Chemical Equation (2) represents the reaction that takes place during this stage.

$$CaCO_3\ (s) \rightarrow CaO\ (s) + CO_2\ (g) \qquad (2)$$

The results reported by the test for the calcined and hydrated material show that there was a slight increase in the concentration of calcium compounds in the system, from 70.40% in the WA sample to 72.90% in the SWCA sample. This slight increase in calcium concentration may be the result of a decrease in the relative concentrations of other elements such as silicates (SiO_2) and phosphates (P_2O_5).

Another important fact to mention is that the hydration of the calcined ash produced an exothermic hydration reaction, with a large amount of heat released. This hydration reaction is typical of the transformation of CaO (calcium oxide) into Calcium Hydroxide ($Ca(OH)_2$), as mentioned by Guimarães (2002) and Melo *et al*. (2018). Chemical Equation (3) represents the probable exothermic chemical reaction of hydration that occurred.

$$CaO\ (s) + H_2O\ (l) \rightarrow Ca(OH)_2\ (s) + \Delta H\ (Heat) \qquad (3)$$

Even with the observation of the exothermic hydration reaction and the change in the tactile-visual aspect of the material after hydration, the data from the XRF test alone does not show the major mineralogical changes that the calcination and hydration stage promotes in the ash. To this end, it was necessary to analyze the change in the diffraction pattern of the calcined material using the XRD test, shown in Figure 56. By varying the peaks associated with each mineralogical phase it is possible to infer more precisely the qualitative composition of the compounds present in the ash.

Figure 56: X-ray diffractogram of ash and commercial lime

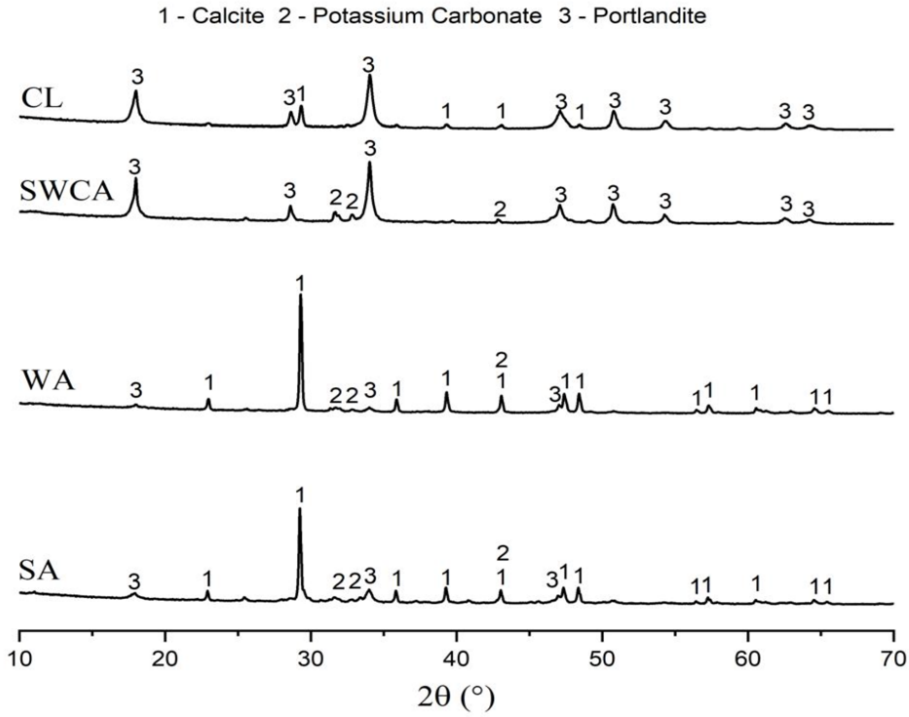

Source: Elaborated by the author

A comparison of the diffraction profiles of the samples showed that the main peaks found were associated with calcite ($CaCO_3$) 29.5° (2θ) basal interplanar distance of 2.71 Å (JCPDS 5-0586) and Portlandite, $Ca(OH)_2$, basal interplanar distance of 2.24 Å (JCPDS 4-

0733). The sieved ash sample (SA) as well as the washed ash sample (WA) showed pronounced peaks associated with the mineral calcite, while the calcined ash (SWCA) showed a predominance of Portlandite, indicating that, in fact, the uncalcined ash is rich in calcium carbonates, while the calcined ash (SWCA) and commercial lime (CL) are rich in calcium hydroxide.

Because ash is a complex material, only the peaks associated with the predominant phases were identified at first. The raw test data will have to be further processed for possible quantification using the Rietveld method to quantify the mineralogical phases present.

Based on the data from the XRF and XRD tests, important indications were found that ash without calcination tends to behave as a chemically non-reactive material, as mentioned in Vaske (2012) and Cabrera *et al.,* (2014). These authors have reported that biomass ash can be used as a filler material, having only a granulometric influence or producing a filler effect in cementitious matrices or granular paving layers.

Picchi *et al.* (1988), dealing with the reactions that occur in systems that use lime, mention that calcium carbonate ($CaCO_3$) does not contribute significantly to the strength of materials, acting as an inert material or as a weak cement in concretes or mortars that have undergone carbonation reactions. On the other hand, the calcined ash (SWCA) showed a diffractometric profile similar to that of commercial lime, which is a strong indication that it can act in the stabilization of plastic soils or in any other applications in which hydrated lime is useful.

4.2 *Soil Characterization*

To initially characterize the soils, tests were carried out on their actual grain density, grain size by sedimentation and consistency limits. Based on these tests, it is possible to classify the soils evaluated into the usual classifications for soils, especially the AASHTO classification, which categorizes soils according to their expected behavior in paving applications.

4.2.1 *Characterization results*

The specific gravity is important data for determining volumetric parameters and for carrying out sedimentation granulometry, which is an essential test for characterizing fine clay soils. For soil 1, the specific gravity was 2.508 g/cm³ and for soil 2, the density was 2.471 g/cm³. Figure 57 shows the particle size curves of the two soils evaluated. From these curves it can be seen that the two soils are quite fine-grained, indicating the presence of

around 50% clay particles in Soil 1 and around 56% of this fraction in Soil 2. The percentage of materials retained on the 2 mm sieve, which corresponds to the coarse fraction of the soil, is less than 3% for the two soils evaluated, showing the fine gradation of the materials.

Figure 57: Soil particle size curve

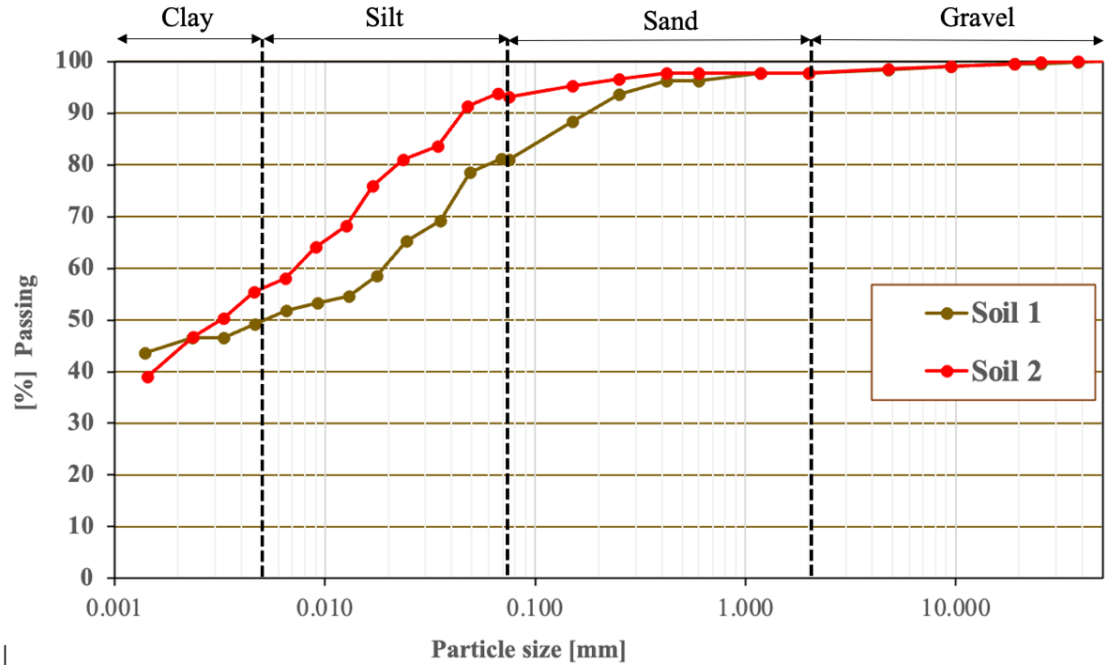

Source: Elaborated by the author

Liquidity Limit and Plasticity tests were carried out on the soil samples without additions, and the data is shown in Table 20. Caputo (1996) points out that soils with plasticity index (PI) between 1 and 7 are considered weakly plastic. According to the author, moderately plastic soils have a PI range between 7 and 15, while highly plastic soils have a PI greater than 15. The soils analyzed in this study are therefore classified as highly plastic according to the author's criteria.

Table 20: Soil consistency limits

	LL	PL	PI	AASHTO Classification
Soil 1	44%	22%	22%	A-7-6
Soil 2	52%	31%	21%	A-7-6

Source: Elaborated by the author

Placing the two clays on the plasticity chart proposed by Casagrande (1932), as shown in Figure 58, it can be seen that both soils are close to the line A which separates high and low compressibility clays. While Soil 1 can be classified as a low-compressibility clay (CL), Soil 2 exhibits the behavior of a high-compressibility silt (MH), although the particle size

distribution indicates a predominance of clay fractions. The proximity to the A-line boundary and the inherent variations in determining the consistency limits justify this discrepancy between the particle size distribution and the resulting classification.

Figure 58: Plasticity chart for classification of soils

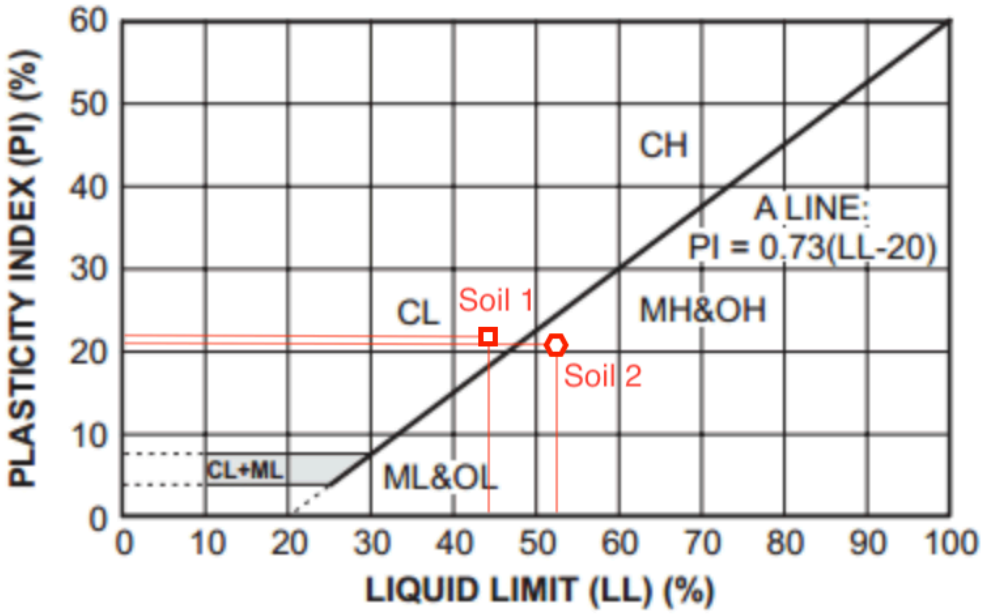

Source: Adapted from (CASAGRANDE ,1932)

Therefore, according to the classification described by Caputo (1996) both soils are considered to have high plasticity. However, according to the SUCS classification and based on Casagrande's plasticity chart (1932), soil 1 can be classified as a low compressibility clay while soil 2 can be classified as a high compressibility silt. This difference in classifications can be explained by the higher level of correlation between the Limit of Liquidity (LL) and compressibility, which is better than the correlation between the Plasticity Index (PI) and compressibility, according to Cunha (2012).

From paving applications point of view, the most common classification for soils used for this purpose is AASHTO, which considers the percentages passing the 10, 40 and 200 mesh sieves, the consistency limits and the calculation of the group index. As the percentage passing the 200-mesh sieve was higher than 36%, the liquidity limits were both higher than 41%, the plasticity indices were higher than 11%, and the Group Indices (GI) were 18.43 and 27.9 respectively. Both soils were classified according to AASHTO as class A-7-6, with expected behavior for use in subgrade from Fair to Poor, confirming the data described in Table 21.

Table 21: AASHTO soil classification

Sieve	Soil 1	Soil 2
N° 10	97.7%	97.8%
N° 40	96.3%	97.8%
N° 200	82.1%	93.3%
LL	44%	52%
PI	22%	21%
GI	18.4	27.9
AASHTO Classification	A-7-6	A-7-6

Source: Elaborated by the author

Having therefore been classified as very clayey soils, traditional soil classification systems suggest that the expected behavior of these materials is inadequate. In these cases, according to Hilt and Davidson (1960), a good alternative for improving the performance of these materials would be chemical stabilization using hydrated lime.

4.2.2 *Compaction of soil and mixtures*

In order to determine the most promising mixtures, it is first necessary to know the compaction parameters of the soils in natura and mixtures. Due to the limited quantity of calcined ash produced (SWCA), it was decided to use small specimens to evaluate the most promising mixtures. Therefore, miniature compaction curves were determined for each of the 26 combinations of materials evaluated. Figure 59 and Figure 60 show the compaction curves for the mixtures made with soils one and two respectively and Figure 61 and Figure 62, as well as Table 22, show the optimum parameters for each soil mixture with each type of ash in its different stages.

Table 22 shows the optimum moisture and maximum dry density parameters for each of the 26 samples evaluated, where S1 and S2 are the soils without additions and the other abbreviations correspond to the mixtures of the respective soil and its tested additive.

Figure 59: Miniature compaction curve - Soil 1

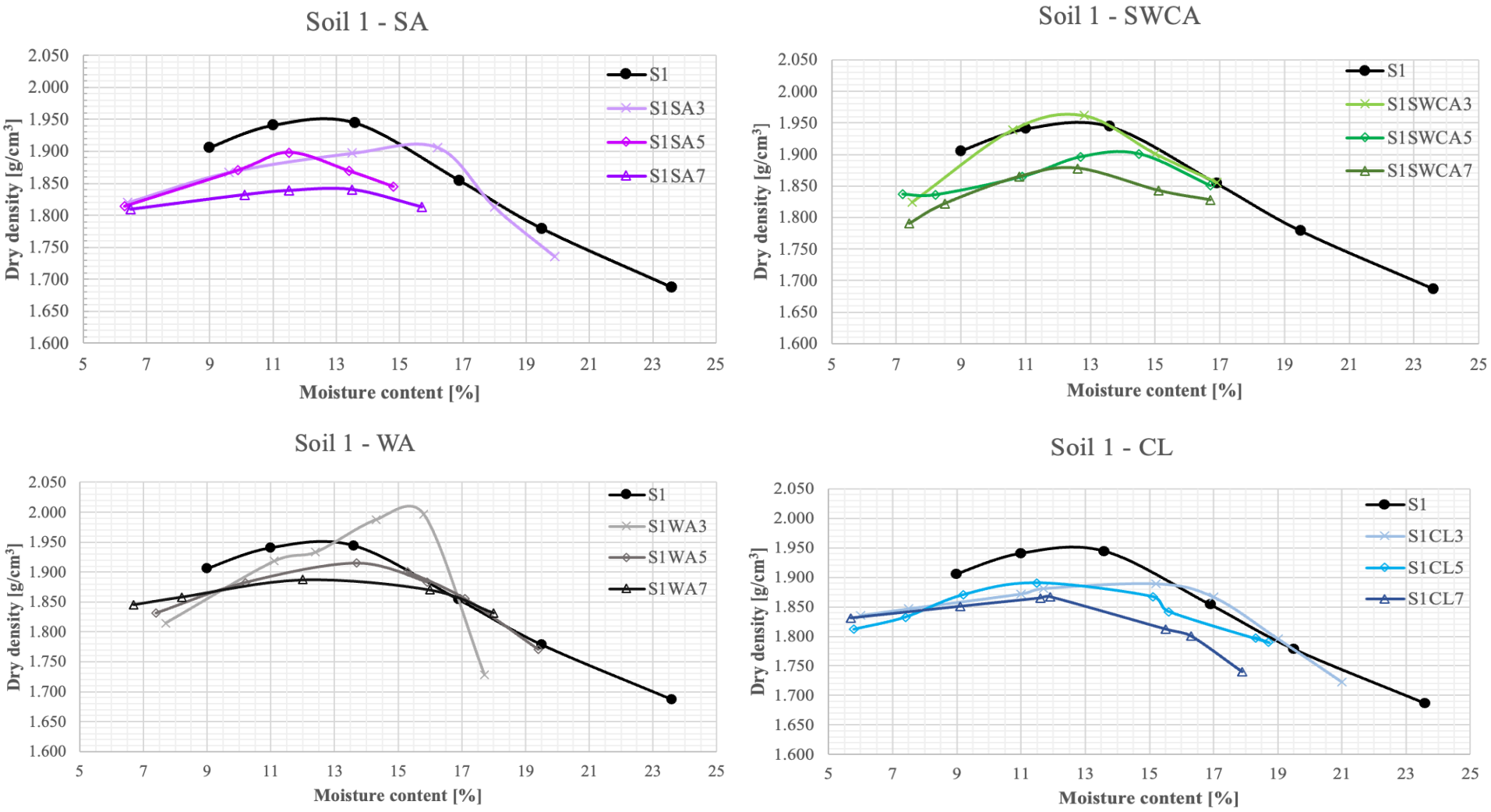

Source: Elaborated by the author

Figure 60: Miniature compaction curve - Soil 2

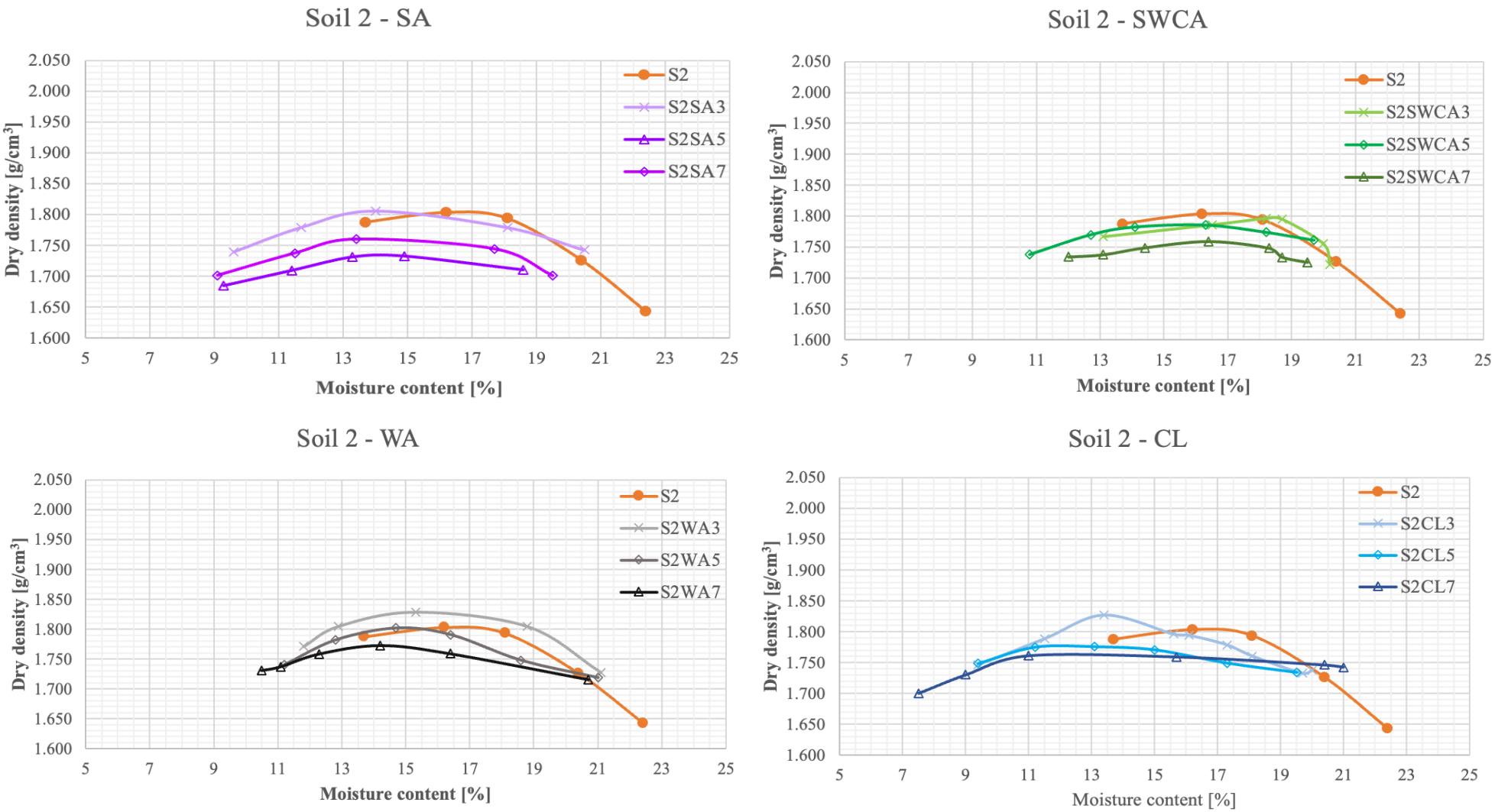

Source: Elaborated by the author

Figure 61: Variation in optimum moisture content for mixtures with soil 1 and 2

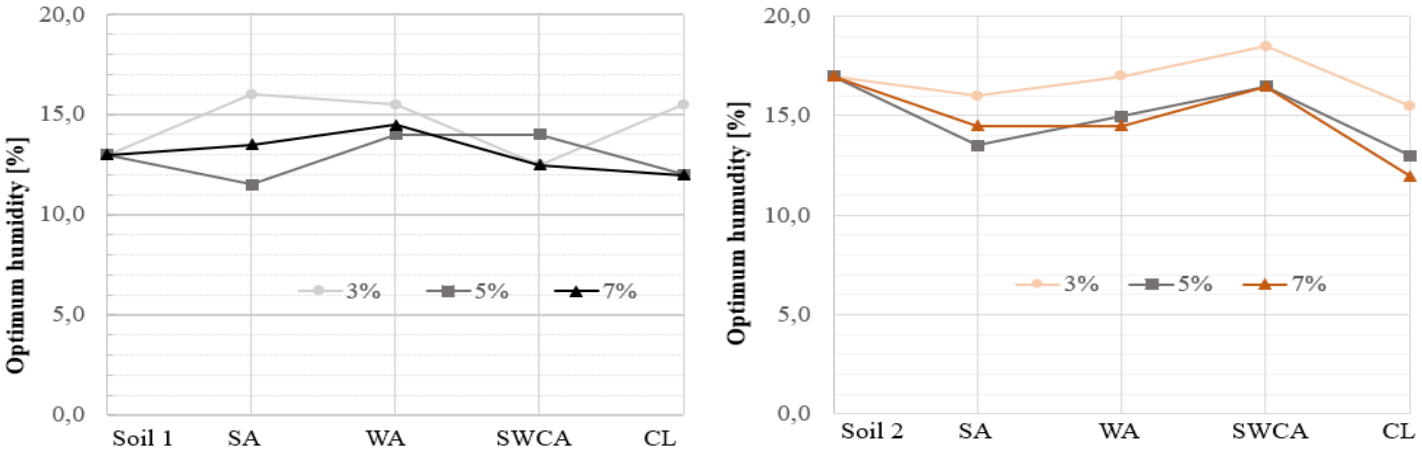

Figura 58: Variation in maximum specific dry mass soil 1 and 2

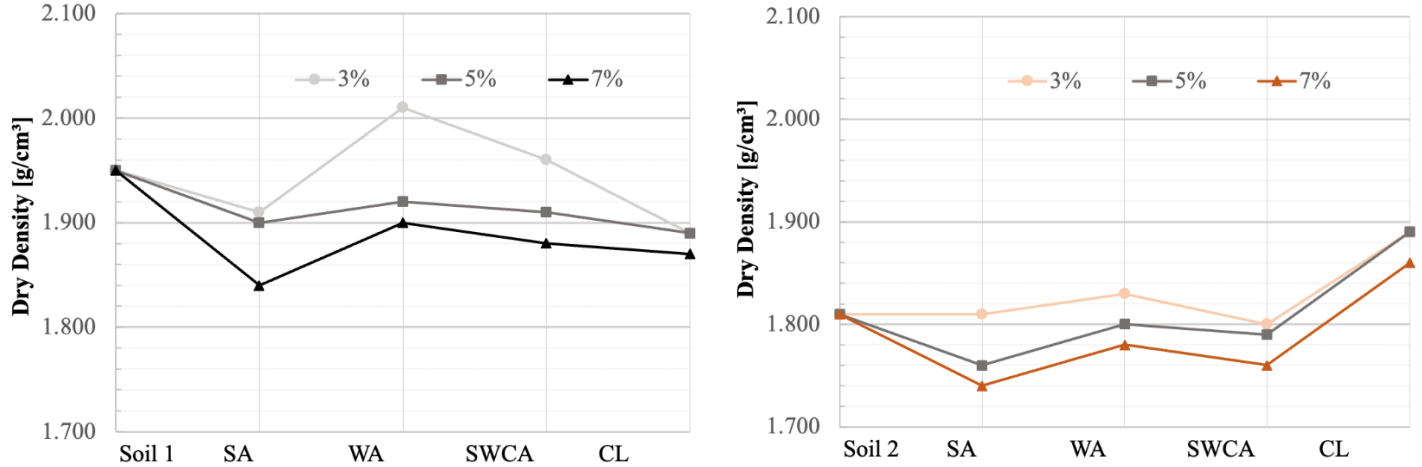

Source: Elaborated by the author

Table 22: Miniature compaction parameters

N	Sample	Additive [%]	Optimum moisture [%]	Máx. Dry density [g/cm³]
1	S1	-	13.0	1.950
2	S1SA3	(3)	16.0	1.910
3	S1SA5	(5)	11.5	1,900
4	S1SA7	(7)	13.5	1.840
5	S1WA3	(3)	15.5	2.010
6	S1WA5	(5)	14.0	1.920
7	S1WA7	(7)	14.5	1.900
8	S1SWCA3	(3)	12.5	1.960
9	S1SWCA5	(5)	14.0	1.910
10	S1SWCA7	(7)	12.5	1.880
11	S1CL3	(3)	15.5	1.890
12	S1CL5	(5)	12.0	1.890
13	S1CL7	(7)	12.0	1.870
14	S2	-	17.0	1.810
15	S2SA3	(3)	16.0	1.810
16	S2SA5	(5)	13.5	1.760
17	S2SA7	(7)	14.5	1.740
18	S2WA3	(3)	17.0	1.830
19	S2WA5	(5)	15.0	1.800
20	S2WA7	(7)	14.5	1.780
21	S2SWCA3	(3)	18.5	1.800
22	S2SWCA5	(5)	16.5	1.790
23	S2SWCA7	(7)	16.5	1.760
24	S2CL3	(3)	15.5	1.890
25	S2CL5	(5)	13.0	1.890
26	S2CL7	(7)	12.0	1.860

Source: Elaborated by the author

Regarding the behavior of the curves as a function of additive content, shown in Figure 59 and Figure 60, in general, the higher the ash content, the lower the maximum dry specific mass of the mixture. This trend was observed in almost all the mixtures and can be explained by the fact that the ash has a lower grain density than the soil grain density.

This general downward trend in the maximum dry specific mass of the mixture was not observed in soil 1 for the mixtures with WA and SWCA at 3%. In soil 2, this trend was not observed for the mixtures with WA and CL, also at the 3% level. These behaviors can possibly be explained by the better workability of these mixtures at the lower contents, promoted by a possible adequate balance in the interaction generating better packing.

In general, the curves show that the higher the ash content, the lower the optimum moisture content, as can be seen in almost all the mixtures with soil 2. This behavior can be attributed to the coarser particle size distribution of the ashes, which are more silty, in contrast to the soils, which are predominantly clayey. Additionally, possible flocculation reactions of clay particles upon contact with the ash may alter the grain structure, reducing plasticity and leading the material to behave more like a granular soil. As a result, lower

optimum moisture values are observed.

4.3 *Choosing the best additive contents*

The selection of optimal additive contents is based on mechanical performance criteria, including saturation resistance, which evaluates whether the mixtures can endure full immersion without disintegration, as well as unconfined UCS, bearing capacity (Mini-CBR), and volumetric stability (expansion and shrinkage).

4.3.1 *Unconfined compressive strength (UCS) and susceptibility to saturation*

Figure 62 shows the saturated compressive strengths obtained for all the 26 mixtures evaluated with 28 days of curing. The mixtures that disintegrated during the saturation stage prior to the test were given strengths of 0 MPa. According to Little (1995), mixtures with saturated unconfined compressive strength values above 0.345 MPa can be considered stabilized; values exceeding 0.689 MPa are suitable for use in subbase layers, and those above 1.034 MPa are appropriate for base layers.

Figure 62: Unconfined compressive strength of mixtures (Miniature) at 28 days.

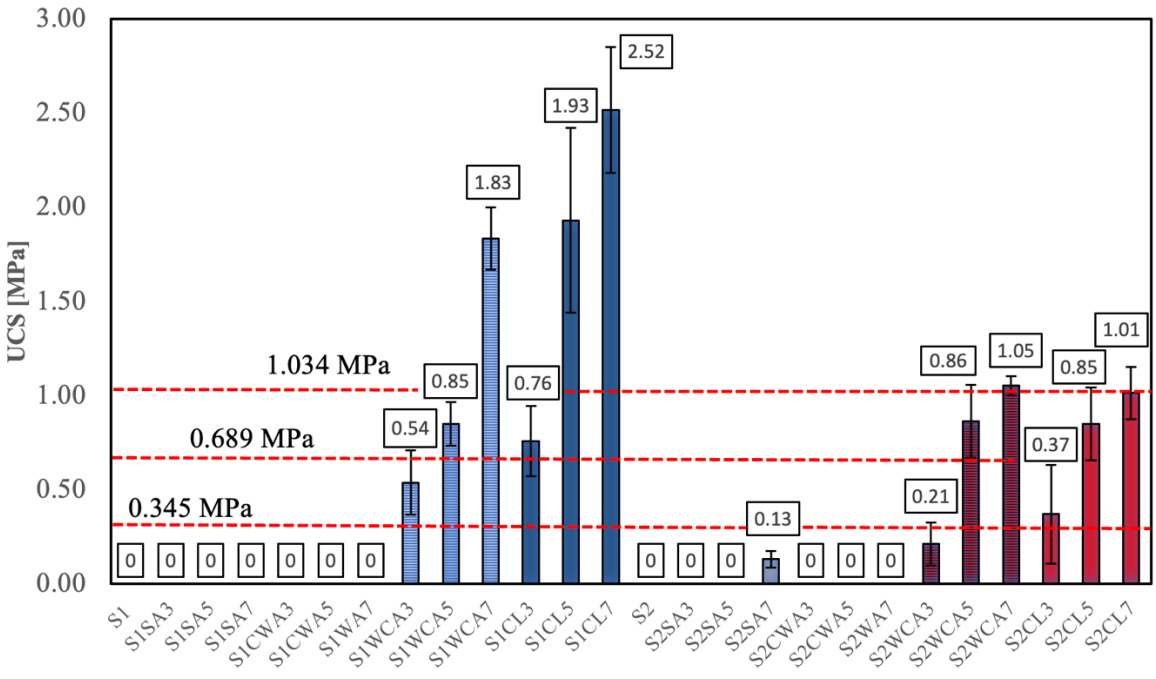

Source: Elaborated by the author

Figure 62 shows that for the soils evaluated, all the samples with uncalcined ash disintegrated except for S2SA7 mixture (Soil 2 + 7% Sieved Ashes). These samples that crumbled were assigned zero UCS values, indicating that for the used contents, the uncalcined ashes do not stabilize the soils evaluated. However, the result of 0.13 MPa

obtained for sample S2SA7 may be an indication that for higher contents, uncalcined ash could promote gains in strength, as reported in the works by Okagbue (2007) and Medeiros (2023). This may be associated with the free CaO content available in the ash at the time of application to the soil. This CaO content depends on the type of biomass burned, and its availability to react depends on how much this ash has been exposed to moisture and air, converting the free CaO into Calcium Carbonate, which is an inert material.

For the mixtures of soil 1 with calcined ash (SWCA), increasing UCS values were found as the SWCA content increased. The mixtures with 3%, 5% and 7% achieved values of 0.54 MPa, 0.85 MPa and 1.85 MPa, respectively. The same behavior was observed for the mixtures with commercial lime, which showed values of 0.76 MPa, 1.93 MPa and 2.52 MPa for the 3%, 5% and 7% respectively.

A similar behavior was observed for the mixtures of soil 2 and calcined ash. The increase in SWCA content is directly proportional to the increase in compressive strength, with the mixtures returning values of 0.21 MPa, 0.86 MPa and 1.05 MPa for the 3%, 5% and 7% content. Although strength gains were observed with the addition of calcined ash and commercial lime, these were lower than in soil 1, indicating that soil 1 is more reactive to stabilizers than soil 2. This behavior may be associated with the cation exchange capacity of the material, as demonstrated in the work by Araújo (2009).

The miniature UCS results showed that the mixtures with non-calcined ash did not react chemically, as evidenced by the crumbling of the specimens. It was expected that the soil mixtures with non-calcined ash would not show UCS values above 0.345 Mpa, which is the criteria for considering that a soil has been chemically stabilized with lime, according to Núñes (1991) and Lovato (2004). This expectation was confirmed after the miniature specimens were saturated.

This non-stabilization behavior can be explained by the fact that the mineralogical composition of these materials is mostly calcite ($CaCO_3$), which according to Picchi *et al.* (1988) does not contribute significantly to the strength of the materials, acting as an inert material or as a weak cement in concretes or mortars that have undergone carbonation reactions.

On the other hand, the mixtures with calcined ash were chemically stabilized, as evidenced by the increase in UCS as the calcined ash content increased. This behavior can be explained by the development of pozzolanic reactions between calcium hydroxide ($Ca(OH)_2$) and the silica-aluminum clay minerals normally present in clay soils, as described by Eades and Grim (1963).

Little (1995) indicates that the minimum UCS values required by the Illinois Highway Department for the use of soil-lime mixtures in sub-base layers is (0.689 MPa) and base (1.034 MPa). Given these criteria, the mixtures with 5 and 7% calcined ash, as well as the mixture of soil 1 with 7% commercial lime, are suitable for use in sub-base layers.

The mixtures with 7% calcined ash, on the other hand, met the strength requirement and can be used in base layers, indicating promising results for the use of these materials in paving layers.

4.3.2 *Bearing capacity of mixtures and susceptibility to saturation*

Although it is important to determine whether the mixtures can be considered stabilized or not, other parameters such as expansion and shrinkage percentages are necessary as acceptance criteria for the mixtures. Since expansion and shrinkage parameters can be determined in the Mini-CBR test, the bearing capacities of all mixtures were also determined to establish a basis for comparison. Figure 63 and Figure 64 presents the bearing capacity values, and the corresponding expansion and shrinkage results obtained for each soil and each mixture.

The dry bearing capacity (Mini-CBR) of soil 1 was 34.8%, higher than the bearing capacity of soil 2, which was 26.2%. According to Villbor and Nogami (2009) dry bearing capacities by Mini-CBR above 30% are considered very high and between 12% and 30% are considered high, indicating that these materials have good bearing capacities in the dry state, however when saturated the bearing capacity drops below 4%, and therefore considered low.

The addition of sieved ash to soils 1 and 2 produced an increase in dry bearing capacity, except for the 3% content in soil 1. When saturated, however, the mixtures with SA suffered significant drops in bearing capacity. According to Villibor and Nogami (2009), losses in bearing capacity above 70% are classified as high, between 40% and 70% as medium, and below 40% as low. Adding 3% SA to soil 1 produced losses that fall into the medium, high, and low categories for the 3%, 5%, and 7% contents, respectively. For soil 2, the SA additions produced high losses for the 3% and 5% contents, and medium losses for the 7% content. Although the qualitative classification of bearing capacity loss varied considerably, all mixtures showed a reduction upon saturation, once again indicating that the uncalcined ashes at the evaluated contents do not stabilize the soil. It should be noted that there is no minimum Mini-CBR threshold formally established by standards for pavement layers; the test provides a qualitative indication of bearing capacity and moisture sensitivity, to be considered together with other mechanical criteria.

Figure 63: Bearing Capacity (Mini-CBR) and its variation values for Soils 1 and 2.

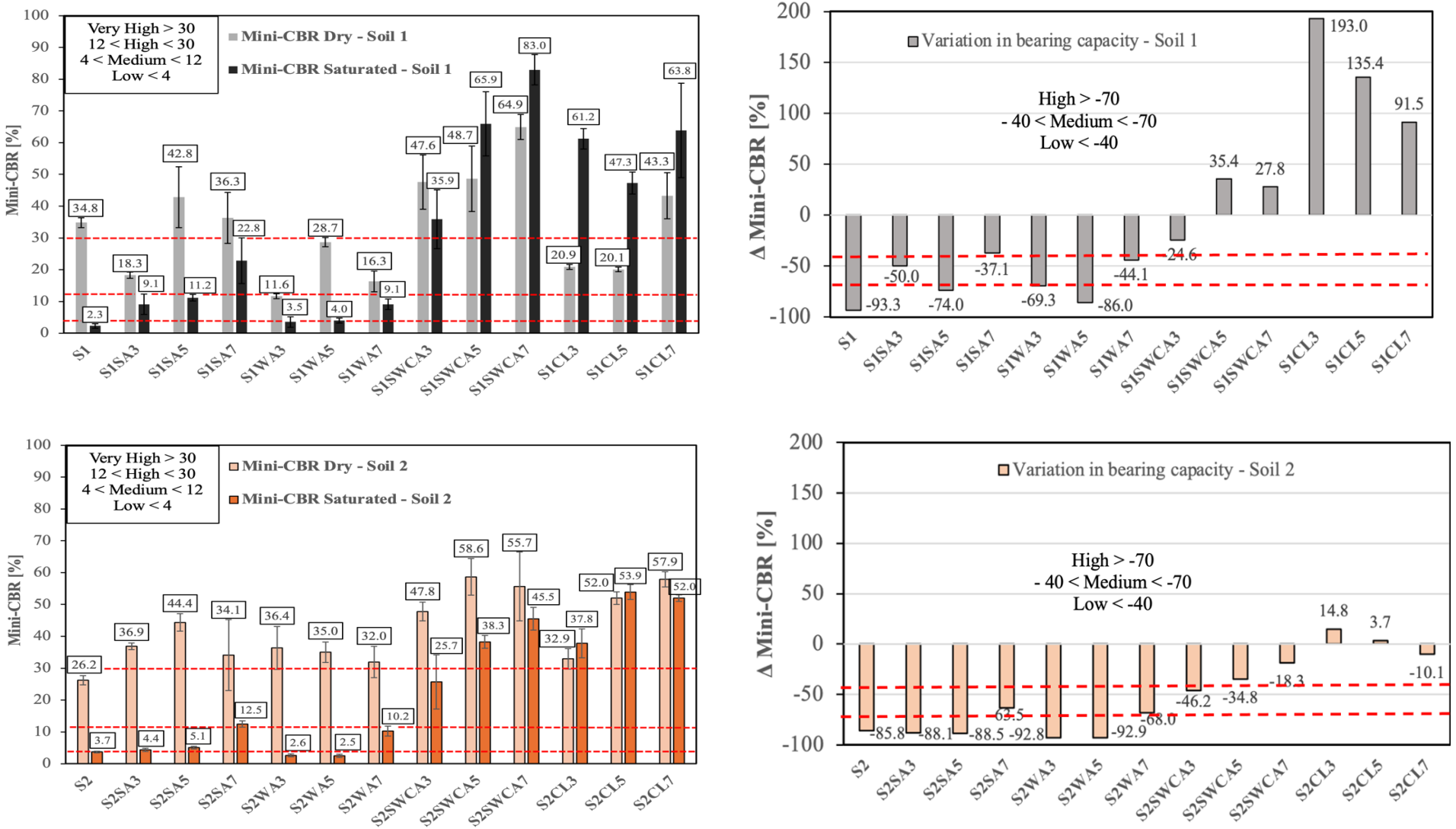

Source: Elaborated by the author

Figure 64 : Expansion and Shrinkage of Soils 1 and 2.

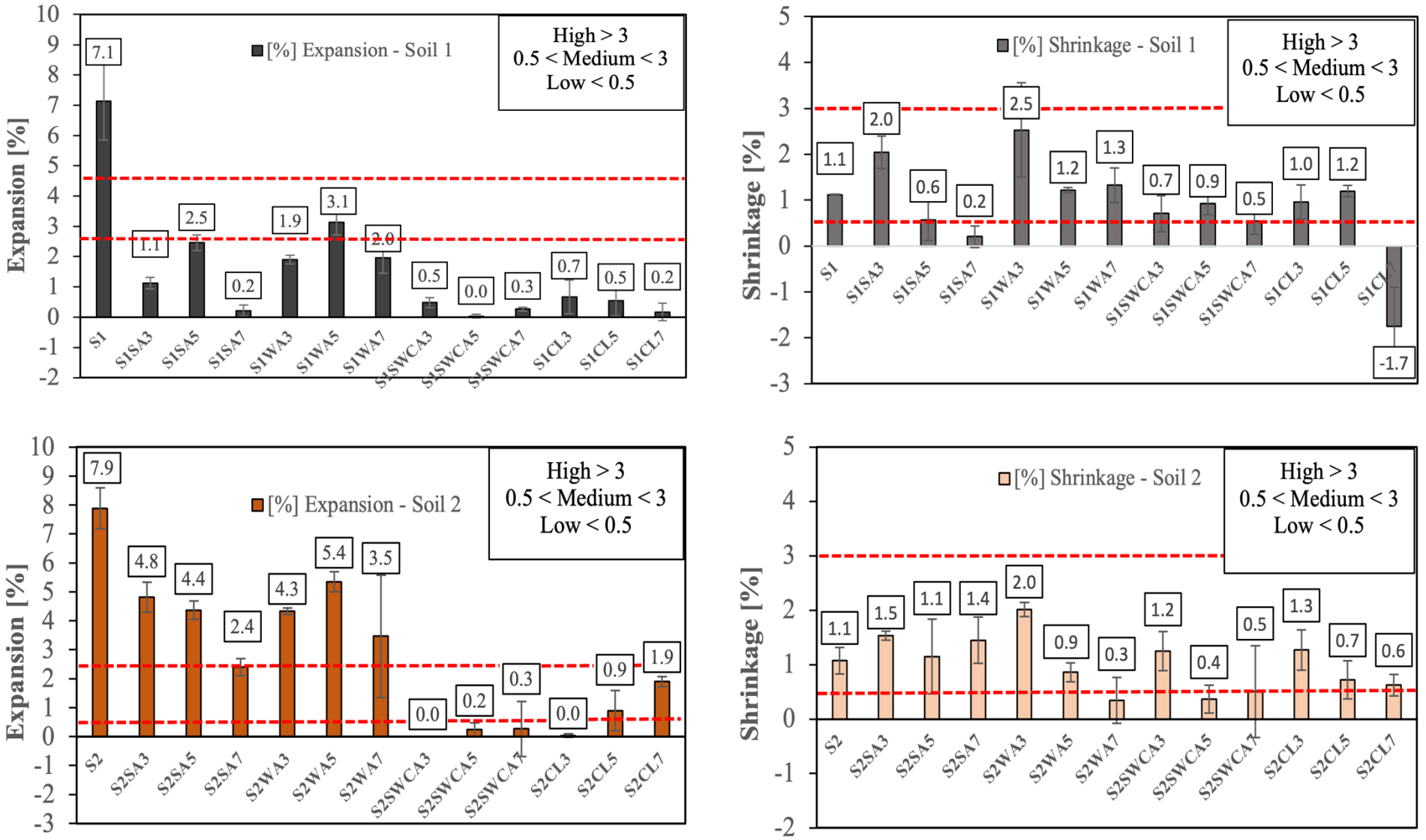

Source: Elaborated by the author

For the mixtures with washed ash (WA), when compared to those with sieved ash (SA), a decrease in bearing capacity was observed in both dry and saturated conditions, indicating that the washing process did not contribute to strength gains at the evaluated levels. The reduction in bearing capacity due to saturation was even more pronounced with the addition of WA. It can therefore be seen that for the mixtures with uncalcined ashes, SA and WA, regardless of the content, Mini-CBR values remained below 45% in the dry condition and below 25% in the saturated condition. All samples showed a decrease in bearing capacity when subjected to saturation, indicating that the ashes did not promote cementation of the mixtures.

Samples with calcined and hydrated ash (SWCA), on the other hand, exhibited increases in bearing capacity when compared to uncalcined ashes. In the dry state, even at the lowest percentages, higher values were observed than for the uncalcined ash. After saturation, although decreases in bearing capacity were observed for the 3% SWCA content in soil 1 and for all contents in soil 2, the saturated values remained of the same order of magnitude as the dry values of the uncalcined ash mixtures. Losses in bearing capacity due to saturation of the SWCA mixtures were generally classified as low (<40%), except for the 3% content, which showed medium losses of 44.1% and 68%. For the mixtures with 5% and 7% SWCA in soil 1, increases in bearing capacity were observed even under saturated conditions, indicating the development of cementing reactions that enhanced resistance.

The improvement mechanisms of these mixtures are primarily associated with cation exchange, flocculation, and pozzolanic reactions, which alter the original soil properties and make them less susceptible to moisture variations. Esses processos, entre outros fatores, dependem do teor de compostos de cálcio reativos disponíveis para a occurrence das reações de estabilização (ZHOU et al., 2019) (AKULA; LITTLE, 2020) e (ZAINI et al., 2024).

Okagbue (2007) reported that the CBR of mixtures of uncalcined wood ash with a clay soil was higher in the dry condition compared to the saturated condition, corroborating the results observed in this study for the uncalcined mixtures. The reduction in the potential of washed ash (WA) can be explained, according to Melo (2018), by the precipitation of calcium compounds during the hot water washing process, which makes them less reactive and therefore reduces their contribution to stabilization mechanisms.

It is therefore evident that unwashed ashes retain a certain concentration of soluble compounds that contribute to improvements in bearing capacity but still provide limited gains at the evaluated contents. Calcined materials, on the other hand, benefit from an increased

availability of reactive calcium compounds, which promotes drastic improvements in bearing capacity.

4.3.3 *Expansion and shrinkage of mixtures*

According to the criteria of Villibor and Nogami (2009), expansions and contractions above 3% are considered high, between 0.5% and 3% are considered medium and below 0.5% are considered low. For the mixtures with ash without calcination for both soils and contents evaluated, medium to high expansions and contractions were observed, except for the 7% SA content for soil 1, which showed an expansion and contraction of 0.2%.

For the samples with calcined ash, there were significant drops in volumetric variation under conditions of saturation and loss of moisture. From expansion point of view, for all the contents evaluated and for the two soils in question, expansion values less than or equal to 0.5 % were observed, indicating that the addition of calcined ash reduced the expansibility of these soils to values considered low.

Both natural soils exhibit average shrinkage values of approximately 1.1%. The addition of unwashed ash (SA) at lower contents increases the shrinkage in both soils. However, in Soil 1, higher SA contents lead to reduced shrinkage, whereas in Soil 2, the shrinkage values remain relatively stable, close to those of the natural soil. For mixtures containing washed ash (WA) and calcined ash (SWCA), a consistent reduction in shrinkage is observed in both soils as the ash content increases. In the case of mixtures with commercial lime, Soil 1 shows shrinkage values similar to those of the untreated soil, except for the 7% content, which showed unexpected expansion, attributed to issues with the quality of the lime used. Soil 2 exhibits reductions in shrinkage at 5% and 7% lime contents.

Several studies (Dash; Hussain, 2015; Zagvozda; Rukavina; Dimter, 2020; Ünver; Lav; Çokça, 2021; Pushpakumara; Mendis, 2022) have evaluated the effects of hydrated lime and different biomass ashes on the swelling and shrinkage behavior of soils. These authors reported that both hydrated lime and biomass ashes, whether used individually or in combination, reduce expansiveness and shrinkage, thereby improving the volumetric stability of the mixtures. Optimal results, however, depend on specific addition ratios and curing times.

4.3 *Mixtures ranking*

To establish a ranking of the most promising mixtures, a score of 1 was assigned to the mixture that showed the best performance in the following criteria: Unconfined

Compressive Strength (UCS), expansion below 0.5%, shrinkage below 0.5%, best bearing capacity under saturated conditions and best bearing capacity under dry conditions. For the other mixtures with lower performance at a given content, a score of 0 was assigned. Table 23 presents the ranking of the most promising mixtures.

Table 23: Most promising mixtures for each ash batch

	UCS [MPa]	Score	Exp. [%]	Score	Shrink. [%]	Score	Sat. [%]	Score	Dry [%]	Score	Total	Best
S1	0	0	7.1	0	1.1	0	2.3	0	34.8	0	0	
S1SA3	0	0	1.1	0	2.0	0	9.1	0	18.3	0	0	
S1SA5	0	0	2.5	0	0.6	0	11.2	0	42.9	1	1	
S1SA7	0	0	0.2	1	0.2	1	22.9	1	36.3	0	3	S1SA7
S1WA3	0	0	1.9	0	2.5	0	3.6	0	11.6	0	0	
S1WA5	0	0	3.1	0	1.2	1	4.0	0	28.7	1	2	S1WA5
S1WA7	0	0	2.0	1	1.3	0	9.1	1	16.3	0	2	
S1SWCA3	0.54	0	0.5	0	0.7	0	36.0	0	47.7	0	0	
S1SWCA5	0.85	0	0.0	1	0.9	0	65.9	0	48.7	0	1	
S1SWCA7	1.83	1	0.3	0	0.4	1	83.0	1	64.9	1	4	S1SWCA7
S1CL3	0.76	0	1.0	0	1.0	1	61.2	0	20.9	0	2	
S1CL5	1.93	0	0.5	0	1.2	0	47.3	0	20.1	0	0	
S1CL7	2.52	1	0.2	1	-1.7	0	83.0	1	43.3	1	3	S1CL7
S2	0	0	7.9	0	1.1	0	3.7	0	26.2	0	0	
S2SA3	0	0	4.8	0	1.5	0	4.4	0	36.9	0	0	
S2SA5	0	0	4.4	0	1.1	1	5.1	0	44.4	1	2	
S2SA7	0.13	1	2.4	1	1.4	0	12.5	1	34.2	0	3	S2SA7
S2WA3	0	0	4.3	0	2.0	0	2.6	0	36.4	1	1	
S2WA5	0	0	3.6	0	0.9	0	2.5	0	35.0	0	0	
S2WA7	0	0	3.5	1	0.5	1	10.3	1	32.0	0	3	S2WA7
S2SWCA3	0.21	0	0.0	0	1.2	0	25.7	0	47.8	0	0	
S2SWCA5	0.86	0	0.2	0	0.5	0	38.3	0	58.7	1	1	
S2SWCA7	1.05	1	0.3	1	0.5	1	45.5	1	55.7	0	4	S2SWCA7
S2CL3	0.37	0	0.0	0	1.3	0	37.8	0	32.9	0	0	
S2CL5	0.85	0	0.9	0	0.6	0	53.9	1	52.0	0	1	
S2CL7	1.01	1	0.5	1	0.6	1	52.0	0	57.9	1	4	S2CL7

Source: Elaborated by the author

Considering the scoring assigned to the mixtures that showed superior performance in each criterion, the 7% content was identified as the most effective for nearly all evaluated additives, with the exception of the S1WA5 mixture, which was selected due to its lower additive content.

4.4 *Testing the* most promising mixtures

Once the most promising mixtures have been defined some additional test such mechanical, consistency, expansion and environmental tests were carried out. The additional mechanical tests aim to assess the strength of the most promising mixtures using methodologies and criteria appropriate to chemically stabilized and unstabilized materials,

while the consistency and expansion tests assess the impact of the additions on the plastic and expansive behavior of the mixtures, since these are important variables for using materials in paving.

The environmental tests, in turn, assess the impact of leaching heavy metals and other contaminating compounds that may be present in the ash, according to criteria established by national and international legislation.

4.4.1 *Consistency tests*

The graphs presented in Figure 65 illustrate the consistency behavior of the soils and their respective mixtures. For Soil 1 and Soil 2, the results are shown in Figure 65 (a) and (b), respectively. When analyzing each graph horizontally, one can observe the consistency parameters of the soils and their mixtures for a given reacting period. Vertically arranged graphs illustrate the variation of consistency parameters over the three curing times under analysis (0, 28, and 90 days).

Figure 65: Consistency variation of mixtures

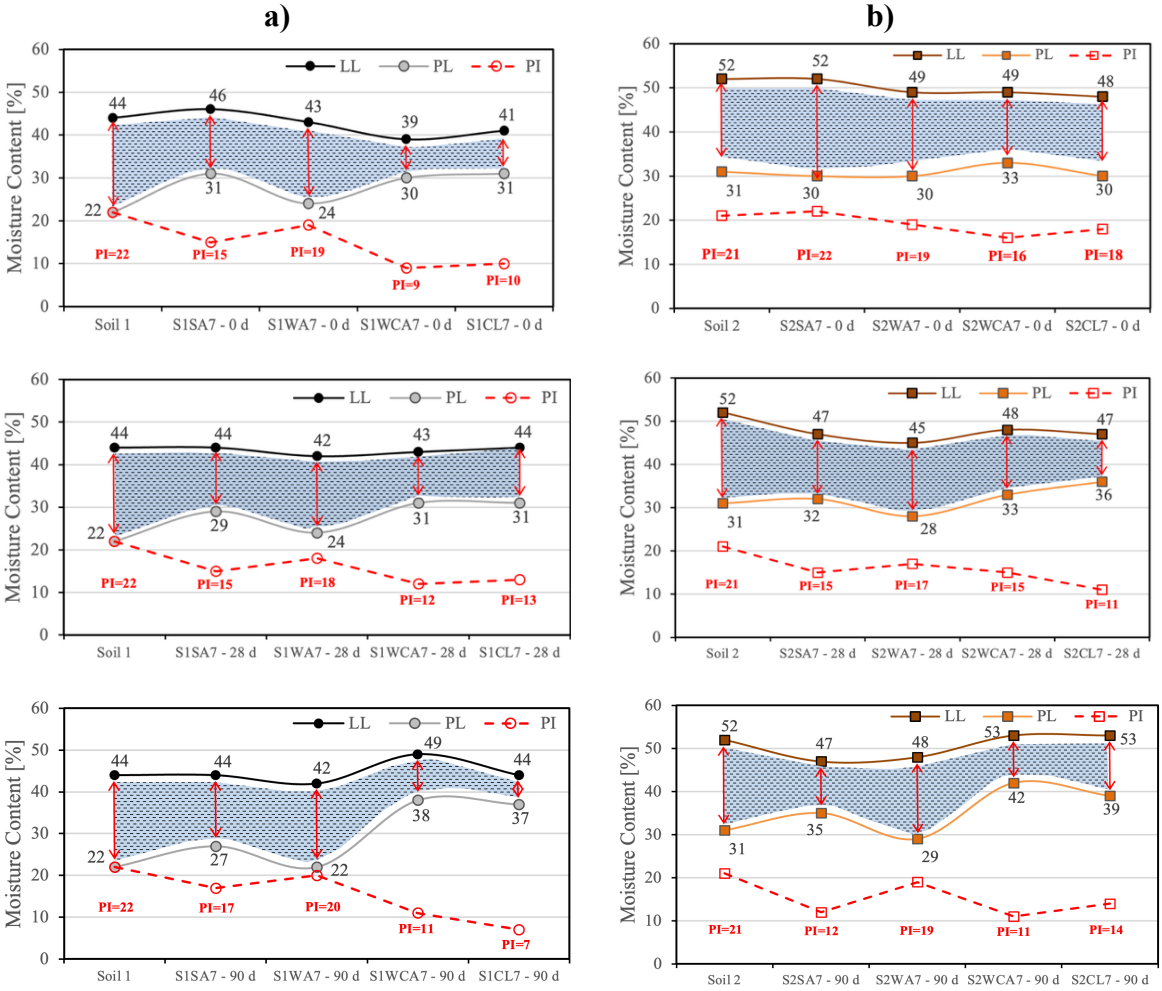

Source: Elaborated by the author

In general, it is observed that, regardless of the processing stage, the addition of ash significantly reduces the Plasticity Index (PI) of the mixtures. This behavior becomes evident when comparing the PI of the natural soils with that of the ash-containing mixtures. In practical terms, this reduction in PI means a decrease in the plastic behavior of the mixtures, making them less susceptible to plastic deformations resulting from moisture increases in the pavement structure.

On a case-by-case basis, it is found that the addition of unwashed ash (SA) reduces the PI of the mixtures more than washed ash (WA). This behavior is observed both immediately after ash addition (0 days) and after 28 and 90 days of curing. The only exception occurred in Soil 2 at 0 days, where the mixture with unwashed ash showed a PI of 22, while the washed ash mixture exhibited a slightly lower value of 19. These results are consistent with the findings of Medeiros (2023), Yadav *et al*. (2019), Okagbue (2007), and Diamond and Kinter (1965), who report that the addition of lime or various biomass ashes reduces the PI of evaluated soils.

The addition of calcined ash, when compared to uncalcined ashes and natural soils, significantly reduces the PI, which strongly indicates the higher reactivity of this material. Okagbue (2007) states that the set of reactions observed in a soil-lime system can also be attributed to a soil-biomass ash system. Thus, supporting the aforementioned author's assumptions, in all cases a reduction in the plastic domain (i.e., reduction in PI) due to calcined ash was observed, reaching levels comparable to those induced by commercial lime. In Soil 1, the addition of calcined ash reduced the PI of the mixture to approximately half of that of the natural soil, from 22 to 11 after 90 days of curing. In Soil 2, the PI was similarly reduced to 11 from an initial value of 21.

Commercial lime (CL) exhibits similar behavior to calcined ash (SWCA). In Soil 1, the addition of CL results in virtually the same PI values at 0 and 28 days of curing when compared to SWCA. Only after 90 days does the mixture with CL reduce the PI to about one-third, from 22 to 7, while the SWCA mixture reduced it to 11. In Soil 2, both materials showed comparable behavior; however, after 90 days, SWCA outperformed CL, reducing the PI from 21 to 11, whereas CL achieved a reduction to 14.

Moving on to the Plastic Limit (PL), similar general behaviors are observed in both soils across the curing periods. Specifically, the addition of unwashed ash (SA) tends to increase the PL of the mixtures, corroborating the findings of Medeiros (2023). Although this

general trend was not observed in the Soil 2 mixture at 0 days of curing, all other conditions were consistent with this behavior.

For the mixtures with washed ash (WA), the PL values were nearly equivalent to those of the natural soils. This suggests that the addition of WA has minimal effect on PL and reveals opposite tendencies in mixtures with Soils 1 and 2. This may indicate that the lower concentration of soluble compounds extracted during washing, such as potassium, limits the potential for cation exchange and flocculation reactions, which are responsible for immediate PL increases, as noted by Diamond and Kinter (1965), Picchi *et al*. (1988), and Okagbue (2007).

In Soil 1, a slight increase in PL is observed, while in Soil 2, a small reduction is noted. Specifically, in Soil 1, the PL increases from 22 (natura) to 24 in the WA mixture at 0 and 28 days, returning to 22 after 90 days. In Soil 2, the PL decreases from 31 to 30 at 0 days, with changes of 3 and 2 points at 28 and 90 days, respectively.

In mixtures with calcined ash (SWCA), however, an increase in PL is observed in all conditions. In Soil 1, PL increases from 22 to 30 immediately after SWCA addition, reaching 31 at 28 days and 38 at 90 days. In Soil 2, a similar but less pronounced trend is observed: PL increases from 31 to 33 initially, remains stable at 28 days, and rises to 42 at 90 days. These differences may be attributed to variations in the types and concentrations of exchangeable cations in each soil's clay minerals, influencing the likelihood of these reactions (Diamond and Kinter, 1965). According to these authors, time also contributes to system changes; while initial effects may be minor (Lund; Ramsay, 1959), time-dependent changes may occur, as also reported by Wolfe and Allen (1964).

Mixtures with commercial lime (CL) exhibit PL values similar to those of SWCA mixtures. Both materials significantly influence this parameter, showing a trend of increasing PL with curing time, again supporting Lund and Ramsay (1959), Wolfe and Allen (1964), and Diamond and Kinter (1965). It is noteworthy that in Soil 1, this increase is more abrupt, while in Soil 2 it is more gradual and continuous. In natural Soil 1, PL increases from 22 to 31 immediately after CL addition, remains stable at 28 days, and reaches 37 at 90 days. In Soil 2, PL increases from 30 (0 days) to 36 (28 days), and reaches 39 after 90 days.

From the perspective of the Liquid Limit (LL), the addition of uncalcined ashes (SA and WA) has less influence on Soil 1 mixtures compared to Soil 2 mixtures. In Soil 1, LL remains stable around the natural value of 44, with a slight decreasing trend observed in WA mixtures, which show LL values of 42 at 28 and 90 days. In Soil 2, while the LL was minimally affected at 0 days, more significant reductions are seen from 28 days onward. The

natural soil LL of 52 drops to 47 (SA) and 45 (WA). At 90 days, the LL of the SA mixture remains stable, while that of the WA mixture increases slightly from 45 to 48.

In mixtures with calcined ash and commercial lime, immediate addition of these materials reduces the LL compared to natural soils. At 28 days, in Soil 1, LL returns to values close to the original, while in Soil 2, it slightly decreases, maintaining similar magnitudes as at 0 days. By 90 days, LL returns to initial levels in all mixtures, except for Soil 1 with SWCA, which reaches 49 (natural = 44).

These results support Diamond and Kinter (1965), who highlight the difficulty of generalizing LL behavior following lime addition, with various studies reporting different trends (Wang; Mateos; Davidson, 1963; Zolkov, 1962). Others, such as Lund and Ramsay (1959), Woods and Yoder (1952), and Taylor and Arman (1960), report that both trends may occur depending on soil type.

In summary, it is evident that the addition of ash, regardless of its processing level, reduces the PI of mixtures. While uncalcined ashes (SA and WA) result in smaller reductions, calcined ash and commercial lime (SWCA and CL) promote more significant decreases.

It is also noted that unwashed ash (SA) has a greater impact on PL than washed ash (WA), suggesting that the reduced potassium concentration from washing lowers the material's reactivity. Authors such as Diamond and Kinter (1965) and Picchi *et al.* (1988) state that cation exchange and flocculation are fast-acting mechanisms in soil-lime systems, which Okagbue (2007) also attributes to soil-ash systems.

Furthermore, larger fluctuations in PL and LL are observed with increasing curing time, particularly in mixtures with calcined ash (SWCA) and commercial lime (CL). This behavior indicates that while uncalcined ashes tend to develop fast reactions (cation exchange and flocculation), calcined ash and commercial lime also promote pozzolanic reactions, which are responsible for long-term strength gains, as described by Diamond and Kinter (1965).

4.4.2 *California Bearing Ratio (CBR)*

While Section 4.1.6.1 presents Mini-CBR data for all mixtures at the three evaluated contents, the graphs shown in Figure 66 and Figure 67 illustrate the behavior of the California Bearing Ratio (CBR) and expansion of the soils and the best-performing mixtures over three curing periods (0, 28, and 90 days). The repetition of the bearing capacity and expansion tests, previously conducted on a miniature scale and now performed using conventional methods, is justified by the limited availability of calcined ashes and by the importance of

providing data that support the empirical pavement design criteria applied to the most promising mixtures.

Figure 66: CBR performance of soils and the most promising mixtures

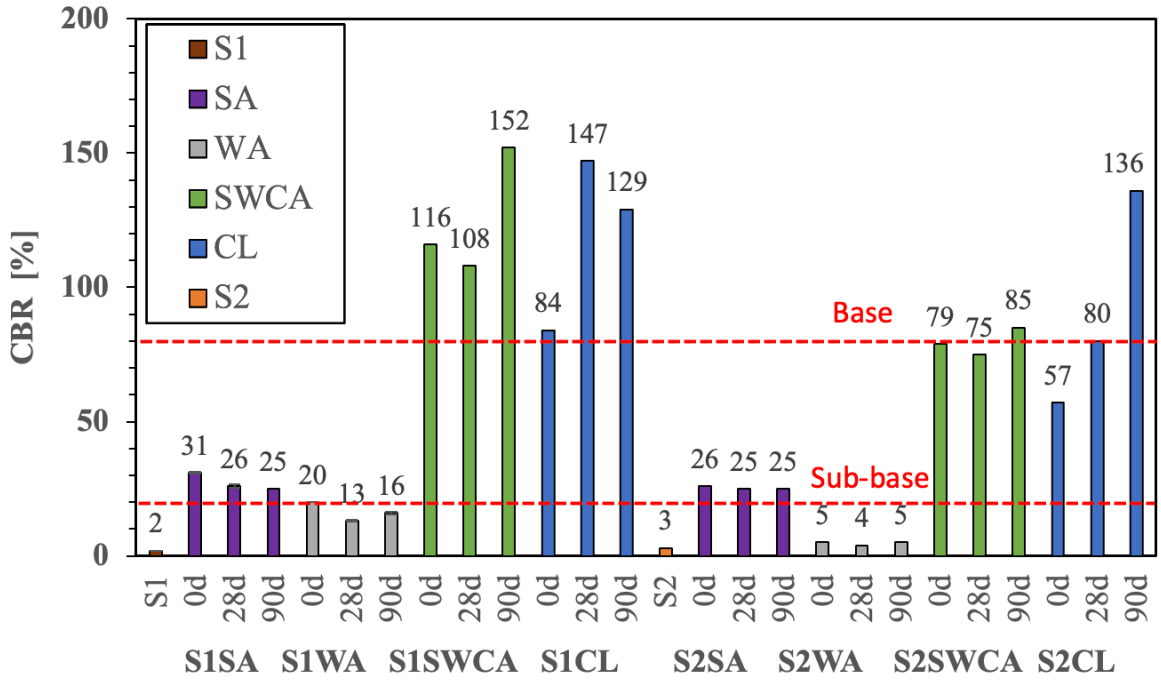

Source: Elaborated by the author

Figure 67: Expansion of soils and the most promising mixtures

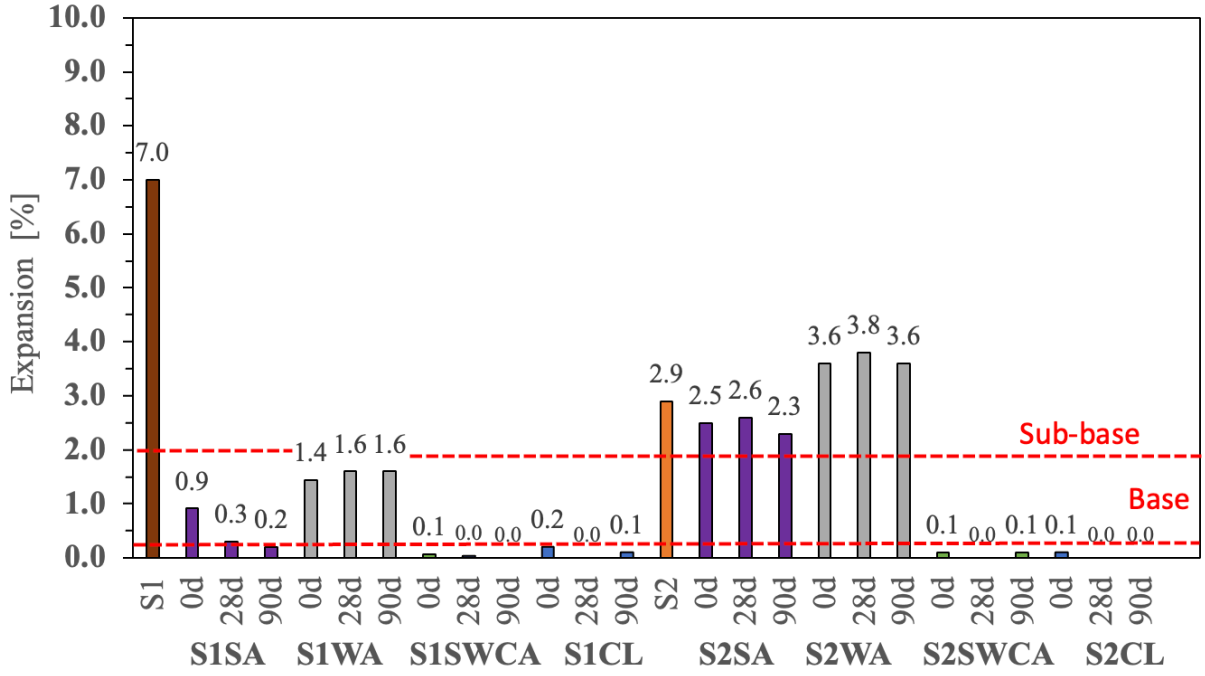

Source: Elaborated by the author

To better synthesize the results presented in Figures 66 and 67 and to align them with the acceptance criteria established by DNIT (2006), Table 24 summarizes the performance

of the soils and mixtures in terms of CBR and expansion. This comparative framework highlights which materials are suitable for use in different pavement layers (subgrade, subbase, and base) and which are unsuitable, considering both mechanical strength and volumetric stability.

Table 24: Suitability of soils and mixtures for pavement layers based on CBR and expansion criteria

Material / Mixture	CBR behavior	Expansion behavior	Pavement layer suitability
Natural soils Soil 1: CBR 2% Soil 2: CBR 3%	Very low CBR (2–3%), below requirements	High expansion (7.0% and 2.9%)	Unsuitable as subgrade/subbase without stabilization
Unwashed ash (SA)	CBR ↑ (Soil 1: 31→25%; Soil 2: ~25%, stable) but reduction over time (Soil 1)	Expansion ↓ (Soil 1: 0.9→0.2%), but ineffective for Soil 2 (~2.5%)	Soil 1: acceptable for subbase (CBR >20%, expansion <1%); Soil 2: unsuitable due to high expansion
Washed ash (WA)	Slight CBR ↑ vs natural soils; lower than SA; Soil 1: only 20% at 0 d; Soil 2: ~5%	Expansion ↓ but less effective than SA (Soil 1: 1.4–1.6%; Soil 2: ~2.5%)	Soil 1: marginal for subbase at 0 d; Soil 2: unsuitable
Calcined ash (SWCA)	Strong CBR ↑ (Soil 1: 116–129%; Soil 2: 75–85%)	Expansion ≈ 0% (<0.5%)	Suitable for base layers (CBR >80%, expansion <0.5%)
Commercial lime (CL)	High CBR (Soil 1: >80%; Soil 2: 57–136%)	Expansion ≈ 0% (<0.5%)	Suitable for base layers

It was found that bearing capacity (CBR) of Soils 1 and 2 is 2% and 3%, respectively, and their expansion is 7.0% and 2.9%. Since DNIT (2006) requires subgrades to have CBR values ≥ 2% and expansion ≤ 2%, these natural soils are considered unsuitable for use in pavement layers without the incorporation of stabilizing agents.

It is also observed that the addition of unwashed ashes (SA) increases the CBR of both soils, with a trend of decreasing bearing capacity over time for Soil 1 and stable behavior for Soil 2, corroborating the findings reported by Okagbue (2007). For Soil 1, CBR values of 31%, 26%, and 25% were recorded at 0, 28, and 90 days, respectively, indicating a slight reduction over time. In contrast, for Soil 2, the values remained stable at 26%, 25%, and 25% for the same curing periods. From the perspective of expansion, a decreasing trend was observed in both soils. For Soil 1, expansion reduced from 0.9% to 0.3% and 0.2% at 0, 28, and 90 days, respectively. For Soil 2, however, the unwashed ashes (SA) were less effective

in controlling expansiveness, with values of 2.5%, 2.6%, and 2.3% over the same curing periods.

Okagbue (2007) suggests that the strength and consequent reduction in bearing capacity observed between 7 and 14 days in clayey soil mixtures with wood ash occur due to the rapid consumption of free lime during the first weeks of curing, leaving little or no available lime to sustain the pozzolanic reactions responsible for strength gain in clay–lime mixtures.

According to DNIT (2006) and considering only the CBR criterion, mixtures with unwashed ashes (SA) can be used as reinforcement for subgrade and/or subbase layers, since the pavement manual requires a CBR greater than 20% for the latter application. However, from the perspective of expansion, only Soil 1 meets the criteria established by the Brazilian standard, which recommends that expansions in subbase layers be less than 1%, thus classifying Soil 1 as suitable and Soil 2 as unsuitable for this purpose.

The mixtures of soils with washed ashes (WA) show an increase in CBR compared to the natural soils but a decrease relative to the mixtures with unwashed ashes (SA). Only the mixture with Soil 1 at 0 days reached a CBR of 20%, which would qualify the mixture for use as a subbase. However, a decreasing trend in CBR is observed over time, with values of 13% and 16% at 28 and 90 days for Soil 1, respectively. In contrast, Soil 2 exhibits stable behavior with CBR values around 5%, rendering these mixtures unsuitable for use as subbase material.

Regarding expansion, it is observed that the addition of washed ashes (WA) reduces this parameter compared to the natural soils for both soils, although more significantly for Soil 1. However, compared to unwashed ashes (SA), washed ashes (WA) are less effective in reducing expansion, with values of 1.4%, 1.6%, and 1.6% at 0, 28, and 90 days of curing for Soil 1, respectively, while for Soil 2, the values are 2.5%, 2.6%, and 2.3% for the same curing periods.

From the perspective of calcined ashes (SWCA), there are significant increases in CBR values for both soils. For Soil 1, CBR values were notably higher than those of Soil 2, with values of 116%, 108%, and 129% at 0, 28, and 90 days of curing, respectively. For Soil 2, CBR values of 79%, 75%, and 85% were observed for the same curing periods. Regarding expansion, the addition of calcined ashes (SWCA) reduced the parameter to nearly zero for both soils across all curing periods evaluated, rendering the mixtures suitable for use in base layers. This suitability is due to expansions below 0.5% at all curing times and CBR values exceeding 80% at the longer curing periods.

A similar behavior is observed for the mixtures with commercial lime (CL). For Soil 1, all CBR values exceed 80%, with 84%, 147%, and 129% recorded at 0, 28, and 90 days of curing, respectively. In Soil 2, CBR values of 57%, 80%, and 136% were observed for the same curing periods. Regarding expansion, the addition of commercial lime (CL) drastically reduces this parameter to values fully acceptable for use in base layers, with all observed expansions below 0.5%.

It is observed that the CBR and expansion behavior of the most promising mixtures corroborates the results obtained in the miniature tests. The addition of uncalcined ashes (SA and WA), especially the unwashed ashes (SA), improves the bearing capacity and reduces the expansiveness of the soils, although to a much lesser extent than the calcined materials (SWCA and CL). This makes the mixtures with Soil 1 suitable for use in subbase layers when using unwashed ashes (SA), and in pavement base layers when using calcined materials (SWCA and CL). For mixtures with Soil 2, only the addition of calcined materials renders the soil suitable for base layers, since the unwashed ashes (SA) did not reduce the expansiveness of the mixture to desirable levels.

The gains in bearing capacity resulting from the addition of ashes—particularly the unwashed ashes and calcined materials (SA, SWCA, and CL)—are related to the immediate flocculation and cation exchange reactions caused by the CaO content present in these materials, as suggested by authors such as Okagbue (2007) and Zagvozda *et al.* (2017). In the case of washed ashes, the free CaO meets the water during the washing process, converting it into hydroxides, as mentioned by Melo (2018). These hydroxides, when exposed to air during drying and storage stages, can be converted into calcium carbonate, a material with low reactivity according to Picchi *et al*. (1988), thereby reducing the reactivity of these ashes and interfering with the chemical stabilization process.

According to Vasconcelos (2018), although the CBR test is not the most appropriate method to evaluate the mechanical behavior of stabilized mixtures—since its methodology is based on penetration resistance rather than on the stiffness resulting from chemical stabilization processes—it is still widely used as a traditional means of comparing granular materials employed in pavement layers.

4.4.3 *Resilient modulus*

Resilient Modulus (MR) tests are conducted on mixtures containing Calcined Ashes (SWCA) and Commercial Lime (CL) after 0, 28, and 90 days of curing. Five models were tested to identify those that best represent the experimental MR data. For the mixtures

considered stabilized, those cured for 28 and 90 days, the DNIT 181/2018-ME protocol, which does not include confining stresses, was initially applied. Due to technical constraints, vertical deformations for these mixtures were measured at the top of the specimen rather than at the central third, as recommended by the standard. Table 25 presents the parameters obtained under unconfined conditions, following DNIT 181/2018-ME. Natural soils and mixtures with 0 days of curing were not tested without confining stress, as they are not considered stabilized materials.

Table 25: Resilient Modulus regression parameters – (DNIT – 181/2018)

Sample	$MR = k1 \times \sigma d^{k2}$ [MPa]		
	k_1	k_2	R^2
S1	-	-	-
S2	-	-	-
S1SWCA7 -0d	-		
S1SWCA7 -	798.2	0.271	0.927
S1SWCA7 -	1266.2	0.416	0.952
S1CL7 – 0d	-	-	-
S1CL7 - 28d	555.1	0.282	0.876
S1CL7 - 90d	1180.2	0.568	0.998
S2SWCA7 -0d	-	-	-
S2SWCA7 -	840.1	0.028	0.040
S2SWCA7 -	852.8	0.457	0.989
S2CL7 - 0d	-	-	-
S2CL7 - 28d	259.1	0.303	0.997
S2CL7 - 90d	739.9	0.426	0.999

Source: Elaborated by the author

Additionally, for all mixtures, the testing protocol established by DNIT 134/2018-ME is applied. This standard is suitable for unbound materials and involves the application of lateral confining stresses and measurement of displacements at the top of the specimens. Table 26 and Table 27 present the parameters for simple and composite models based on experimental data obtained under confining stresses, in accordance with DNIT 134/2018-ME.

Table 26 : Resilient Modulus parameters (DNIT-134/2018)

	$MR = k1 \times \sigma d^{k2}$ [MPa]			$MR = k1 \times \sigma 3^{k2}$ [MPa]			$MR = k1 \times \theta^{k2}$ [MPa]		
	k_1	k_2	R^2	k_1	k_2	R^2	k_1	k_2	R^2
S1	119.2	-0.346	0.881	104.7	-0.318	0.504	164.4	-0.364	0.688
S2	63.6	-0.385	0.772	53.3	-0.367	0.479	90.21	-0.415	0.643
S1SWCA7 -0d	Specimen disintegrated during the conditioning phase								
S1SWCA7 -28d	1002.5	0.195	0.508	1743.9	0.327	0.857	1390.1	0.327	0.857
S1SWCA7 -90d	2627.7	0.354	0.742	5321.7	0.496	0.907	3733.3	0.496	0.907

S1CL7 – 0d	38.89	-0.713	0.124	132728.0	0.013	0.005	76.3	-0.427	0.027
S1CL7 - 28d	730.4	0.162	0.540	1182.0	0.278	0.947	974.4	0.278	0.948
S1CL7 - 90d	2424.5	0.393	0.720	5930.7	0.584	0.959	3953.8	0.584	0.954
S2SWCA7 -0d	85.7	-0.146	0.359	92.5	-0.088	0.085	101.7	-0.124	0.186
S2SWCA7 -28d	474.31	0.008	0.002	405.3	-0.043	0.043	417.4	-0.043	0.043
S2SWCA7 -90d	1666.9	0.400	0.734	4132.5	0.600	0.942	2725.9	0.600	0.942
S2CL7 - 0d	91.2	-0.202	0.583	89993.0	-0.164	0.243	100.8	-0.164	0.262
S2CL7 - 28d	496.0	0.468	0.917	883.4	0.555	0.719	601.0	0.555	0.728
S2CL7 - 90d	1626.0	0.395	0.720	4054.1	0.597	0.951	2678.8	0.597	0.948

Source: Elaborated by the author

Table 27 Resilient Modulus parameters – Compound models - (DNIT-134/2018)

	$MR = k1 \times \sigma 3^{k2} \times \sigma d^{k3}$ [MPa]				**$MR = k1 \times (\theta/Patm)^{k2} \times (\tau oct/Patm)^{k3}$ [MPa]**			
	k_1	**k_2**	**K_3**	**R^2**	**k_1**	**k_2**	**K_3**	**R^2**
S1	153.1	0.081	-0.343	0.878	189.4	0.125	-0.387	0.877
S2	85.1	0.071	-0.355	0.803	113.5	0.105	-0.390	0.802
S1SWCA7 -0d	Specimen disintegrated during the conditioning phase							
S1SWCA7 -28d	1905.9	0.327	0.035	0.869	373.2	0.518	-0.160	0.865
S1SWCA7 -90d	5302.2	0.385	0.140	0.968	639.6	0.626	-0.103	0.963
S1CL7 – 0d	3957	0.628	0.372	0.999	77.1	0.324	-0.324	0.702
S1CL7 - 28d	1216	0.270	0.021	0.954	319.5	0.429	-0.141	0.950
S1CL7 - 90d	5530.3	0.467	0.123	0.992	459.9	0.764	-0.176	0.991
S2SWCA7 -0d	108.6	0.173	-0.263	0.479	74.5	0.278	-0.367	0.486
S2SWCA7 -28d	394.4	-0.103	-0.064	0.131	572.7	-0.155	0.119	0.118
S2SWCA7 -90d	3795.8	0.406	0.143	0.996	320.2	0.741	-0.140	0.997
S2CL7 - 0d	108.3	0.113	-0.272	0.626	100.7	0.182	-0.341	0.629
S2CL7 - 28d	685.9	0.223	0.313	0.975	137.0	0.349	0.184	0.973
S2CL7 - 90d	3761.4	0.468	0.133	0.996	310.4	0.753	-0.155	0.995

Source: Elaborated by the author

It is observed that none of the five models consistently provides the best fit to the experimental data for all mixtures. However, it is found that the composite model dependent on σ_3 and σd represents the greatest number of mixtures with high R^2 values. Table 28 shows the composite models with the average modulus value. The relevance of presenting average values lies solely in making the overall behavior more explicit through a single representative number; nevertheless, it is important to recognize that relying exclusively on the mean is not appropriate, since stress conditions vary with depth in the pavement structure and, consequently, so does the resilient response.

Table 28: Average resilient modulus

Sample	**$MR = k1 \times \sigma 3^{k2} \times \sigma d^{k3}$ [MPa]**				**Average Modulus** [MPa]
	k_1	**k_2**	**K_3**	**R^2**	
S1	153.1	0.081	-0.343	0.878	267.1

S2	85.1	0.071	-0.355	0.803	157.8
S1SWCA7 -0d	-				
S1SWCA7 -28d	1905.9	0.327	0.035	0.869	618.5
S1SWCA7 -90d	5302.2	0.385	0.140	0.968	1110.4
S1CL7 – 0d	3957	0.628	0.372	0.999	130.4
S1CL7 - 28d	1216	0.270	0.021	0.954	487.6
S1CL7 - 90d	5530.3	0.467	0.123	0.992	936.8
S2SWCA7 -0d	108.6	0.173	-0.263	0.479	120.7
S2SWCA7 -28d	394.4	-0.103	-0.064	0.131	466.3
S2SWCA7 -90d	3795.8	0.406	0.143	0.996	625.9
S2CL7 - 0d	108.3	0.113	-0.272	0.626	146.1
S2CL7 - 28d	685.9	0.223	0.313	0.975	154.9
S2CL7 - 90d	3761.4	0.468	0.133	0.996	618.7

Source: Elaborated by the author

To simplify and visually assess the behavior of the resilient modulus of the soils and mixtures, composite models based on the confining stress protocol (DNIT-134/2018) were taken and the surfaces of these models were generated. Figure 68 and Figure 69 illustrates the resilient behavior of these materials.

Figure 68: Resilient Modulus surface for in natura soils.

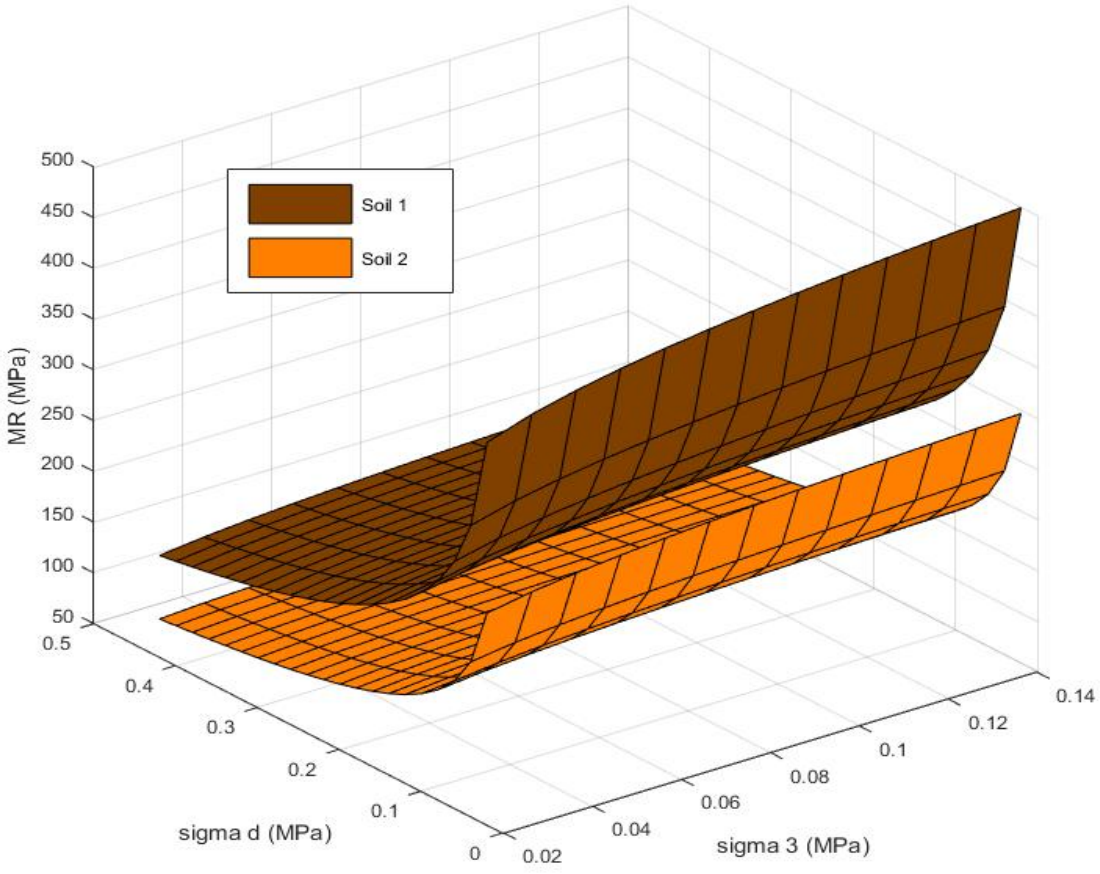

Source: Elaborated by the author

Figure 69: Resilient Modulus surface for mixtures

a) S1SWCA

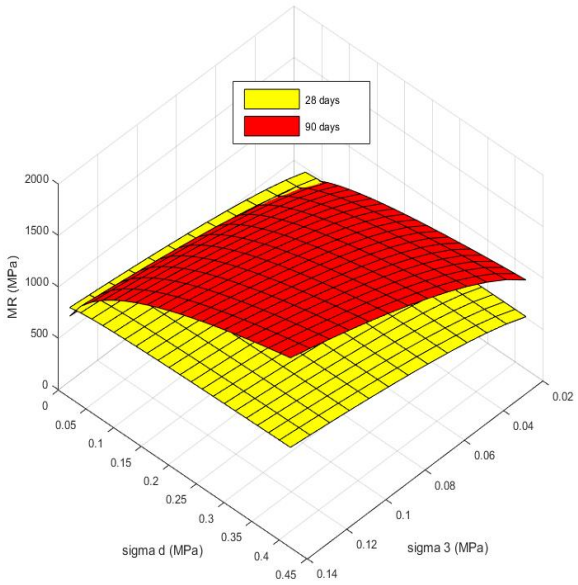

b) S2SWCA

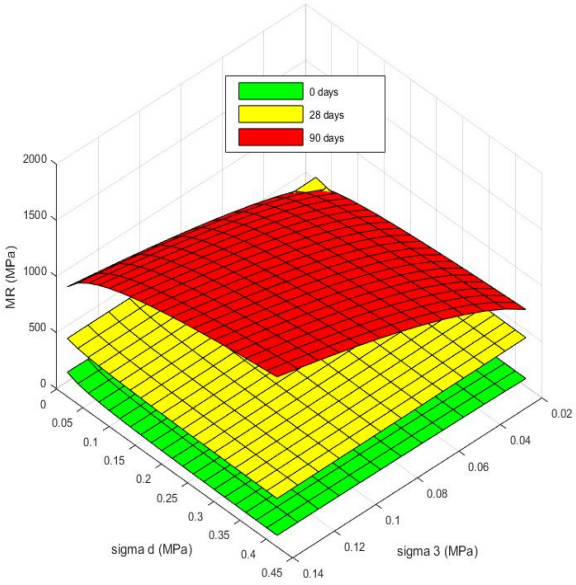

c) S1CL

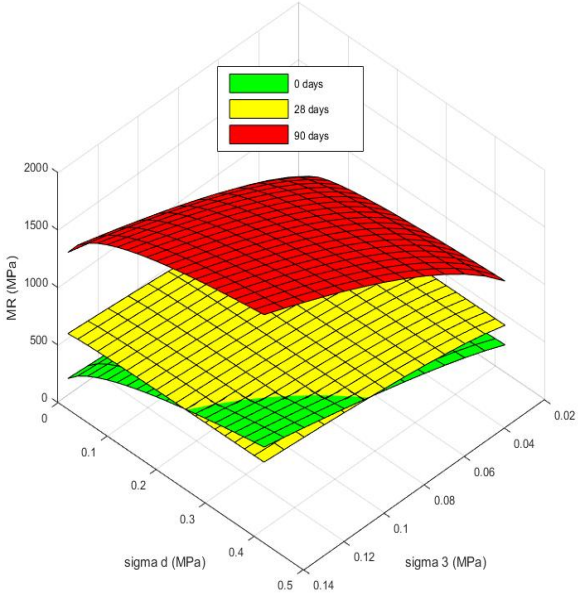

d) S2CL

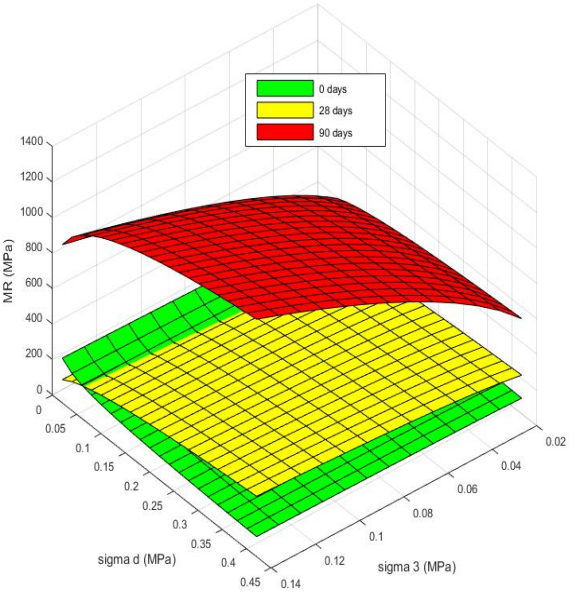

Source: Elaborated by the author

It is observed that the natural soils exhibit a strong dependence on deviator stresses (σd) and little influence from confining stresses (σ_3). The Resilient Modulus (MR) values of Natural Soil 1 are approximately twice those observed for Natural Soil 2 under the same stress conditions. For lower deviator stress values (σd), Soil 1 presents MR values around 400 MPa, while Soil 2 reaches approximately 200 MPa. Under the highest applied deviator stresses, MR values decrease to approximately 200 MPa for Soil 1 and 100 MPa for Soil 2.

Furthermore, it is observed that an increase in deviator stress (σd) leads to a reduction in MR values for both natural soils. This behavior is consistent with the findings of Achampong, Usmen, and Kagawa (1997) and aligns with the textural characteristics of the

materials, as more plastic soils, due to their higher cohesion and compressibility, tend to exhibit lower resilient stiffness under higher stress levels (Puppala, Mohammad, and Allen, 1996; AASHTO, 2007).

In mixtures with the addition of calcined ashes (SWCA) at 0 days of curing, a reduction in the resilient capacity of both soils is observed. In the case of Soil 1, this effect is more pronounced, to the point that the specimen did not withstand the preconditioning phase prior to testing. For Soil 2, significant losses in MR are observed at low deviator stress levels, with relatively stable values at higher σd levels compared to the natural soil. These losses may be associated with immediate reactions between the stabilizing agents and the soil's clay minerals, which negatively affect plasticity and internal cohesion, thereby compromising the initial strength of the mixtures.

With the addition of commercial lime (CL) and no curing period, a reduction in MR values is also observed for Soil 1, culminating in the disintegration of the specimen under higher deviator stresses. In the case of the Soil 2 mixture, MR values are slightly higher than those obtained with SWCA, ranging between 100 and 200 MPa, which are close to the levels observed in natural Soil 2. This behavior suggests that, in Soil 1, the initial reactions with CL were more intense, leading to a more significant reduction in plasticity and cohesion, which negatively affected the resilient response under immediate conditions.

Studies such as those by Quispe (2012) and the technical report by ANTT and CCR Nova Dutra (2014) report that the immediate reactions resulting from the addition of ash or lime made the evaluated soils more friable and less cohesive at early stages. As the primary objective of soil stabilization for pavement purposes is the long-term gain in strength and stiffness, it is less common for studies to examine the resilient behavior of stabilized mixtures without curing. However, for the purpose of understanding stabilization mechanics and for projects involving loading shortly after construction, this initial phase can be relevant.

At 28 days of curing, an increase in Resilient Modulus (MR) is observed at higher deviator stress levels across all mixtures (with SWCA and CL) and for both soils. The reversal of the behavior seen in the natural samples suggests a loss of plasticity and an increase in the internal cohesion of the mixtures, resulting from the progression of cementitious reactions. These reactions contribute to a more elastic response of the materials, as opposed to a plastic behavior, in agreement with the findings of Araujo (2009), Vasconcelos (2018), Bhuwaneshwari, Robinson, and Gandhi (2019), and Mahmood, Hassan, and Fouad (2021).

The mixtures with Soil 1 stabilized with SWCA and CL exhibited MR values ranging from 400 to 600 MPa and from 250 to 400 MPa, respectively. On the other hand, the mixtures with Soil 2 reached MR values on the order of 800 MPa with SWCA and between 170 and 200 MPa with CL. It is noteworthy that the high MR values for Soil 2 with SWCA at 28 days deviate from the expected behavior. This discrepancy may be attributed to accidental moisture loss during the curing period, which could have compromised the representativeness of the results.

This atypical behavior of Soil 2 with SWCA also stands out compared to the results obtained after 90 days of curing. At this stage, the trend of increasing MR values with rising deviator stress is maintained for both Soil 1 and Soil 2, regardless of the stabilizer used (SWCA or CL). In general, mixtures with SWCA exhibited slightly higher values than those with CL. Although this performance may indicate greater reactivity of calcined ashes compared to commercial lime, this hypothesis cannot be confirmed based solely on these data, since possible variations in the internal moisture of the specimens—related to the hygroscopic behavior of the stabilized materials—were neither controlled nor evaluated in this study.

It is therefore observed that all mixtures evaluated at 0 days of curing showed better adherence of the experimental data to the composite model, except for sample S1SWCA7-0d, which disintegrated during the conditioning phase, preventing the test from being performed. This behavior indicates that the immediate reactions caused by the addition of stabilizers significantly modify the resilient performance of the mixtures in the initial period, making the specimens more susceptible to the effects of confining stresses shortly after molding. For the mixtures cured for 28 and 90 days, it was not possible to directly evaluate the influence of confining stresses, since stabilization of the materials is assumed at this stage and the adopted testing protocol does not include the application of variable confining stresses.

4.4.3 *Indirect Tensile Strength (ITS)*

Figure 70 presents the results of the Indirect Tensile Strength (ITS) tests conducted on the mixtures with calcined ashes (SWCA) and commercial lime (CL) after 28 days of curing. The testing protocol was carried out in accordance with the DNER-ME 181/94 standard, which states that the test must be conducted after 24 hours of specimen saturation.

Figure 70: Indirect Tensile Strength (ITS) of stabilized mixtures.

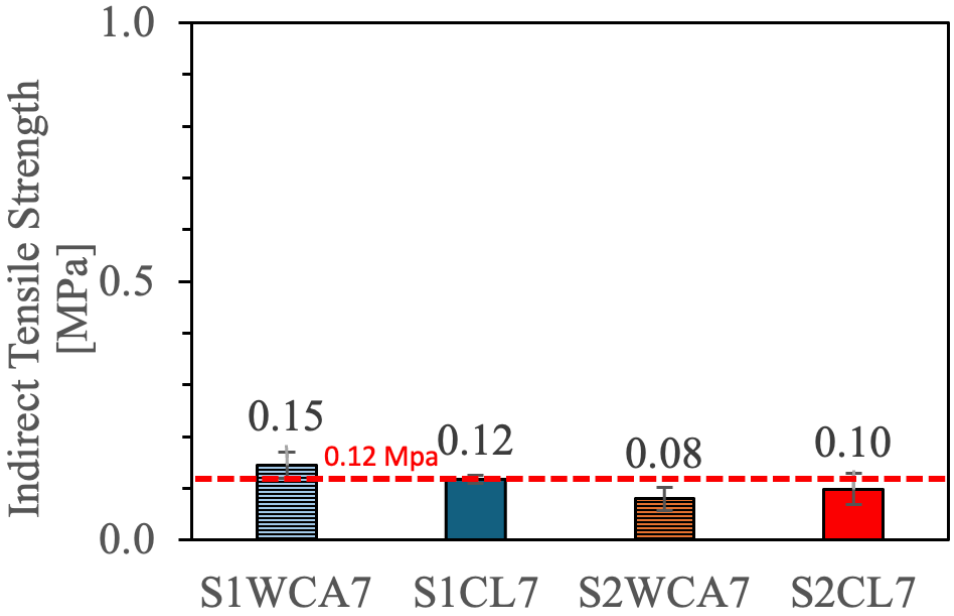

Source: Elaborated by the author

Araújo (2009) states that the tensile strength in lime-soil mixtures indicates the onset of pozzolanic reactions, and that a value of 0.12 MPa represents the boundary between the modified and cemented phases for this type of mixture, while Vasconcelos (2018) suggests a value of 0.10 MPa as the threshold for considering mixtures as cemented. It is observed that the mixtures presented Indirect Tensile Strength (ITS) values ranging from 0.08 to 0.15 MPa. Better performance was observed in the mixtures containing Soil 1, in contrast to those with Soil 2, which indicates greater reactivity of the stabilizing agents with the first soil.

It is likely that Soil 1 contains a higher proportion of kaolinite-type clay minerals, whereas Soil 2 may contain a greater presence of illite. Studies such Ninov and Donchev, 2008) and Maier, Beuntner and Thienel (2021) have shown that kaolinite exhibits high reactivity, with rapid reactions and the formation of durable cementitious products. Illite, on the other hand, although reactive, presents a slower and less complete reaction than kaolinite, with its performance strongly dependent on curing temperature and time. XRD tests may be conducted in the future for a more detailed investigation of the mineralogical profile of the soils.

According to Thompson (1966), the Unconfined Compressive Strength (UCS) and Indirect Tensile Strength (ITS) are related by the expression ITS = 0.13 × UCS, while the TRB (1987) indicates that this relationship is ITS = 0.25 × UCS. Figure 71 compares the expected ITS values based on the relationships proposed by these authors with the ITS values observed in this study.

Figure 71: Expected values *vs* Obtained Values (ITS)

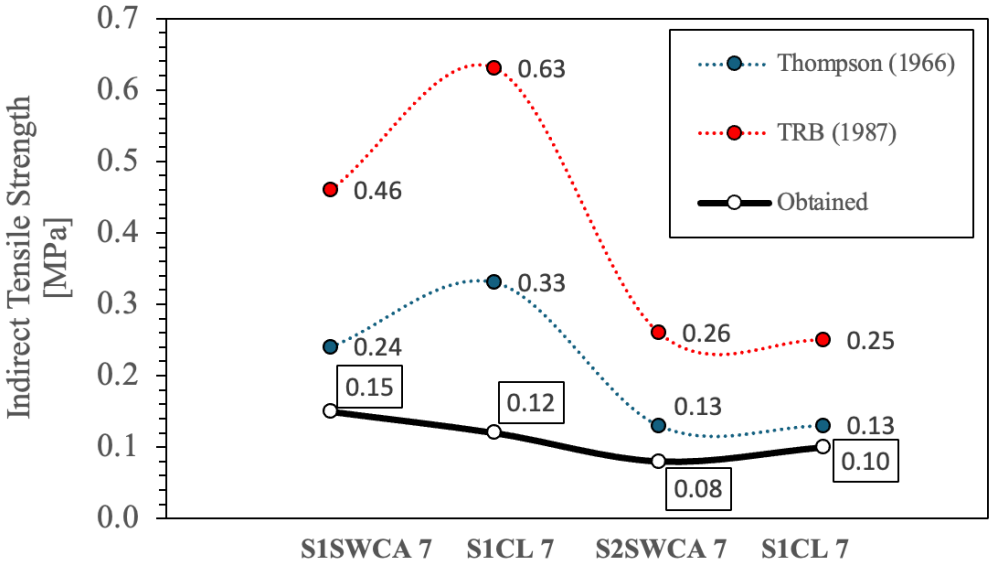

Source: Elaborated by the author

It is observed that the values obtained in this study are lower than those expected based on the correlations proposed by the referenced authors. It is believed that the saturation stage prior to specimen testing accounts for this discrepancy between the expected and observed strength values. In this context, it is important to emphasize the need for future studies to further investigate the relationship between moisture content and both the ITS and fatigue performance of semi-cemented mixtures.

4.4.4 *Fatigue Test*

Figure 72 and Figure 73 present the laboratory fatigue test results for the mixtures containing Soils 1 and 2. While the vertical axis represents the ratio between the applied tensile stress and the tensile strength of the mixture (ITS), the horizontal axis represents the number of load applications until total failure of the specimens.

The overall behavior of the mixtures is as expected: the lower the tensile stress ratio, the higher the number of cycles to specimen failure. For Soil 1, the mixtures stabilized with calcined ashes (SWCA) and commercial lime (CL) showed similar performance, with comparable numbers of cycles to failure, all on the order of 10^5. A similar trend was observed for the mixtures with Soil 2; although at higher stress ratios the specimens failed after a low number of cycles, for the lower stress levels, the number of load applications to failure also reached the order of 10^5.

Figure 72: Fatigue results for S1 mixtures

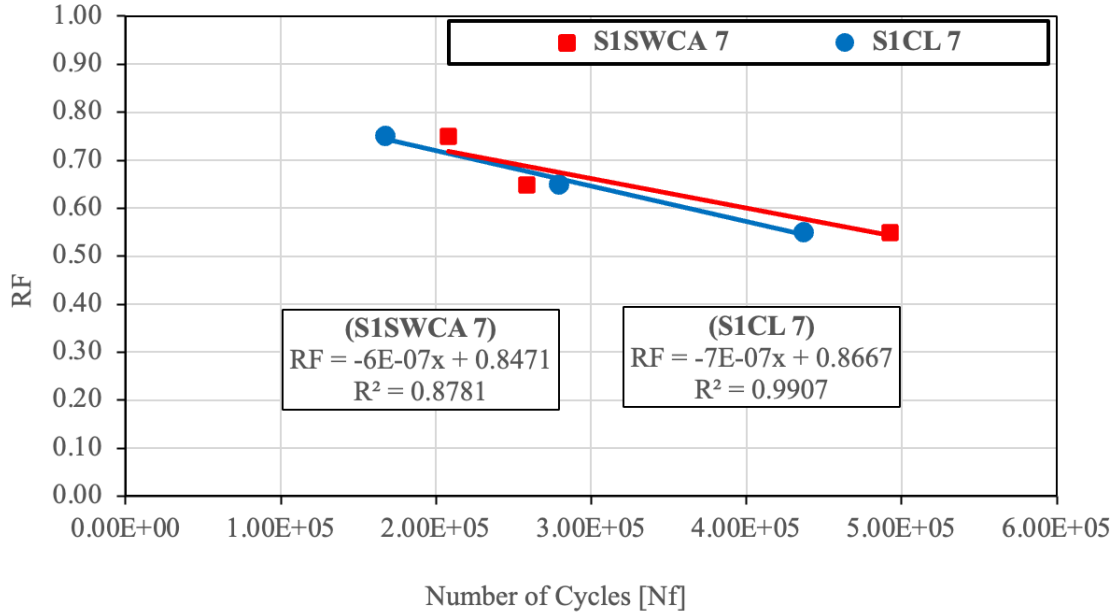

Source: Elaborated by the author

Figure 73: Fatigue results for S2 mixtures

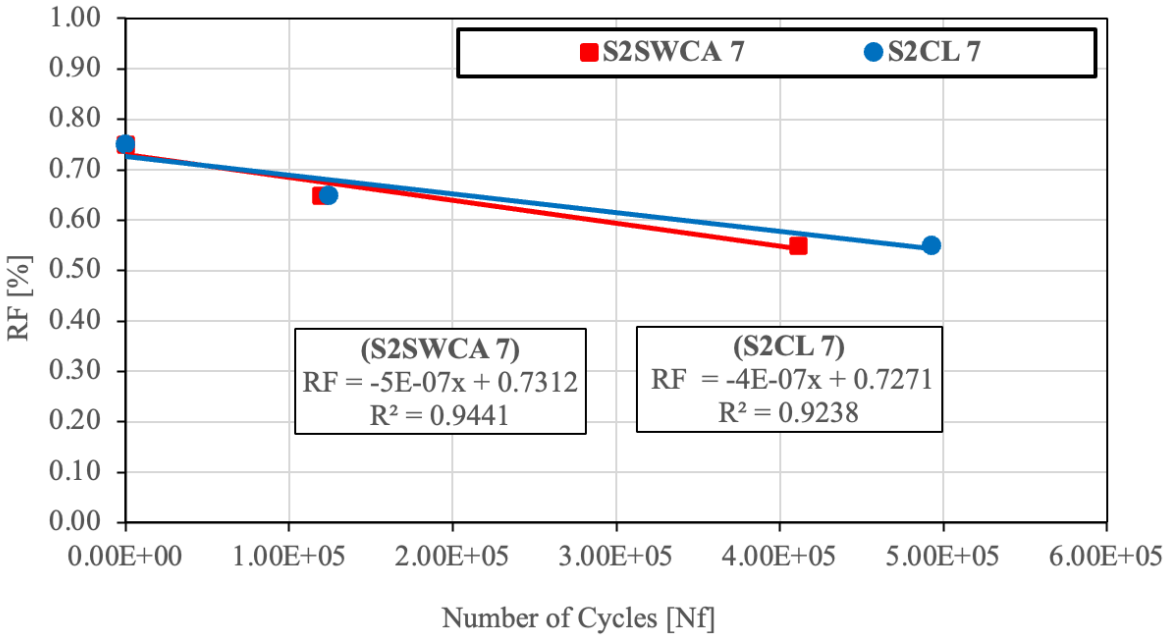

Source: Elaborated by the author

To relate the laboratory fatigue behavior to the predicted field performance, it is first necessary to determine the fatigue equation based on the model proposed by Balbo (1993) (Equation 6) and on the laboratory data. For this purpose, a base-10 logarithmic transformation is applied to the number of load applications (N) for each stress ratio (RF). Then, the intercept (k1) and slope (k2) parameters are determined for each model, thus obtaining the prediction models. Figure 74 and Figure 75 present the laboratory fatigue behavior and the prediction models.

$$N = 10^{(k1 - k2 \times \%RF)} \qquad (6)$$

Figure 74: Determining fatigue equations for S1 mixtures.

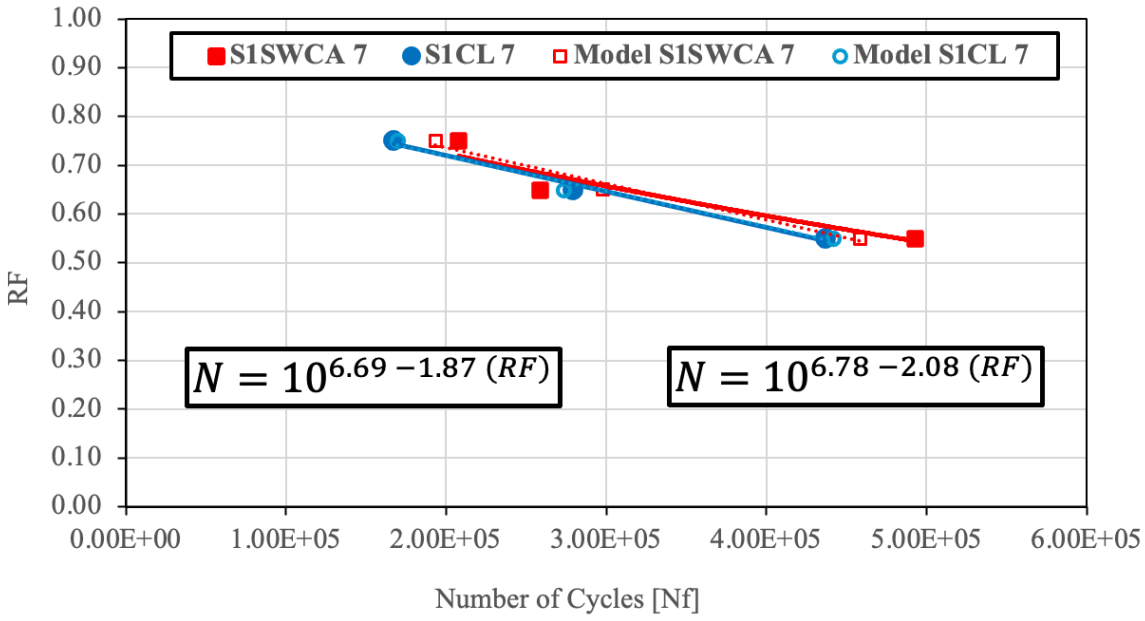

Source: Elaborated by the author.

Figure 75: Determining fatigue equations for S2 mixtures.

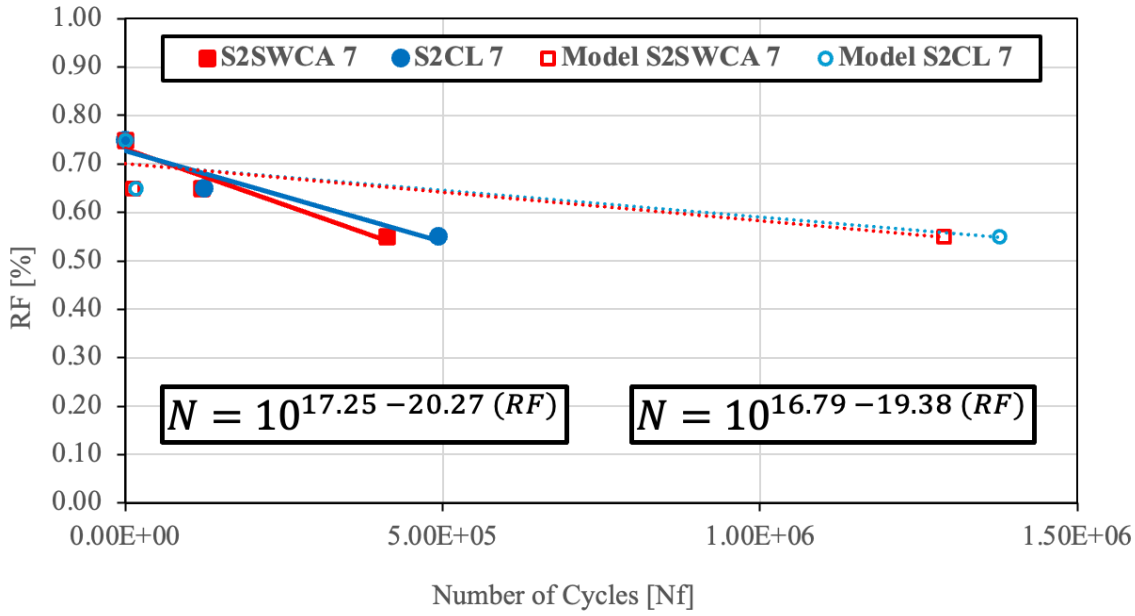

Source: Elaborated by the author

The models for Soil 1 showed satisfactory agreement with the experimental data, whereas the model for Soil 2 did not. This difference is mainly due to the proximity between the values of the number of blows (N) to failure observed in the mixtures with Soil 1, which remain on the order of 10^5 for the three RF levels evaluated, favoring the consistency of the

fit. On the other hand, in the mixtures with Soil 2, the highest RF level resulted in an extremely low number of blows, which compromises the representativeness of the model and explains its inferior performance.

Once the fatigue equations are determined using the Balbo (1993) model, it is possible to estimate the field fatigue performance of the evaluated materials. According to Monteiro et al. (2023), this model is suitable for predicting the fatigue behavior of chemically stabilized mixtures, where N represents the number of load repetitions to failure, %RF is the ratio between the applied tensile stress and the tensile strength of the mixture (expressed as a percentage), and k_1 and k_2 are empirical calibration coefficients. The fatigue equations obtained are presented in Table 29.

Table 29: Fatigue equation for the mixtures

S1SWCA 7	$N = 10^{6.69-1.87\,(RF)}$
S1CL 7	$N = 10^{6.78\,-2.08\,(RF)}$
S2SWCA 7	$N = 10^{17.25\,-\,20.27\,(RF)}$
S2CL 7	$N = 10^{16.79\,-\,19.38\,(RF)}$

Source: Elaborated by the author

Based on these equations, tensile stresses at the bottom fiber of hypothetical pavement sections designed with the evaluated materials are estimated using the AEMC design software developed by DNIT (2023), which allows the assessment of fatigue life in scenarios where such mixtures are incorporated into pavement structures. Considerations on field fatigue performance are discussed in the Design Section.

4.5 *Environmental Analysis*

The Brazilian standard ABNT NBR 10004 classifies solid waste as either hazardous or non-hazardous, with the latter further subdivided into inert and non-inert waste. According to the standard, hazardous waste is characterized by properties such as flammability, corrosivity, reactivity, toxicity, or pathogenicity.

4.5.1 *Classification of solid waste*

The ashes evaluated in this study, based on the criteria outlined in the standard, are not considered to exhibit flammability, reactivity, or pathogenicity. Therefore, the analysis focuses on assessing the corrosivity and toxicity of these materials. To this goal, pH testing is conducted to evaluate the corrosive potential of the residues, while solubilization and

leaching tests are performed to analyze the extracts and determine the presence and concentration of potentially toxic compounds.

4.5.2 *Characterization of pH and corrosivity*

Figure 76 presents the results of the pH determination of samples diluted in water at a 1:1 mass ratio, as established by ABNT NBR 10004.

Figure 76 : pH of 1:1 mass solutions

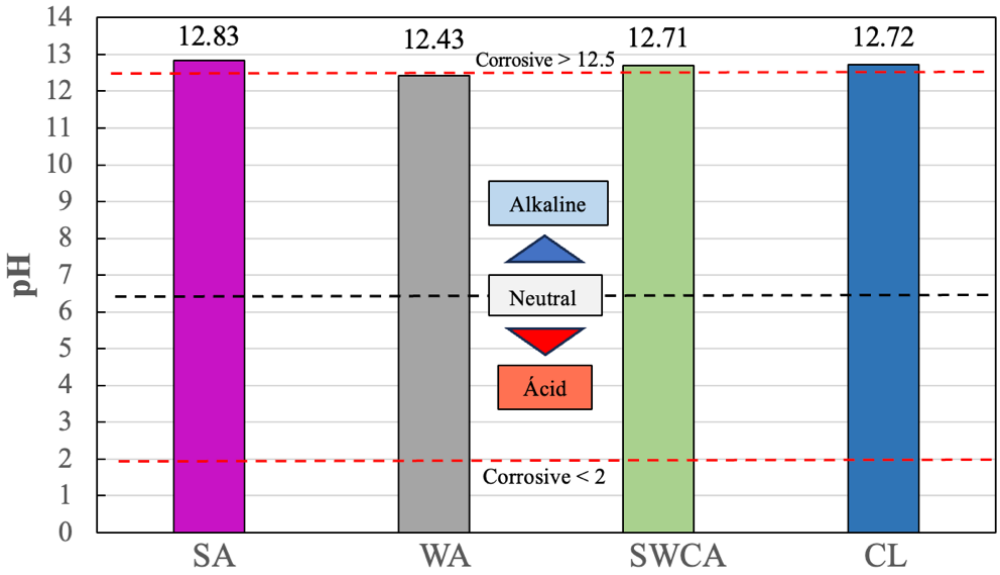

Source: Elaborated by the author

All samples analyzed exhibited an alkaline character on the pH scale. This behavior is expected, as noted by Etiégni and Campbell (1991), who reported that wood ash typically presents pH values ranging from 9 to 13.5, while saturated solutions of hydrated lime may reach pH values between 12.4 and 12.8 (Estrela, 2005). Etiégni and Campbell (1991) further indicate that the alkalinity of wood ash is directly related to the content of carbonates, bicarbonates, oxides, and hydroxides present in the material. These compounds are predominantly composed of calcium (Ca), potassium (K), magnesium (Mg), silicon (Si), and phosphorus (P), which constitute the main chemical components of wood ash.

It is further observed that all samples exceeded the upper alkalinity threshold of pH 12.5, and are therefore classified as corrosive and, consequently, hazardous—except for the Washed Ash (WA) sample. According to Melo (2018), the washing process, as described by the author and applied in this study, has proven effective in reducing the potassium content typically found in wood ash, as well as other soluble compounds. It is believed that the reduction in potassium concentration from 10.82% to 0.70% in the washed ash (WA) contributed significantly to the decrease in alkalinity of the evaluated solution.

Furthermore, although the potassium content in the calcined ash (SWCA) was 0.65%—and therefore lower than that of the washed ash (WA)—the pH of the SWCA sample was higher than that of the WA sample. This behavior is believed to be associated with the conversion of calcium carbonate into calcium hydroxide during the calcination process. Since carbonate is a less alkaline compound than hydroxide (Malešič *et al.*, 2019), the formation of calcium hydroxide results in greater availability of Ca^{2+} and OH^- ions in the system, thereby increasing the pH.

4.6.3 *Toxicity assessment*

Once the corrosiveness of the materials had been verified, the toxicity of the ash and lime was assessed. The search for toxic substances listed in Annexes A to D of the ABNT NBR 10004 standard, as well as pesticides and other organic residues, was not carried out, as it is unlikely that the ash will show traces of these compounds after wood combustion. Furthermore, the high cost and analytical complexity of the tests to determine the presence of these materials reinforced the decision to limit the toxicity analysis only to the inorganic materials listed in Annex 7 of the standard.

Preliminary indications of the presence of certain toxic constituents in the ashes and commercial lime are provided by the XRF results for the four materials, as presented in Table 10, Section 4.1.2. However, the total content of contaminants is a poor indicator of the environmental risk posed by a waste (Król, Mizerna, and Bożym, 2020), since X-ray fluorescence (XRF) analyzes the sample in its solid (powder) state and does not allow for the assessment of the potential release of these pollutants into the environment. These results, therefore, serve only as indicators of the presence or absence of such contaminants.

In the unwashed ashes (SA), seven elements identified by XRF are listed as toxic according to the standard. These elements are sulfur (SO_3), chlorine (Cl), manganese (Mn), iron (Fe), copper (Cu), zinc (Zn), and barium (Ba). In the washed ashes (WA), two additional elements were detected beyond those found in the unwashed ashes (SA): aluminum (Al) and tin (Sn), with aluminum being classified as toxic. It is believed that during the washing process in boiling water, the ashes reacted with the walls of the metal container, resulting in the incorporation of these metallic contaminants into the washed ashes.

In the calcined ashes (SWCA), a reduction in the number of compounds present in the material is observed, which is attributed to volatilization during calcination at 875°C. However, vanadium (V) was detected in the ashes, an element commonly found in special metal alloys. It is believed that the presence of this element is due to minor contamination

inside the muffle furnace, as this specific equipment is typically used for conditioning metal alloys in the metallurgy department at UFC.

In the commercial lime sample, seven toxic elements were also detected by XRF, corresponding to those found in the unwashed ashes (SA) except for barium (Ba). Although the commercial lime sample did not show traces of barium, traces of arsenic (As) were detected, which is considered a highly toxic metal.

Based on the indication of the presence of contaminants in the evaluated materials, solubilization and leaching tests were conducted in accordance with the Brazilian standards ABNT NBR 10005 and 10006, respectively. Table 30 and Table 31 present the concentrations of metals and other hazardous compounds extracted from the ashes. These tables compare the detected concentrations with the legal limits established by the Brazilian solid waste classification standard, ABNT NBR 10004.

Table 30 : Metal concentration in solubilized sample

Metal	**Regulatory Concentration [mg/L]**	**SA**		**WA**		**SWCA**		**CL**	
Aluminum	0.2	N. E		N. E		N. E		N. E	
Arsenic	0.01	N. E		N. E		N. E		N. E	
Barium	0.7	N. E		N. E		N. E		N. E	
Cadmium	0.005	0.006	D. M	0	OK	0	OK	0	OK
Lead	0.01	0.3	D. M	0.01	OK	0	OK	0.05	D.M
Chloride	250	3195	D. M	142	OK	106.5	OK	35.5	OK
Copper	2.0	2.09	D. M	0.297	OK	0.304	OK	0.342	OK
Chromium	0.05	0.357	D. M	0.023	OK	0.054	D.M	0.035	OK
Iron	0.3	0.296	OK	0	OK	0	OK	0	OK
Manganese	0.1	0.026	OK	0	OK	0	OK	0	OK
Mercury	0.001	N. E		N. E		N. E		N. E	
Silver	0.05	0	OK	0	OK	0	OK	0	OK
Selenium	0.01	N. E		N. E		N. E		N. E	
Sodium	200	1546	D. M	53.58	OK	122.3	OK	10.15	OK
Zinc	5.0	13.35	D. M	0.815	OK	0.62	OK	0.0175	OK
Sulfate	250	325.2	D. M	15.53	OK	9.02	OK	0.145	OK
*N. E	Not Evaluated								
**D. M	Don`t Meet Regulatory concentration								
***Ok	Under regulatory concentration								

Source: Elaborated by the author

Of the 16 compounds applicable to biomass ashes, 11 were investigated, while 5 were not assessed due to the unavailability of necessary equipment and reagents for evaluation. It was found that the unwashed ash samples (SA) are toxic, since among the 11 elements analyzed in their solubilized extracts, only iron (Fe), manganese (Mn), and silver (Ag) did not exceed the permissible concentration limits. Notably, lead (Pb), chlorides (Cl), chromium (Cr), sodium (Na), and zinc (Zn) exceeded the legal limits by approximately 30, 12, 7, 7, and 2 times, respectively.

For the washed ashes (WA), all 11 evaluated elements were found at concentrations below the regulatory limits. Therefore, it is concluded that the washing step was effective in reducing contaminant concentrations. However, it is important to emphasize the need to assess the treatment of the washing effluents, since these effluents not only contain elements that can be converted into agricultural fertilizers and cleaning materials (MELO, 2018) but also may carry toxic elements with potential contaminant effects.

The calcined ashes (SWCA), in turn, presented 10 elements within the legal limits, with only chromium (Cr) slightly exceeding the maximum allowable concentration at 0.054 mg/L, compared to the legal limit of 0.05 mg/L. It is considered that the increase in chromium concentration relative to the washed ashes (WA), which was 0.023 mg/L, may be associated with contamination from the furnace during the calcination step, since the calcined ashes are obtained from the washed ashes. Thus, it is emphasized that although the calcined ashes (SWCA) exceeded the ABNT NBR 10004 limit for chromium (Cr), this concentration increase may be related to the conditions of the calcination furnace rather than the ashes themselves.

For the commercial lime, it was found that the concentration of lead (Pb) is five times higher than the regulatory limit of 0.01 mg/L, with a measured value of 0.05 mg/L. Although the concentrations of all other evaluated elements are considered safe, the elevated lead content in the commercial lime sample renders it toxic according to the limits established by ABNT NBR 10004.

Table 31 : Metal concentration in leached sample

Metal	**Regulatory Concentration [mg/L]**	**SA**	**WA**	**SWCA**	**CL**
Arsenic	1.0	N. E	N. E	N. E	N. E
Barium	70.0	N. E	N. E	N. E	N. E

Cadmium	0.5	0	Ok	0	Ok	0	Ok	0	Ok
Lead	1.0	0.21	Ok	0.28	Ok	0.29	Ok	0.29	Ok
Chromium	5.0	0.113	Ok	0.082	Ok	0.103	Ok	0.096	Ok
Fluoride	150.0	N. E		N. E		N. E		N. E	
Mercury	0.1	N. E		N. E		N. E		N. E	
Silver	5.0	0	Ok	0	Ok	0	Ok	0	Ok
Selenium	1.0	N. E		N. E		N. E		N. E	
*N. E	Not Evaluated								
**Ok	Under regulatory concentration								

Source: Elaborated by the author

Based on the results obtained from the leaching tests, it was observed that all evaluated samples presented concentrations of toxic elements below the limits established by the ABNT NBR 10004 standard. It is important to note that, as recommended by the ABNT NBR 10005 standard, the use of acidic solutions is advised in these tests, since the solubility of contaminants in solid waste is strongly influenced by the pH of the solution. In acidic media, toxic elements tend to exhibit greater mobility and availability in aqueous systems, as discussed by Consoli, Lopes Junior e Heineck (2009) and Alloway (2013).

The low concentrations of metals found in the leachate extracts go against the expected behavior for this test, as the concentrations of lead (Pb), chromium (Cr), and cadmium (Cd), for example, were higher in the solubilized extracts (water as solvent) than in the leachate extracts (acidic solvent). However, this behavior can be explained by the small difference in pH between the solubilized and leachate extracts, as shown in Figure 77.

Figure 77: pH of solubilized and leached samples

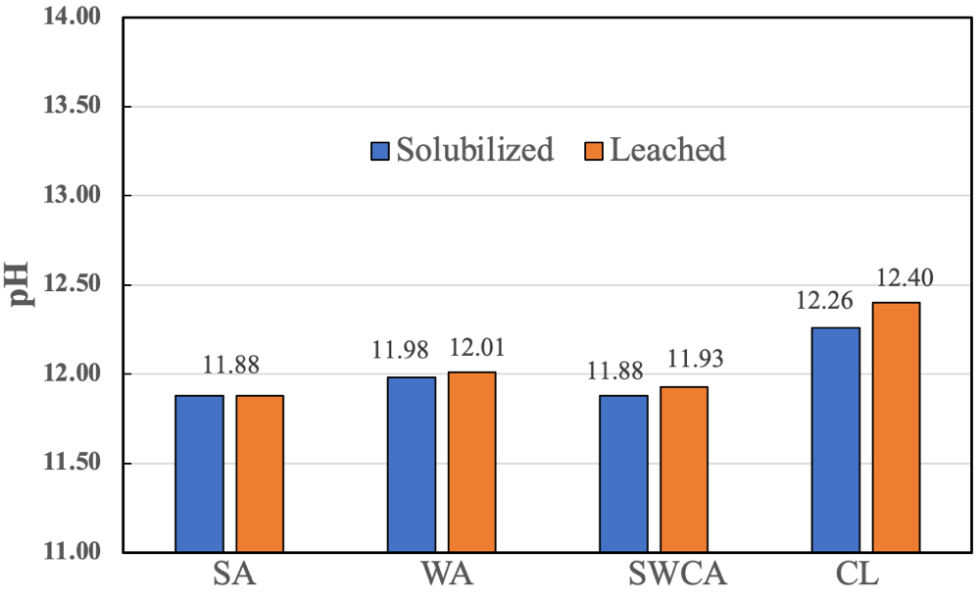

Source: Elaborated by the author

The maintenance of pH at strongly alkaline levels in the leachate extracts suggests that the acidic solution recommended by NBR 10005 was not effective in acidifying the medium. This limitation compromises the mobilization of potentially toxic compounds, since, as pointed out by Baird (2002) and Król, Mizerna, and Bożym (2020), an increase in pH—especially through alkaline stabilizing agents—tends to significantly reduce the solubility of inorganic contaminants.

Furthermore, the solubilization and leaching tests differ in terms of contact time, type, and concentration of the solvent, which directly influences the concentration of dissolved metals. While leaching employs an acidic solution, continuous agitation for 14–18 hours, and a 1:20 (mass:volume) ratio, solubilization uses distilled water, prolonged contact for 7 days, and a much higher ash concentration, resulting in more concentrated extracts.

Based on the results obtained, the ash and commercial lime samples were classified as hazardous solid wastes, except for the washed ashes (WA), which presented acceptable levels of contaminants. The data demonstrate the effectiveness of the washing process in reducing the concentrations of toxic elements. In the case of the calcined ashes (SWCA), the presence of chromium was attributed to cross-contamination inside the calcination furnace, indicating that the observed toxicity does not inherently arise from the material itself, but rather from the experimental conditions of the thermal processing.

The strongly alkaline nature of the ashes reduces the solubility and, consequently, the mobility of toxic metals, as described by Consoli, Lopes Junior e Heineck (2009), Alloway (2013) and Król,Mizerna and Bożym (2020). However, in natural environments, variations in soil pH and the presence of other substances can significantly alter this dynamic, which emphasizes the importance of leaching studies under conditions representative of the field. In this context, column leaching tests are considered important to more accurately represent the percolation and transport conditions of toxic elements in compacted soil samples.

Column leaching tests were conducted on samples of natural soil and preliminary trials on Soil 1 stabilized with 7% calcined ashes. In the natural soil samples, it is believed that percolation occurred without the formation of preferential flow paths, as evidenced by the slow flow observed in the collection beaker for the percolating liquid, as shown in Figure 78. Pressures between 1 and 1.5 bar were applied, and approximately 700 mL of leachate was collected within about 5 minutes.

Figure 78: Collection of percolated liquid – soil 1

Source: Elaborated by the author

For the Soil 1 sample with calcined ashes (S1SWCA7), it was not possible to collect percolated liquid, thereby preventing environmental analyses of this material under compacted conditions. In Figure 79 (a), the condition of the specimen surface previously in contact with the pressurized liquid is shown, while Figure 79 (b) depicts the non-saturation/percolation condition of the specimen following disaggregation and dismantling of the testing apparatus.

Figure 79: Appearence of the test specimen after test failure

a) Surface **b)** Disaggregated

Source: Elaborated by the author

It was observed that, even after the intermittent application of pressures up to 3 bar over a period of two months, no significant percolation occurred through the compacted specimen. The disassembly of the experimental apparatus revealed that the interior of the sample remained unsaturated, which demonstrates the low hydraulic permeability of the tested material. Further attempts were not conducted due to operational difficulties that prevented access to the equipment.

Despite the impossibility of performing the percolation test under compacted conditions (column leaching), there is evidence suggesting that the calcined ashes (SWCA) may have acted as a chemical stabilizer, producing an encapsulating effect as described by Vasconcelos (2018).

4.6 Hypothetical pavement section design

Based on the geotechnical characteristics of the region, the type of highway, and the traffic data presented in section 3.5, some hypothetical pavement sections are proposed. Although the Cariri Metropolitan Region (CMR) presents a great diversity of soils, Mascarenhas (2016) and Xavier (2018) identified the presence of sandy-silty soils in Juazeiro do Norte. Therefore, a silty material was adopted for the subgrade and a sandy one for the sub-base.

Since the focus of this study is on evaluating materials suitable for the base and subbase of the pavement, the materials for the asphalt surface, sub-base, and subgrade were kept constant. All layers were optimized so that the minimum thickness was used. The differences between the design sections are thus highlighted comparatively by the variation in the material used in the base layer. Figure 80 and Figure 81 illustrate the first set of solutions using chemically stabilized bases.

Figure 80: Hypothetical section 1.1

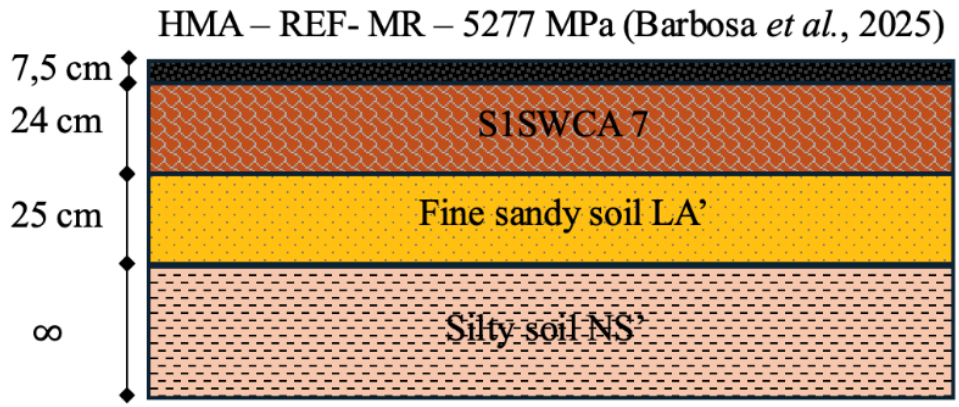

Source: Elaborated by the author

Figure 81: Hypothetical section 1.2

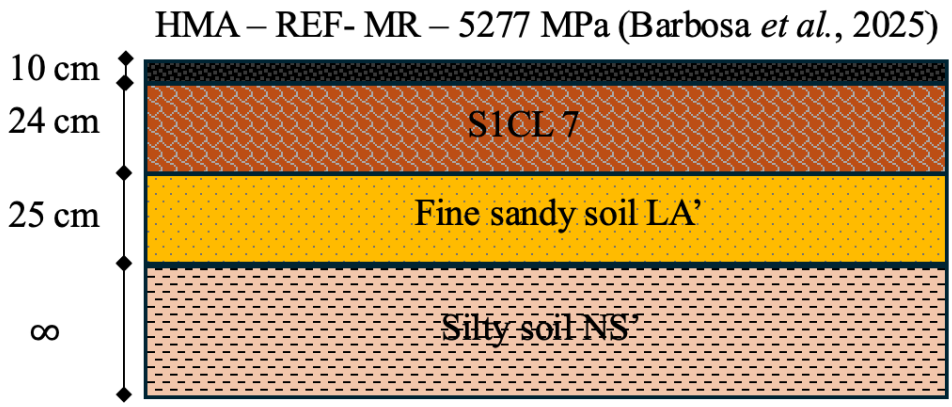

Source: Elaborated by the author

It is observed that, in the comparison between Sections 1.1 and 1.2, the use of the mixture with calcined ashes (S1SWCA 7) leads to a reduction in asphalt layer thickness from 10 cm to 7.5 cm, highlighting the superior performance of the mixture with calcined ashes compared to the mixture with commercial lime (S1CL 7). This result is attributed to the higher resilient modulus of the mixture with calcined ashes under the specific stress conditions to which the sections are subjected. While Section 1.1 exhibits a resilient response of 645 MPa, Section 1.2 presents a value of 510 MPa. It is considered that this 135 MPa difference between layers is responsible for the need to increase the thickness of the stiffer layer (the surface course).

It is also worth noting that, although the design process aimed to keep the layer thicknesses similar for better comparison, using the same surface thickness for the solution with commercial lime (S1CL 7) exceeds the maximum recommended limit of 40 cm per layer, making an increase in the surface layer thickness the most straightforward adjustment.

Additionally, to establish a basis for comparison between the mixtures evaluated in this study and similar mixtures reported in the literature, a pavement section was designed using a clayey lateritic soil stabilized with 7,5 % of lime with data reported by Medeiros (2017). This mixture was selected due to the clayey nature of the soil and because the lime content of 7.5% is very close to the contents used in the context of this design. Figure 82 ilustrastes the proposed section.

Figure 82: Hypothetival section 1.3

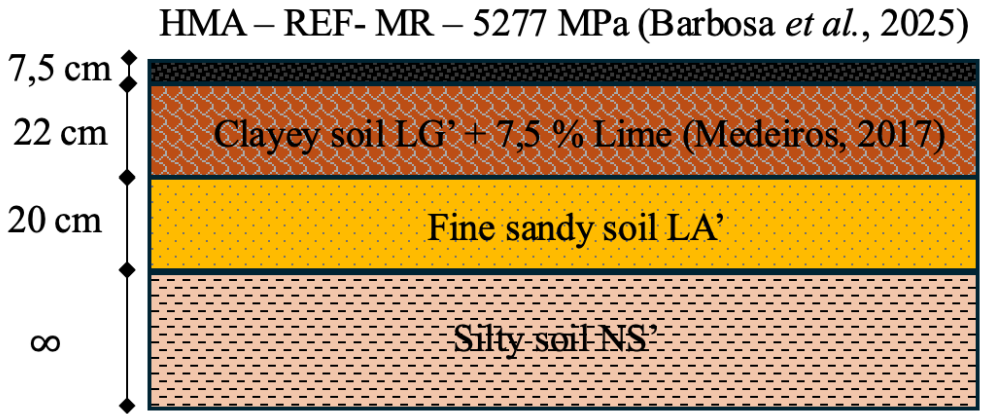

Source: Elaborated by the author

It is found that the use of the mixture evaluated by Medeiros (2017) as a chemically stabilized base layer results in a section similar to that proposed with the mixture containing calcined ashes (S1SWCA 7). The thicknesses of asphalt surface could be maintained, except for the base and subbase layer, which could be reduced by 2 cm and 5 cm respectively, indicating better mechanical performance for the mixture proposed by Medeiros (2017).

The difference between the mixtures, as reflected in the pavement design, may be related to the higher lime content used (7.5%) and/or superior characteristics of the soil evaluated by the author. The heterogeneity of soils and the resulting diversity of mechanical behaviors due to the soil–stabilizer interaction justify the differences between the designed sections. Nevertheless, it is observed that the pavement design results with the mixtures evaluated in this study align with the behavior of mixtures reported in the literature, demonstrating the technical feasibility of using calcined ashes in pavement solutions.

In local projects, soil–aggregate mixtures and simple graded crushed stone are traditionally used as base and/or sub-base layers instead of chemically stabilized solutions. Although chemical stabilization can be technically advantageous in many situations, the technology is still not widely adopted, especially in less developed regions of Brazil, due to several interrelated factors. Despite their high durability, superior mechanical strength, and better long-term performance, chemically stabilized mixtures still face barriers related to high initial costs, lack of technical training, and resistance to innovation. Furthermore, they remain susceptible to fatigue cracking, which must be carefully considered in design. In this context, hypothetical pavement sections were designed using traditionally employed solutions. These sections are illustrated in Figure 83 and Figure 84, while Table 32 presents the cracking and rutting data for all proposed sections.

Figure 83: Hypothetical section 2.1

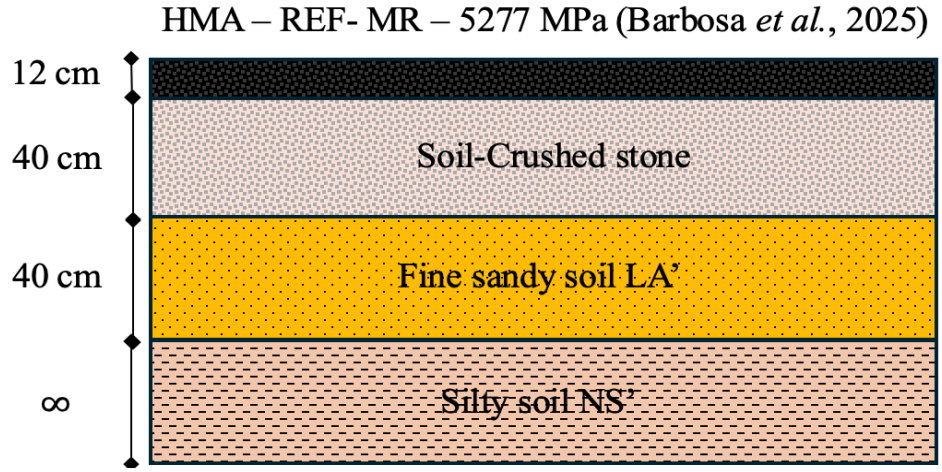

Source: Elaborated by the author

Figure 84: Hypothetical section 2.2

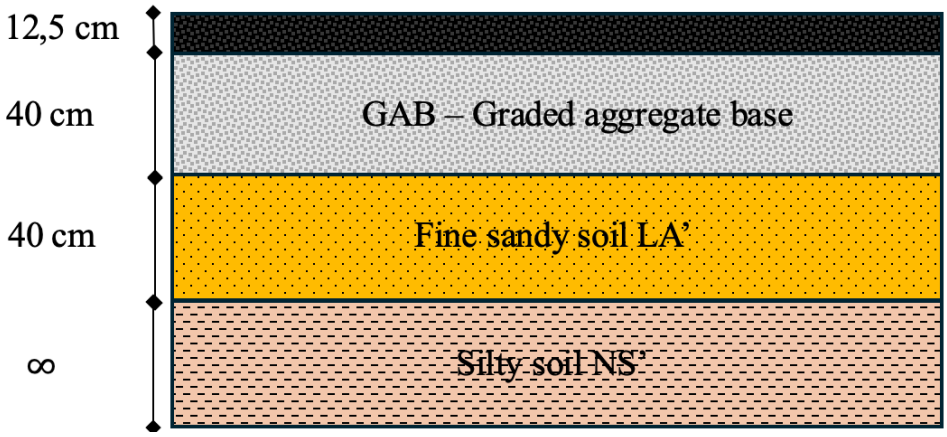

Source: Elaborated by the author

Table 32: Cracking permanent deformation of hipothetical solutions

	Chemically stabilized			Granular materials	
Solution	1.1	1.2	1.3	2.1	2.2
Cracking [%]	29,9	29,2	29,7	28,3	29,0
ATR [mm]	1,4	1,4	1,2	4,9	3,8

Source: Elaborated by the author

The solutions with chemically stabilized bases can generally be constructed with thinner sections. It remains to be assessed whether this reduction in layer thickness is cost competitive. Despite the promising behavior of the chemically stabilized mixtures, it is important to emphasize the need to assess their fatigue performance. For this purpose, the predicted fatigue life of the mixtures is calculated using the adjusted model by Balbo (1993).

The input variables for the calculation are the Indirect Tensile Strength (ITS) and the tensile stress at the bottom fiber of the base layer, calculated with AEMC DNIT software,

case by case. The Fatigue Ratio (RF) being the ratio between the first and the second. Based on this, the predicted number of load cycles is determined, as shown in Table 33.

Table 33: Fatigue life prediction for S1SWCA 7 and S1CL 7 mixtures

	ITS [Mpa]	**σt Calc. [Mpa]**	**RF**	**Fatigue model Balbo (1993)**	**Nf**
S1SWCA 7	0.15	0.098667	0.657	$N = 10^{6.69-1.87\,(RF)}$	2.88×10^5
S1CL 7	0.12	0.090593	0.754	$N = 10^{6.78\,-2.08\,(RF)}$	1.65×10^5

Source: Elaborated by the author

Considering that the traffic values expressed by the number **N** were on the order of 10^6 for the pavement layer design, it is observed, based on the proposed model, that the mixtures exhibit low fatigue resistance, as the predictions indicate values on the order of 10^5.

The adopted fatigue prediction model is sensitive to the ratio between the tensile stress at the bottom fiber of the base and the Indirect Tensile Strength (ITS) of the mixture. The lower this ratio, the better the fatigue performance of the mixture. In this context, it is worth noting that the DNIT standard for ITS (DNER-ME-181/94) requires to be tested after a saturation stage, whereas the standard for fatigue testing does not mention this step.

It is understood that the moisture content or degree of saturation can influence the mechanical behavior of soils, reducing tensile strength, especially considering that soil–lime mixtures are classified as semi-cemented and do not exhibit purely linear-elastic behavior. Furthermore, it cannot be stated that, even after potential early cracking of the base, it completely loses its bearing capacity, since the mechanisms of lime stabilization go beyond cementation, including flocculation and changes in soil structure.

In this context, it is understood that the ITS and fatigue testing protocols have the limitation of not accounting for the influence of conducting these tests under different moisture conditions. Therefore, it cannot be assumed that the prediction model is accurate under such conditions. As such, understanding the fatigue mechanisms under varying moisture conditions for semi-cemented mixtures may be the subject of future investigations, and the potential use of soil–calcined ash mixtures cannot be ruled out, especially when considering strategies to prevent crack reflection from the base to the surface layer and further studies on the retention of bearing capacity even after fatigue damage.

Therefore, it is necessary to assess the cost feasibility of these solutions to determine whether the use of stabilizing agents is financially competitive, given that all solutions can be technically viable.

4.6.1 *Cost feasibility*

The cost feasibility analysis compares four pavement sections: solutions 1.1,1.2, 2.1 and 2.2. The costs considered include direct costs related to materials and logistical expenses. This preliminary analysis does not include costs associated with environmental licensing, equipment mobilization/demobilization, indirect administrative costs, or other aspects inherent to the technologies used, such as water demand for curing, traffic disruptions, quality control, and laboratory testing.

Sections 1.1 and 1.2 (chemical stabilization solutions) use clayey soil (S1) as the base material, stabilized with 7% of calcined ash and commercial hydrated lime type CH I, respectively. Sections 2.1 and 2.2, in contrast, adopt granular layer solutions: the former uses a mixture of soil + 30% of crushed stone 1 and 40% of crushed stone 0, while the latter uses a graded aggregate base (GAB).

All soils are assumed to be sourced from borrow pits located at an average distance of 5 km. For the solutions involving stabilizers, the additional variable is the acquisition of ash and lime. Thus, the costs considered for these sections include the acquisition and transportation of granular materials and borrow soils, excavation and loading, as well as spreading and compaction operations.

Since the ash does not have an established commercial value, its cost was estimated based on the price of lime. For the calcined ash, a value equivalent to 150% of the cost of hydrated lime was adopted, considering the similarities in their industrial production processes, especially regarding the calcination stage. Table 34 details the items considered in this cost estimate, the unit cost, the unit of measurement used, and a brief justification regarding the sources of the unit costs adopted.

Table 34: Unit costs

Cost item	Estimated unit cost	Unit	Justification / Source
Borrow pit soil - Excavation	R$ 8,00	R$/m³	Average value from SICRO (2023) for excavation using a hydraulic excavator in dry soil conditions, including loading onto trucks.
Borrow pit soil - Hauling	R$ 4,00	R$/m³	Part of the excavation cost composition, separated here for analytical purposes.
Borrow pit soil - Transportation (5 km)	R$ 7,50	R$/m³	Estimate based on haulage by dump truck (12 m³ capacity), at R$ 1.50 per m³·km, totaling R$ 7,50 for a 5 km distance.
Borrow pit soil - Compaction	R$ 12,00	R$/m³	Based on SICRO compositions and crew productivity.

On-site Soil-Aggregate Mixing	R$ 15,00	R$/m³	Based on the use of motor graders or front loaders to perform in-situ mixing of soil and aggregates, including equipment operation, labor, and fuel costs.
Hauling (Soil and Aggregate)	R$ 12,00	R$/m³	Estimated for average transportation of both soil and crushed stone (brita), considering longer distances (up to 10 km) and higher unit weights of aggregates. Includes cost of diesel, equipment depreciation, and driver/operator labor for dump trucks.
Spreading	R$ 6,50	R$/m³	Based on the use of motor graders for material distribution, with average productivity rates and crew costs. Includes minor leveling adjustments before compaction, in line with SICRO mechanical spreading rates.
Compaction (Soil-Aggregate)	R$ 9,00	R$/m³	Derived from SICRO and practical productivity data for vibratory rollers compacting mixed layers. Slightly lower than pure soil compaction due to better self-compaction behavior of granular materials.
Moistening	R$ 5,00	R$/m³	includes the use of water trucks (pipa) to achieve optimum moisture content for compaction. Accounts for fuel, operator, and water costs for a standard daily volume application over compacted layers.
Asphalt Binder (CAP 50/70)	R$ 3,800.00	R$/t	2024 average market price (based on SINAPI and regional suppliers; excludes freight)
Aggregates (coarse/fine)	R$ 140.00	R$/t	Includes crushed stone (sizes 0 and 1) and stone dust from quarries (5–10 km)
Mixing at Asphalt Plant	R$ 50.00	R$/t	Covers plant operation, energy consumption, and dosage control
Hauling to Job Site (up to 20 km)	R$ 50.00	R$/t	Using thermal dump trucks (round trip)
Spreading (Paving)	R$ 25.00	R$/t	Includes paver operation and thickness control
Compaction	R$ 30.00	R$/t	Based on tandem and pneumatic roller productivity (200–300 t/day)
Quality Control	R$ 12.00	R$/t	Includes binder content checks, gradation, thickness, and temperature monitoring
Hidrated Lime (CH I)	R$ 500,00	R$/t	The price reflects bulk purchase in 1-ton big bags, excluding taxes and freight, and is aligned with recent price references from SINAPI (2024) and quotations from distributors active in infrastructure projects.
Calcined Ash (7%) – Base	R$ 750,00	R$/t	Estimated at 150% of the market price of cement (R$ 500/t), considering additional washing and calcination steps.

Graded aggregate base - Material	R$ 90,00	R$/m³	Estimate based on average market prices in the brazilian Northeast region; includes material acquisition from quarries and profit margin.
Graded aggregate base - Transport	R$ 30,00	R$/m³	Estimated based on a fleet of dump trucks (average capacity of 12 m³), considering an average hauling distance of 20 km to the site.
Graded aggregate base – Execution (Placement and compaction)	R$ 40,00	R$/m³	Based on cost composition from SICRO (DNIT, 2023) for execution using a vibratory roller and motor grader.

Source: Elaborated by the author

Considering the road segment is dual carriageway with each lane measuring 8 meters in width and 3.5 kilometers in length, the design areas and volumes were calculated using the following formulas, with consolidated results presented.

Total paved area = 2 × Lane width × Section length = 2 × 8 m × 3500 m = 56.000 m^2

In addition, once the unit costs for materials and services listed in Table 34 are known, a cost composition per cubic meter of layer is developed, as shown in Table 35. Based on this, and knowing the total paved area, the costs, and the design thicknesses of each layer, the cost of each pavement solution is determined, as presented in Table 36.

Table 35: Cost Breakdown of the pavement layers

Component	Unit Cost	Un.	Subtotal (R$)
Asphalt Layer			
Asphalt Binder (Penet. grade 50/70)	R$ 3800,00	0.044 t	R$ 167,20
Aggregates	R$ 140,00	0.956 t	R$ 133,84
Mixing at Asphalt Plant	R$ 50,00	1 t	R$ 50,00
Hauling to Job Site	R$ 50,00	1 t	R$ 50,00
Spreading (Paving)	R$ 25,00	1 t	R$ 25,00
Compaction	R$ 30,00	1 t	R$ 30,00
Quality Control	R$ 12,00	1 t	R$ 12,00
Total Cost / t			**R$ 468,04/t**
Total Cost / m³			**R$ 1.101,89/m³**
Soil + 7% Calcined ash base course			
Soil (excavation + transportation)	R$ 15.50/m³	1 m³	R$ 15.50
Calcined Ash	R$ 750.00/t	0.13 t/m³	R$ 97,50
Ash Transportation	R$ 4.00/m³	0.13 m³	R$ 0.52
Execution (placement, mixing,spreading)	R$ 20.00/m³	1 m³	R$ 20.00
Moistening	R$ 5,00/m³	1 m³	R$ 5,00
Soil compaction	R$ 12.00/m³	1 m³	$ 12.00
Total			**R$ 150,52/m³**
Soil + 7% Lime base course			
Soil (excavation + transportation)	R$ 15.50/m³	1 m³	R$ 15.50

Hydrated Lime CH I Type	R$ 500.00/t	0.13 t/m³	R$ 65.00
Lime Transportation	R$ 4.00/m³	0.13 m³	R$ 0.28
Execution (placement, mixing, spreading)	R$ 20.00/m³	1 m³	R$ 20.00
Moistening	R$ 5,00/m³	1 m³	R$ 5,00
Soil compaction	R$ 12.00/m³	1 m³	$ 12.00
Total			**R$ 117,02/m³**
Soil + (30% + 40% Crushed Stone base course)			
Soil (excavation + transportation)	R$ 15.50/m³	0,3 m³	R$ 4,65
Crushed Stone 1	R$140.00/t	0,3 m³	R$ 42.00
Crushed Stone 0	R$140.00/t	0,4 m³	R$ 56.00
Soil Transportation	R$ 7.50/m³	1 m³	R$ 7.50
Stone Transportation	R$ 12.00/m³	0,7 m³	R$ 8.40
Moistening	R$ 5,00/m³	1 m³	R$ 5,00
Execution (placement and compaction)	R$ 40.00/m³	1 m³	R$ 40.00
Total			**R$ 156.05/m³**
GAB base course			
Material GAB	R$ 90.00/m³	1 m³	R$ 90.00/m³
Transportation GAB	R$ 30.00/m³	1 m³	R$ 30.00/m³
Moistening	R$ 5,00/m³	1 m³	R$ 5,00
Execution (placement and compaction)	R$ 40.00/m³	1 m³	R$ 40.00/m³
Total			**R$ 163.55/m³**
Borrow Pit Soil Subbase			
Soil (excavation + transportation)	R$ 15.50/m³	1 m³	R$ 15.50
Spreading	R$ 6,50 m³	1 m³	R$ 6,50
Moistening	R$ 5,00/m³	1 m³	R$ 5,00
Soil compaction	R$ 12.00/m³	1 m³	$ 12.00
Total			**R$ 39.00/m³**

Source: Elaborated by the author

Table 36: Cost of Each Proposed Solution

Solution	Layer	Material Description	Thickness [cm]	Total Cost [R$/m³]	Layer Vol. [m³]	Layer cost [R$]	Solution cost [R$]
1.1	Asphalt Layer	Asphalt Concrete	7.5	1101,89	4200	4.626.738,00	7.195,534.80
	Base	S1 + 7% Calcined Ash	24	150,52	13440	2.022.796,80	
	Subbase	Sandy Soil	25	39,00	14000	546.000,00	
1.2	Asphalt Layer	Asphalt Concrete	10	1.101,89	5600	6.170.584,00	7,896,327.20
	Base	S1 + 7% Hydrated Lime	24	117,02	13440	1.179.763,20	
	Subbase	Sandy Soil	25	39,00	14000	546.000,00	
2.1	Asphalt Layer	Asphalt Concrete	12	1.101,89	6720	7.404.700.80	11,773,820.80
	Base	Soil + Crushed Stone (0 + 1)	40	156,05	22400	3.495.520,00	
	Subbase	Sandy Soil	40	39,00	22400	873.600,00	
2.2	Asphalt Layer	Asphalt Concrete	12.5	1101,89	7000	7.713.230,00	12,250,350.00
	Base	Granular Aggregate Base (GAB)	40	163,55	22400	3.696.000,00	
	Subbase	Sandy Soil	40	39,00	22400	873.600,00	

Source: Elaborated by the author

Cost estimates indicate that project solutions with chemically stabilized bases prove to be more economical than sections with non-stabilized materials. The reduction in layer thickness, resulting from the improved mechanical behavior of the chemically stabilized mixtures, was the decisive factor for this. It is highlighted that the cost of adopting solutions with granular materials practically doubles the project's value, indicating that the solution with calcined ash, besides being advantageous from an environmental standpoint, can be very competitive from a technical and economic perspective. The Figure 85 shows the comparative cost of each solution.

Figure 85: Cost of each proposed solution

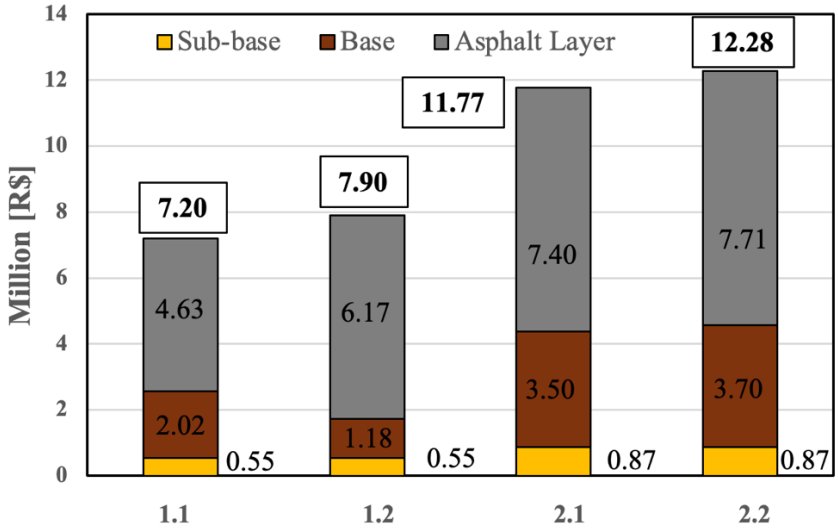

Source: Elaborated by the author

Considering that the main sensitive premise for the competitiveness of the alternative section is based on the inference between the cost of ash and the cost of commercial lime, a brief sensitivity analysis is included. This analysis is based on the breakeven point at which an increase in the cost of ash would make the costs between the sections equivalent. Table summarizes the steps for this analysis.

Table 37: Summary of sensitivity analysis calculations

Step	Calculation	Value
Step1: Ash Mass per m3	0.07×1.88 t/m3	0.1316 t/m3
Step 2: Total Ash Mass	0.1316 t/m3×13,440 m3	1,769.5 t
Step 3: Fixed Cost of Section 1.1	Pavement + Subbase + Base (excluding ash)	R$ 5,261,776.20
Step 4: Total Cost of Section 1.2	Reference value to match	R$ 7,896,347.20
Step 5: Cost Difference	7,896,347.20 − 5,261,776.20	R$ 2,634,571.00
Step 6: Cost per Ton (x)	2,634,571.00 / 1,769.5 t	R$ 1,488.68 / t

Source: Elaborated by the author

It is ascertained that the cost of calcined ash would need to be raised from R$ 750.00 per ton to R$ 1,488.68 per ton (an increase of approximately 98.5%) for project solutions 1.1 and 1.2 to present equivalent costs. Alternatively, considering a reference price for commercial lime of R$ 500.00 per ton, as long as the cost of the ash does not exceed approximately three times the value of the commercial lime—or about 198.5% above the unit price of cement (R$ 500.00/t)—solution 1.1 maintains its position as the most economically competitive.

Therefore, although the economic viability analysis presented herein is based on hypothetical premises and inferences that may not reflect the entirety of the econometric variables, it is postulated that the alternative solution, which employs biomass ash and local soil, can be considered competitive and a sustainable option for the construction of road segments, as exemplified by the beltway project of an inland municipality in Brazil.

5 CONCLUSIONS

This research investigated the feasibility of using calcium-rich wood ash as an alternative input for soil stabilization, aiming at its application in pavement sublayers. The proposed approach involved processing the ash and evaluating its effects on low-strength clayey soils through chemical, physical, and mechanical tests.

The results indicated that the use of wood ash, especially after the calcination stage, leads to significant improvements in the mechanical properties of the soils, including increased strength, stability under full immersion saturation, and reductions in plasticity and expansiveness. In addition, pavement design using this type of technology can lead to economic gains due to the significant reduction in layer thicknesses, especially when compared to solutions that use granular materials. These findings demonstrate the technical potential of the material as a stabilizing agent, serving as a substitute for traditional stabilizer such as lime.

From an environmental perspective, the use of wood ash contributes to reducing the volume of waste sent to landfills, while also avoiding the extraction of conventional raw materials such as limestone. These results suggest that adopting this residue as a stabilizer in road construction can be considered a circular economy strategy and a means of mitigating environmental impacts.

In addition to its technical performance, the sustainability of the approach is noteworthy, as it utilizes a renewable-origin residue and contributes to lowering the carbon footprint of road infrastructure works. Thus, the study reinforces the importance of valorizing industrial waste in pavement engineering, proposing solutions that combine performance, technical feasibility, and environmental responsibility.

5.1 Main findings of the research

5.1.1 Regarding the processing of ash

The ash processing steps proved effective in improving its properties as a stabilizing additive: sieving reduced the presence of organic material (charcoal); washing decreased the content of potassium compounds, which are detrimental to the formation of cementitious compounds during calcination and also increased the calcium concentration in the system; and calcination was efficient in modifying the material's mineralogy.

The most significant chemical transformations occurred during the calcination process, as evidenced by X-ray diffraction (XRD) analyses. A replacement of calcite ($CaCO_3$) peaks with intense portlandite ($Ca(OH)_2$) peaks was observed, indicating the conversion of calcium

oxide into calcium hydroxide. This mineralogical change was corroborated by the exothermic hydration reactions and the associated heat release.

5.1.2 Regarding choosing the most promising additive contents

The selection of the most promising mixtures was based on mechanical performance criteria such as saturation stability without disintegration, volumetric stability (expansions and contractions within regulatory limits), and higher mechanical strengths. The results indicated that the best-performing mixtures were those with the highest additive contents (7%).

5.1.3 Regarding mixtures plasticity

In general, the addition of ash progressively reduces the plasticity of the mixtures with increasing reaction time. The greatest reductions were observed for the calcined materials (SWCA and CL) and the unwashed ash (SA). Although the PI values are not considered acceptable according to conventional classifications (such as AASHTO) for use in pavement base and subbase layers, it is understood that there are limitations in traditional classification systems, and PI values above 6 do not necessarily imply inferior performance, as demonstrated by the mechanical tests.

5.1.4 Regarding the mechanical behavior of soils and mixtures

The two evaluated soils were classified as A-7-6 according to the AASHTO system, characterizing them as low-strength clays with high expansion indices and low CBR values, unsuitable for use in granular pavement layers in their natural state.

The addition of unwashed ashes (SA) led to a significant reduction in plasticity, an increase in load-bearing capacity (approximately 10 to 15 times), and a reduction in the expansiveness of the mixtures. However, these ashes did not provide sufficient stability after curing and saturation, making it impossible to classify them as stabilizers at the evaluated contents.

On the other hand, the washed ashes (WA) showed inferior performance, with only modest improvements in geotechnical properties, indicating that the washing process reduces the effectiveness of the ash as a stabilizing agent.

The calcined ashes (SWCA) demonstrated superior performance in all analyzed aspects, significantly improving plasticity, bearing capacity, immersion saturation resistance, and expansiveness, even at lower contents. The results were comparable to those of commercial

lime (CL), with mixtures containing 7% SWCA or CL meeting the requirements for base layers, while those with 5% were suitable for subbase applications.

Mixtures with SA presented CBR values above 20% and expansion below 1% for soil 1, making them suitable for subgrade reinforcement and subbase layers. For soil 2, despite improved load-bearing capacity, expansion rates remained high, making its use unfeasible at the studied dosages. However, there is evidence that higher biomass ash contents may enable its use, as suggested by Lahtinen (2001) and Macsik and Svedberg (2006).

Mixtures with SWCA and CL remained stable after 28 days of curing and showed strength gains with increasing additive content, reinforcing the potential of calcined ash as a viable stabilizing material for pavement applications.

The resilient behavior of the natural soils was consistent with that of plastic soils, presenting average resilient modulus (MR) values considered low. The addition of SWCA negatively affected the MR in the early curing stages, leading to specimen disintegration. After 28 and 90 days, however, a significant increase in MR values was observed, indicating the progressive development of cementitious reactions.

The indirect tensile strength (ITS) tests indicated more pronounced cementitious reactions in the mixtures with soil 1. However, the values for all mixtures approached the threshold of 0.1 MPa, which is the value above and below which mixtures are considered cemented and non-cemented, respectively. It is also worth noting that the ITS tests were carried out immediately after the specimens were saturated for a period of 24 hours, as specified by the standard for the ITS of chemically stabilized mixtures.

The predicted fatigue life of the stabilized mixtures was considerably low for the level of stress that the designed layer may undergo. This behavior is directly related to the low ITS of the mixtures, which may have been affected by the prior saturation of the specimens. Future studies may be conducted to assess the impact of moisture variations on the ITS and fatigue performance of semi-cemented mixtures.

5.1.5 Regarding cost feasibility

The chemically stabilized mixtures resulted in much slimmer pavement sections compared to the alternatives with granular layers. This behavior led to significant reductions in project costs, with the cost of the most economical section using calcined ashes being 58.7% of the cost of the most expensive section, which used crushed aggregate base (GAB).

Furthermore, through sensitivity analysis, it was found that the cost of the calcined ashes would need to be three times higher than that of commercial lime for the solutions to be cost-equivalent, highlighting the technical, economic, and environmental potential of this alternative.

5.1.6 Regarding environmental analysis

From an environmental standpoint, both the ashes and the commercial lime (CL) are considered corrosive, as they exhibit pH values above 12.5 under the conditions established by regulatory protocols, except for the washed ash (WA). Due to technical limitations, it was not possible to assess the solubility of certain elements such as Aluminum (Al), Arsenic (As), Barium (Ba), Fluoride (F), Mercury (Hg), and Selenium (Se). However, considering the other eleven evaluated elements, the washing process proved effective in removing heavy metals, rendering the washed ashes non-toxic. It was also observed that possible cross-contamination during the calcination stage increased Chromium (Cr) concentrations to slightly above the regulatory limit. Furthermore, lead (Pb) concentrations found in commercial lime (CL) were five times higher than the regulatory threshold.

The leaching evaluation method under compacted conditions appears to be ineffective for assessing highly impermeable mixtures. It was observed that the compacted mixture of calcined ashes (SWCA) with soil 1 showed no percolation even after two months of testing in the column leaching apparatus, suggesting that encapsulation conditions may have been achieved, as no percolation was detected through the mixture. Due to technical limitations, it was not possible to repeat or conduct the test on other mixtures. It is therefore recommended that alternative methods for assessing contaminant potential be considered, such as static immersion leaching tests.

5.2 Main work conclusions

Freshly produced wood ashes exhibit a high content of calcium oxides (CaO), in addition to a variety of other compounds, as demonstrated by XRF analyses. When hydrated, these oxides are expansive and highly reactive, making them unsuitable for soil stabilization in this initial condition due to the risk of volumetric expansion and heat release. Upon exposure to moisture and air, as a function of post-combustion storage conditions, partial hydration and carbonation of the ashes occur, leading to the transformation of CaO into calcium hydroxide ($Ca(OH)_2$) and calcium carbonate ($CaCO_3$). This process is commonly referred to as ash maturation or curing.

Under these conditions, ashes may exhibit variable behavior as a result of the diversity and evolution of the compounds in their composition. In practice, their use can enhance certain mechanical properties depending on the availability of calcium hydroxide for reactions. However, the presence of unhydrated oxides, predominant in freshly produced ashes ("young ashes"), or the excess of carbonated materials, characteristic of more exposed ashes ("mature ashes"), results in inconsistent and unpredictable performance as a stabilizing material. This variability explains the range of outcomes reported in the literature.

In this context, ash processing becomes essential. While the direct use of young ashes may be problematic due to their instability and the presence of contaminants, the application of mature ashes tends to result in behavior typical of inert materials, associated with a "filler effect." Proper processing, through steps such as washing and calcination, is what enables overcoming these limitations and making ashes viable as a stabilizing material. Figure 86 illustrates the decision tree for the application of biomass ash in pavement layers.

Figure 86: Decision tree for the application of biomass ash in pavement layers

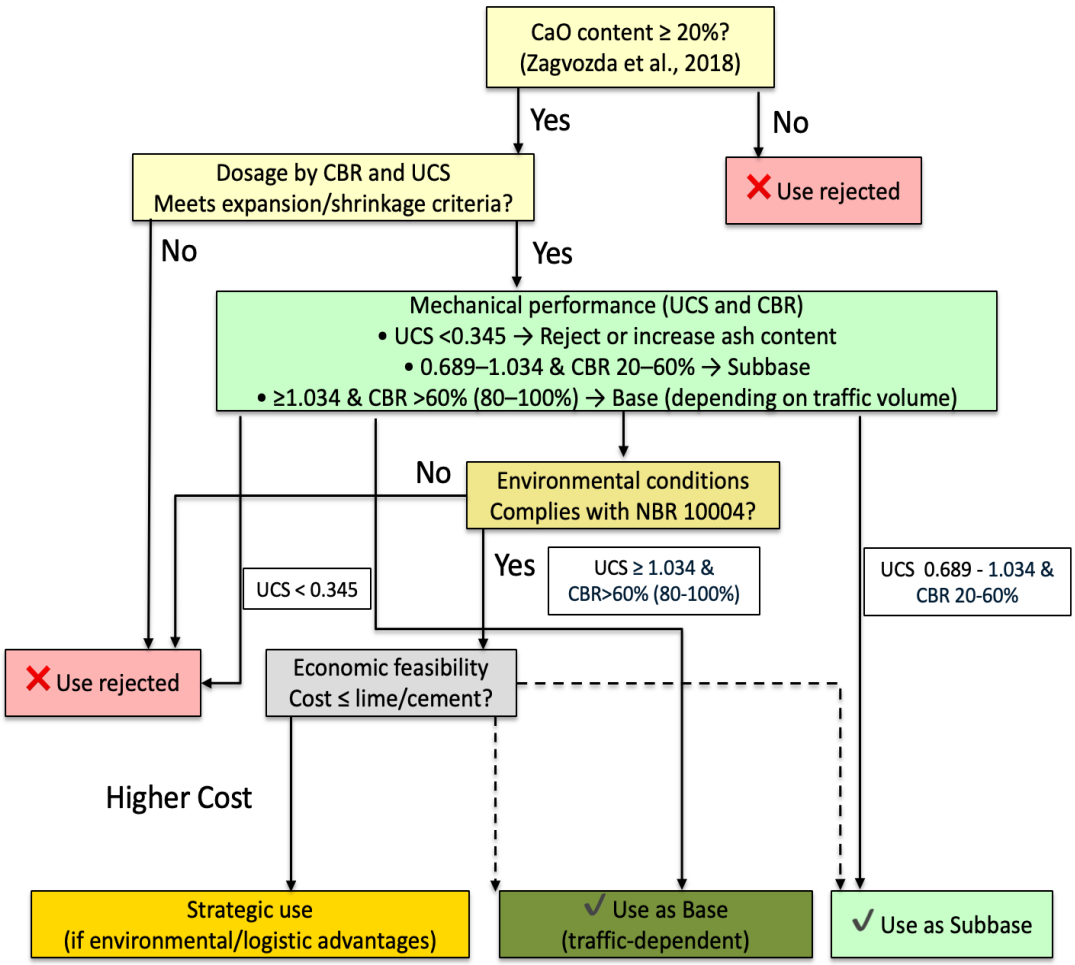

Source: Elaborated by the author, according to the recommendations of Zagvozda et al. (2018) and Little (1995)

5.3 Main research limitations

This study faced a series of practical and methodological limitations, many of which stemmed from operational constraints, laboratory infrastructure, and the feasible scope of experimentation within an academic environment. The main factors that limited the development or scope of the research are outlined below:

Soil volume and experimental scope: The manual preparation of clayey soils, especially the disaggregation process, proved to be extremely labor-intensive and time-consuming. Since compaction tests using standard-size molds would require very large volumes of soil, the compaction curves were determined using a reduced-scale methodology. As a result, it was not possible to evaluate all combinations with 3%, 5%, and 7% ash content across all variables (plasticity, mechanical behavior, and environmental analysis). The detailed analysis was therefore focused on mixtures that showed the most promising performance in preliminary tests.

Limitations in ash processing: The processing of wood ash was constrained by the available infrastructure. During the washing stage, the absence of appropriate containers resistant to the high alkalinity and temperature of the ash-water mixture led to the use of conventional metal buckets, which displayed visible corrosion. This may have resulted in contamination of the ash by metals released from the containers, partially compromising the quality of the input material.

Similarly, the calcination process was carried out using equipment with limited capacity and without refractory containers, potentially affecting the purity and physicochemical performance of the calcined ash. The small volume of material processed at a time also restricted the number of samples produced, limiting test replication and reducing the statistical reliability of the results.

Laboratory scale and absence of field validation: All tests were performed in a laboratory setting under controlled conditions. Environmental and operational variables typical of real-world field applications, such as temperature fluctuations, moisture variations, traffic loads, or dynamic loading conditions, were not tested. Field trials would be essential to validate the practical applicability of the technique in real roadwork scenarios.

Single source of ash used: The ash used in this study was obtained from a single biomass source (specific wood species and combustion process). This limits the generalizability of the findings, as ashes derived from other biomass types or combustion

conditions may exhibit distinct physicochemical characteristics, potentially influencing performance.

Limitations in environmental characterization: Although environmental aspects were considered in the study, not all parameters required by Brazilian regulations could be assessed. The unavailability of certain equipment prevented specific tests, such as the quantification of arsenic and mercury by atomic absorption spectrophotometry. Moreover, limited access to column leaching equipment hindered a more comprehensive evaluation of the long-term contaminant encapsulation potential of the compacted mixtures.

Limited curing time and absence of durability testing: Most mechanical tests were conducted after curing periods of up to 28 days, with a few samples extended to 90 days. However, alternative cementitious materials often develop strength over longer durations due to pozzolanic reactions. The absence of long-term evaluations may have underestimated the mixtures' strength gain potential. Additionally, the study did not assess the behavior of stabilized mixtures under durability conditions, such as wetting–drying or freeze–thaw cycles, which are critical for long-term material performance.

5.4 Recomendations for future research

Based on the results obtained and the limitations encountered throughout this study, further investigations are recommended to deepen the understanding and expand the technical and environmental applicability of the proposed approach. The following research directions are suggested:

- **Influence of ash storage conditions**: Evaluate the impact of storage conditions on the physicochemical and mineralogical properties of calcium-rich ashes, examining how possible transformations affect their performance as a construction material.
- **Long-term durability and stability**: Investigate the behavior of soil–residue mixtures subjected to wetting–drying and freeze–thaw cycles, analyzing their long-term durability and chemical stability.
- **Cost–benefit analysis of ash processing**: Compare the costs and benefits of processing and calcining calcium-rich ashes with untreated ashes, considering different storage conditions, reactivity levels, and technical performance.
- **Full-scale validation**: Conduct field trials and pilot sections using soils stabilized with wood ash, including traffic simulations and continuous performance monitoring, in order to assess the feasibility of the technique under real operational conditions.

- **Expanded environmental characterization**: Perform more comprehensive environmental assessments, including the quantification of elements regulated by Brazilian and international standards, such as arsenic, mercury, cadmium, and lead. Additionally, conduct long-term column leaching tests and static immersion leaching tests to evaluate the potential release of contaminants under different exposure scenarios.
- **Life Cycle Assessment (LCA) and economic feasibility**: Develop a Life Cycle Assessment (LCA) study to measure the environmental impacts of replacing conventional binders with biomass ash in infrastructure works and assess the economic viability of the proposed technique.

REFERENCES

AASHTO – AMERICAN ASSOCIATION OF STATE HIGHWAY AND TRANSPORTATION OFFICIALS. **Standard Method of Test for Determining the Resilient Modulus of Soils and Aggregate Materials (T 307-99).** Washington, D.C., 2007.

ACHAMPONG, F.; USMEN, M.; KAGAWA*, T. Evaluation of resilient modulus for lime- and cement-stabilized synthetic cohesive soils.* ***Transportation Research Record,*** *v. 1589, p. 70–75, 1997. doi:10.3141/1589-12.*

AGRELA, F.; CABRERA, M.; MORALES, M. M.; ZAMORANO, M.; ALSHAAER, M. Biomass fly ash and biomass bottom ash. In: AGRELA, F. (ed.). **New trends in eco-efficient and recycled concrete**. United Kingdom: Elsevier, 2019. cap. 2, p. 23–58.

AKULA, P.; LITTLE, D. *Analytical tests to evaluate pozzolanic reaction in lime stabilized soils.* ***MethodsX,*** *v. 7, 2020. doi:10.1016/j.mex.2020.100928.*

ALLOWAY, B. J. Heavy metals in soils: trace metals and metalloids in soils and their bioavailability. *3. ed. Dordrecht: Springer, 2013. doi:10.1007/978-94-007-4470-7.*

AMERICAN SOCIETY FOR TESTING AND MATERIALS (ASTM). Standard test method for leaching solid material in a column apparatus. **ASTM D4874**. Philadelphia: ASTM, 1995.

ARAÚJO, A. F. Avaliação de misturas de solos estabilizados com cal, em pó e em pasta, para aplicação em rodovias do Estado do Ceará. 2009. 175 f. Dissertação (Mestrado em Engenharia de Transportes) – Universidade Federal do Ceará, Fortaleza, 2009.

ASHRAF, M. A.; RAHMAN, M. M.; HOSSAIN, A. T. S. The effect of cement content and wetting-drying cycles on the strength of cement-stabilized soft soil. ***Journal of Civil Engineering (IEB****), v. 46, n. 1, p. 57–69, 2018.*

ASSOCIAÇÃO BRASILEIRA DE NORMAS TÉCNICAS (ABNT). NBR 10004: Resíduos sólidos – Classificação. Rio de Janeiro: ABNT, 2004.

ASSOCIAÇÃO BRASILEIRA DE NORMAS TÉCNICAS (ABNT). NBR 10005: Lixiviação de resíduos – Procedimento. Rio de Janeiro: ABNT, 2004.

ASSOCIAÇÃO BRASILEIRA DE NORMAS TÉCNICAS (ABNT). NBR 10006: Solubilização de resíduos – Procedimento. Rio de Janeiro: ABNT, 2004.

ASSOCIAÇÃO BRASILEIRA DE NORMAS TÉCNICAS (ABNT). NBR 12770: Solo coesivo – Determinação da resistência à compressão não confinada. Rio de Janeiro: ABNT, 2022.

ASSOCIAÇÃO BRASILEIRA DE NORMAS TÉCNICAS (ABNT). NBR 7175: Cal hidratada para argamassas. Rio de Janeiro: ABNT, 2003.

ASSOCIAÇÃO BRASILEIRA DE NORMAS TÉCNICAS (ABNT). NBR 7182: Solo – Ensaio de compactação – Procedimento. Rio de Janeiro: ABNT, 2016 (versão corrigida em 2020).

BAGHDADI, Z. A.; RAHMAN, M. A. The potential of cement kiln dust for the stabilization of soils. **Building and Environment**, v. 25, p. 285–289, 1990.

BAIRD, C. ***Química ambiental.*** *2. ed. Porto Alegre: Bookman, 2002.*

BALBO, J. T. ***Pavimentação asfáltica: materiais, projeto e restauração.*** *São Paulo: Oficina de Textos, 2007. 560 p. ISBN 978-85-86238-56-7.*

BARROSO, S. H. A.; SANTOS, R. M. Estudo de misturas de solo-cal dos solos da região metropolitana de Fortaleza para aplicação na engenharia rodoviária. In: XIII Congresso Brasileiro de Mecânica dos Solos e Engenharia Geotécnica, Curitiba, 2006.

BARSHAD, I. The effect of the interlayer cations on the expansion of the mica type of crystal lattice. **American Mineralogist**, v. 25, p. 225–238, 1950.

BASU, P. **Combustion and gasification in fluidized beds.** Boca Raton: CRC Press, 2006.

BERRA, M.; MANGIALARDI, T.; PAOLINI, A. E. Reuse of woody biomass fly ash in cement-based materials. ***Construction and Building Materials****, v. 76, p. 286–296, 2015.*

BHUVANESHWARI, S.; ROBINSON, R. G.; GANDHI, S. R. *Resilient modulus of lime-treated expansive soil.* ***Geotechnical and Geological Engineering****, v. 37, n. 1, p. 305–315, 2019. doi:10.1007/s10706-018-0648-8.*

BORLINI, M. C.; SALES, H. F.; VIEIRA, C. M. F.; CONTE, R. A.; PINATTI, D. G.; MONTEIRO, S. N. Cinza da lenha para aplicação em cerâmica vermelha. Parte I: características da cinza. **Cerâmica,** v. 51, p. 192–196, 2005. doi:10.1590/S0366-69132005000300004.

BRASIL. Conselho Nacional do Meio Ambiente (CONAMA). Resolução nº 375, de 29 de agosto de 2006. Diário Oficial da União, Brasília, DF, n. 168, p. 141–143, 30 ago. 2006.

BRASIL. Departamento Nacional de Estradas de Rodagem (DNER). Material finamente pulverizado – Determinação da massa específica real. DNER-ME 085/94. Brasília, DF, 1994.

BRASIL. Departamento Nacional de Estradas de Rodagem (DNER). Solos estabilizados com cinza volante e cal hidratada – Determinação da resistência à compressão simples. DNER-ME 180/94. Brasília, DF, 1994.

BRASIL. Departamento Nacional de Estradas de Rodagem (DNER). Solos estabilizados com cinza volante e cal hidratada – Determinação da resistência à tração por compressão diametral. DNER-ME 181/94. Brasília, DF, 1994.

BRASIL. Departamento Nacional de Infraestrutura de Transportes (DNIT). Especificação de serviço ES DNIT 141/2022-ES: Pavimentação – Base estabilizada granulometricamente. Revisão de 10 out. 2022. Brasília: IPR/DNIT, 2022.

BRASIL. Departamento Nacional de Infraestrutura de Transportes (DNIT). Solos – Compactação em equipamento miniatura – Mini-CBR e expansão – Método de ensaio. DNIT 254/2023-ME. Brasília, DF, 2023.

BRASIL. Departamento Nacional de Infraestrutura de Transportes (DNIT). Pavimentação – Ensaio de fadiga por compressão diametral à tensão controlada em camadas estabilizadas quimicamente – Método de ensaio. DNIT 434/2022-ME. Brasília, DF, 2022.

BRASIL. Departamento Nacional de Infraestrutura de Transportes (DNIT). Instituto de Pesquisas Rodoviárias. Manual de pavimentação. 3. ed. Rio de Janeiro: IPR/DNIT, 2006. (Publicação IPR-719).

BUNGART, R.; HÜTTL, R. F. Production of biomass for energy in post-mining landscapes and nutrient dynamics. **Biomass and Bioenergy**, v. 20, p. 181–187, 2001.

CABRERA, M.; GALVÍN, A. P.; AGRELA, F.; CARVAJAL, M. D.; AYUSO, J. Characterisation and technical feasibility of using biomass bottom ash for civil infrastructures. **Construction and Building Materials**, v. 58, p. 234–244, 2014.

CAILLAT, S.; VAKKILAINEN, E. Large-scale biomass combustion plants: an overview. In: ROSENDAHL, L. (ed.). **Biomass Combustion Science, Technology and Engineering.** Woodhead/Elsevier, 2013. p. 189–224.

CAPUTO, H. P. **Mecânica dos solos e suas aplicações**. 6. ed. Rio de Janeiro: LTC, 1996.

CARROLL, D. Ion exchange in clays and other minerals. **Bulletin of the Geological Society of America,** v. 70, n. 6, p. 749–779, 1959.

CASAGRANDE, A. Research of Atterberg limits of soils. **Public Roads**, v. 13, n. 8, p. 121–136, 1932.

CCR NOVA DUTRA. **Estudo do comportamento mecânico de solos estabilizados com cal hidratada.** Relatório técnico. Guararema, SP: CCR NovaDutra, 2014. 129 f.

CHU, T. Y. Soil stabilization with lime–fly ash mixtures: preliminary studies with silty and clayey soils. **Highway Research Board Bulletin**, v. 108, p. 102–111, 1955.

CONSOLI, N. C.; LOPES JUNIOR, L. S.; HEINECK, K. S. Key parameters for the strength control of lime stabilized soils. **Journal of Materials in Civil Engineering**, v. 21, p. 210–216, 2009.

CORDEIRO, G. C. Utilização de cinzas ultrafinas do bagaço de cana-de-açúcar e da casca de arroz como aditivos minerais em concreto. 2006. Tese (Doutorado) – Universidade Federal do Rio de Janeiro, Rio de Janeiro, 2006.

CORDEIRO, G. C.; TOLEDO FILHO, R. D.; FAIRBAIRN, E. M. R. Effect of calcination temperature on the pozzolanic activity of sugar cane bagasse ash. **Construction and Building Materials,** v. 23, p. 3301–3303, 2009.

CRUZ, N. C. et al. Ashes from fluidized bed combustion of residual forest biomass: recycling to soil as a viable management option. **Environmental Science and Pollution Research**, v. 24, p. 14770–14781, 2017.

CUNHA, C. L. S. Estudo das características de compressibilidade unidimensional e plasticidade de misturas de argila e areia. 2012. Dissertação (Mestrado) – Universidade Federal do Espírito Santo, 2012.

DAHL, J. et al. Results and evaluation of a new heavy metal fractionation technology in grate-fired biomass combustion plants as a basis for an improved ash utilisation. **In: EUROPEAN BIOMASS CONFERENCE,** 12., 2002, Amsterdã. **Proceedings**… Florença: **ETA-Florence Renewable Energies**, 2002. p. 690–694.

DAHL, O.; NURMESNIEMI, H.; PÖYKIÖ, R.; WATKINS, G. Comparison of the characteristics of bottom ash and fly ash from a medium-size (32 MW) district heating plant incinerating forest residues and peat in a fluidized-bed boiler. **Fuel Processing Technology,** v. 90, n. 7–8, p. 871–878, 2009.

DAS, B. M. **Fundamentos de engenharia geotécnica.** São Paulo: Thomson, 2007.

DASH, S.; HUSSAIN, M. Influence of lime on shrinkage behavior of soils. Journal of Materials in Civil Engineering, v. 27, e04015041, 2015. doi:10.1061/(ASCE)MT.1943-5533.0001301.

DEMEYER, A.; VOUNDI NKANA, J. C.; VERLOO, M. G. Characteristics of wood ash and influence on soil properties and nutrient uptake: an overview. **Bioresource Technology,** v. 77, p. 287–295, 2001.

DEMIRBAS, A. Heavy metal contents of fly ashes from selected biomass samples. **Energy Sources,** v. 27, p. 1269–1276, 2005.

DEPARTAMENTO NACIONAL DE INFRAESTRUTURA DE TRANSPORTES (DNER/DNIT). DNER-ME 162: Solos – Ensaio de compactação utilizando amostras **trabalhadas. Rio de Janeiro, 1994a.**

DEPARTAMENTO NACIONAL DE INFRAESTRUTURA DE TRANSPORTES (DNER/DNIT). DNER-ME 049: Solos – Determinação do índice de suporte Califórnia para amostras não trabalhadas. Rio de Janeiro, 1994b.

DEPARTAMENTO NACIONAL DE INFRAESTRUTURA DE TRANSPORTES (DNER/DNIT). DNER-ME 051: Solos – Análise granulométrica. Rio de Janeiro, 1994.

DEPARTAMENTO NACIONAL DE INFRAESTRUTURA DE TRANSPORTES (DNER/DNIT). DNER-ME 082: Solos – Determinação do limite de plasticidade. Rio de Janeiro, 1994.

DEPARTAMENTO NACIONAL DE INFRAESTRUTURA DE TRANSPORTES (DNER/DNIT). DNER-ME 093: Solo – Densidade real. Rio de Janeiro, 1994.

DEPARTAMENTO NACIONAL DE INFRAESTRUTURA DE TRANSPORTES (DNER/DNIT). DNER-ME 122: Solos – Determinação do limite de liquidez – Método de referência e método expedito. Rio de Janeiro, 1994.

DEPARTAMENTO NACIONAL DE INFRAESTRUTURA DE TRANSPORTES (DNIT). DNIT 134-ME: Solos – Determinação do módulo de resiliência. Rio de Janeiro, 2018.

DEPARTAMENTO NACIONAL DE INFRAESTRUTURA DE TRANSPORTES (DNIT). DNIT 181-ME: Pavimentação – Material estabilizado quimicamente – Determinação do módulo de resiliência. Rio de Janeiro, 2018.

DIAMOND, S.; KINTER, E. B. Mechanisms of soil–lime stabilization: an interpretive review. **Highway Research Record,** p. 83–102, 1965.

EADES, J. L.; NICHOLS JR., F. P.; GRIM, R. E. Formation of new minerals with lime stabilization as proven by field experiments in Virginia. Highway Research Board Bulletin, v. 335, p. 31–39, 1963.

EMEH, C.; IGWE, O. The combined effect of wood ash and lime on the engineering properties of expansive soils. **International Journal of Geotechnical Engineering,** v. XX, p. 1–11, 2016. doi:10.1080/19386362.2015.1125412.

EPE – EMPRESA DE PESQUISA ENERGÉTICA. Balanço Energético Nacional (BEN) 2024: ano base 2023. 2024. Disponível em: https://www.epe.gov.br/sites-pt/publicacoes-dados-abertos/publicacoes/PublicacoesArquivos/publicacao-819/topico-723/BEN2024.pdf. Acesso em: 12 jun. 2025.

ESTRELA, C. Eficácia antimicrobiana de pastas de hidróxido de cálcio. 2005. Livre-Docência – Faculdade de Odontologia de Ribeirão Preto, USP. Disponível em: https://endoscience.com.br/publicacoes/eficacia-antimicrobiana-de-pastas-de-hidroxido-de-calcio/. Acesso em: 16 maio 2025.

ETIÉGNI, L.; CAMPBELL, A. G. Physical and chemical characteristics of wood ash. **Bioresource Technology,** v. 37, p. 173–178, 1991.

EUROPEAN UNION. Directive 2009/28/EC of the European Parliament and of the Council of 23 April 2009 on the promotion of the use of energy from renewable sources. Official Journal of the European Union, v. 140, p. 16–62, 2009.

FONSECA, M. C.; NUNES, S. F. Desagregação da carga circulante do pelotamento através do roller press. Belo Horizonte: Samarco Mineração, 2003. (Relatório interno).

FREIRE, J. M. O. et al. Aproveitamento do carbonato de cálcio de resíduos de papel e celulose como agente estabilizante de solo-cimento. In: CBECIMat, 21., 2014, Cuiabá. Anais… Cuiabá: UFMT, 2014.

FREIRE, M.; LOPES, H.; TARELHO, L. A. C. Critical aspects of biomass ashes utilization in soils: composition, leachability, PAH and PCDD/F. **Waste Management,** v. 46, p. 304–315, 2015.

FREITAS, F. B. Determinação da densidade real dos solos. Centro Universitário do Leste de Minas Gerais – Unileste, 2014.

FUNCEME. *Calendário de chuvas do Estado do Ceará. 2025. Disponível em: https://chuvas.funceme.br/ano/municipios/media/2025. Acesso em: 13 jun. 2025.*

GIBBS, F. W. The history of the manufacture of soap. ***Annals of Science****, v. 4, n. 2, p. 169–190, 1939.*

GONDIM, L. M. Estudo experimental de misturas solo–emulsão aplicado às rodovias do agropólo do Baixo Jaguaribe – CE. 2008. Dissertação (Mestrado) – Universidade Federal do Ceará, Fortaleza, 2008.

GUIMARÃES, J. E. P. **A cal: fundamentos e aplicações na engenharia civil**. 2. ed. São Paulo: PINI, 2002.

HERNÁNDEZ, J. J.; LAPUERTA, M.; MONEDERO, E.; PAZO, A. Biomass quality control in power plants: technical and economic implications. **Renewable Energy**, v. 115, p. 908–916, 2018.

HILT, G. H.; DAVIDSON, D. T. Lime fixation in clayey soils. **Highway Research Board,** v. 262, p. 20–32, 1960.

IBGE – Instituto Brasileiro de Geografia e Estatística. Dados diversos. 2021.

INGLES, O. G.; METCALF, J. B. **Soil stabilization: principles and practice.** Melbourne: Butterworths, 1972.

JONES, C. W. Stabilization of expansive clay with hydrated lime and with Portland cement. Highway Research Bulletin, v. 193, p. 40–47, 1958.

KIM, A. G.; KAZONICH, G. Mass release of trace elements from coal combustion by-products. In: INTERNATIONAL ASH UTILIZATION SYMPOSIUM, 13., 1999, Lexington. Proceedings… Lexington: University of Kentucky, 1999. p. 9.

KLEMM, W. A. Kiln dust utilization. Martin Arietta Laboratories Report, MML TR80-12, Baltimore, MD, 1980.

KRÓL, A.; MIZERNA, K.; BOŻYM, M. An assessment of pH-dependent release and mobility of heavy metals from metallurgical slag. **Journal of Hazardous Materials**, v. 384, p. 121502, 2020. doi:10.1016/j.jhazmat.2019.121502.

LAHTINEN, P. Fly ash mixtures as flexible structural materials for low-volume roads. Finnra Reports, n. 70/2001, 102 p.

LITTLE, D. N. Evaluation of structural properties of lime stabilized soils and aggregates. Vol. 1 – Summary of findings. Prepared for the National Lime Association, 1999.

LITTLE, D. N. **Stabilization of pavement subgrades and base courses with lime.** Dubuque: Kendall/Hunt, 1995.

LOO, S. V.; KOPPEJAN, J. **The handbook of biomass combustion and cofiring.** London: Earthscan, 2008.

LOVATO, R. S. Estudo do comportamento mecânico de um solo laterítico estabilizado com cal, aplicado à pavimentação. 2004. Dissertação (Mestrado) – Universidade Federal do Rio Grande do Sul, Porto Alegre, 2004.

LUND, O. L.; RAMSEY, W. J. Experimental lime stabilization in Nebraska. **Highway Research Board Bulletin,** v. 231, p. 24–57, 1959.

MACSIK, J.; SVEDBERG, B. Gravel road stabilization of Ehnsjövägen Hallstavik. **Swedish Thermal Engineering Research Institute Report,** n. 968, 2006.

MAHEDI, M.; ÇETİN, B.; WHITE, D. J. Performance evaluation of cement and slag stabilized expansive soils. **Transportation Research Record**, n. 2672, p. 164–173, 2018. doi:10.1177/0361198118757439.

MAHMOOD, A.; HASSAN, R.; FOUAD, A. An assessment of lime–cement stabilisation on the elastic and resilient moduli of a clayey soil. **International Journal of Pavement Engineering**, 2021. doi:10.1080/10298436.2021.1921772.

MAIER, M.; BEUNTNER, N.; THIENEL, K. Mineralogical characterization and reactivity test of common clays suitable as supplementary cementitious material. **Applied Clay Science**, v. 202, 105990, 2021. doi:10.1016/j.clay.2021.105990.

MALEŠIČ, J. et al. Nano calcium carbonate versus nano calcium hydroxide in alcohols as a deacidification medium for lignocellulosic paper. **Heritage Science**, v. 7, art. 50, 2019. doi:10.1186/s40494-019-0294-6.

MALLELA, J.; VAN QUINTUS, P. E. H.; SMITH, K. L. Consideration of lime-stabilized layers in mechanistic–empirical pavement design. Prepared for The National Lime Association, 2004.

MASCARENHAS, I. M. N. Caracterização geotécnica de solos na Região Metropolitana do Cariri/CE para uso em pavimentação. 2016. Dissertação (Mestrado) – Universidade Federal do Ceará, Fortaleza, 2016.

MASIÁ, A. A. T. et al. Characterising ash of biomass and waste. ***Fuel Processing Technology****, v. 88, n. 11–12, p. 1071–1081, 2007.*

MATALKAH, F.; SOROUSHIAN, P. Use of non-wood biomass combustion ash in development of alkali-activated concrete. **Construction and Building Materials**, v. 121, p. 491–500, 2016.

MATEOS, M. Stabilization of soils with fly ash alone. **Highway Research Board**, v. 52, p. 59–65, 1964.

MCCALLISTER, L. D.; PETRY, T. M. Physical property changes in a lime-treated expansive clay caused by leaching. **Transportation Research Record**, v. 1295, p. 37–44, 1991.

MEDEIROS, L. D. de. Melhoramento do comportamento mecânico de um solo estabilizado com cinza da lenha de algaroba. 2023. Dissertação (Mestrado) – Universidade Federal de Pernambuco, 2023.

MEDEIROS, L. D.; FERREIRA, S. R. de M.; BELLO, M. I. M. da C. V. Evolução da estabilização química em solos expansivos. **Journal of Environmental Analysis and Progress**, v. 8, n. 2, p. 123–139, 2023.

MELLO, L. G. R. S. et al. Análise do impacto do período de projeto de pavimentos no custo global de obras rodoviárias. **Revista Transportes**, v. 24, n. 4, p. 1–13, 2016. doi:10.14295/transportes.v24i4.1056.

MELO, M. C. S. de. Utilização de cinza de algaroba como matéria-prima alternativa para uso em blocos de solo–cal. 2018. Tese (Doutorado) – Universidade Federal de Campina Grande, 2018.

MELO, M. C. S. et al. Cal produzida a partir de cinza de biomassa rica em cálcio. **Cerâmica,** v. 64, n. 371, p. 318–324, 2018. doi:10.1590/0366-69132018643712338.

MENDONÇA, L. A. R. Recursos hídricos da chapada do Araripe. 2001. Tese (Doutorado) – Universidade Federal do Ceará, Fortaleza, 2001.

NAKANISHI, E. Y. Cinza residual da queima de biomassa do capim-elefante (Pennisetum purpureum) como material pozolânico substituto do cimento Portland. 2013. Dissertação (Mestrado) – Universidade de São Paulo, 2013. doi:10.11606/D.74.2013.tde-07102013-094322.

NINOV, J.; DONCHEV, I. Lime stabilization of clay from the 'Mirkovo' deposit. **Journal of Thermal Analysis and Calorimetry,** v. 91, p. 487–490, 2008. doi:10.1007/s10973-006-8304-9.

NOGAMI, J. S.; VILLIBOR, D. F. Ampliação do uso da metodologia MCT no estudo de solos tropicais para pavimentação. **In: REUNIÃO ANUAL DE PAVIMENTAÇÃO,** 28., 1994, Belo Horizonte. Anais… Belo Horizonte: ABPV, 1994.

NOGAMI, J. S.; VILLIBOR, D. F. **Pavimentação de baixo custo com solos lateríticos.** São Paulo: PINI, 1995.

NORDMARK, D. et al. Geochemical behaviour of a gravel road upgraded with wood fly ash. **Journal of Environmental Engineering**, v. 140, n. 10, p. 05014002, 2014.

NÚÑEZ, W. P. Estabilização físico–química de um solo residual de Arenito Botucatu, visando seu emprego na pavimentação. 1991. Dissertação (Mestrado) – UFRGS, 1991.

OBIANIGWE, N.; NGENE, B. U. Soil stabilization for road construction: comparative analysis of a three-prong approach. **IOP Conference Series: Materials Science and Engineering**, v. 413, art. 012015, 2018.

OBURGER, E. et al. Environmental impact assessment of wood ash utilization in forest road construction and maintenance – a field study. **Science of the Total Environment,** v. 544, p. 711–721, 2016.

OKAGBUE, C. O. Stabilization of clay using wood ash. **Journal of Materials in Civil Engineering,** v. 19, n. 1, p. 14–18, 2007. doi:10.1061/(ASCE)0899-1561(2007)19:1(14).

PAPAYIANNI, I.; TSIMAS, S.; MOUTSATSOU, A. Standardization aspects concerning high calcium fly ashes. In: WOCA – World of Coal Ash Conference, 2009, Lexington. **Proceedings…**

PICCHI, F. A.; CINCOTTO, M. A.; BARROS, J. M. C. Tijolos de solo–cal. In: **Tecnologia das Edificações.** São Paulo: PINI, 1988. cap. 090, p. 101–106.

POUEY, M. T. F. **Beneficiamento da casca de arroz residual com vistas à produção de cimento composto e/ou pozolânico.** 2006. Tese (Doutorado) – UFMG, 2006.

PRUSINSKI, J. R.; BHATTACHARJA, S. Effectiveness of Portland cement and lime in stabilizing clay soils. **Transportation Research Record**, n. 1652, p. 215–227, 1999.

PUPPALA, A. J.; MOHAMMAD, L. N.; ALLEN, A. Engineering behavior of lime-treated Louisiana subgrade soil. **Transportation Research Record**, v. 1546, n. 1, p. 24–31, 1996. doi:10.1177/0361198196154600103.

PUSHPAKUMARA, B.; MENDIS, S. Suitability of rice husk ash (RHA) with lime as a soil stabilizer in geotechnical applications. **International Journal of Geo-Engineering,** v. 13, p. 1–12, 2022. doi:10.1186/s40703-021-00169-w.

QUISPE, C. C. **Comportamento de um solo argiloso estabilizado com cinzas de resíduo sólido urbano sob carregamento estático.** 2012. Tese (Doutorado) – PUC-Rio, 2012.

RIBBING, C. M.; BJURSTRÖM, H. G. The Swedish ash programme with focus on bioashes: ashes are a resource in a sustainable society. In: **Recycling of Biomass Ashes**. Berlin: Springer, 2011. p. 147–164.

RUFF, C. G.; DAVIDSON, D. T. Lime and sodium silicate stabilization of montmorillonite clay soil. **Highway Research Board Proceedings**, v. 107, p. 107–128, 1961.

SAKSHAM, S.; JAGDISH, Y.; RAJAT, P. Analysis of stabilization of soil–cement for base of railway track and subgrade. **International Journal of Engineering Research,** v. 6, 2018.

SALES, C. P. Produção e caracterização de cinza de capim-elefante com vistas à sua aplicação como pozolana. 2012. Dissertação (Mestrado) – UENF, 2012.

SANTANA, H. Pontos básicos e elementares da estabilização granulométrica. In: **REUNIÃO ANUAL DE PAVIMENTAÇÃO**, 18., 1983, Porto Alegre. Anais… ABPv, v. 2, p. 417–462.

SEED, H. B. et al. **Prediction of flexible pavement deflections from laboratory repeated-load tests.** Washington, D.C.: TRB, 1967. (NCHRP Report; 35).

SEYE, O.; CORTEZ, L. A. B.; GOMEZ, E. O. Estudo cinético da biomassa a partir de resultados termogravimétricos. In: **3º Encontro de Energia no Meio Rural**, 2000, Campinas.

SILVA, F. C. et al. Use of biomass ash-based materials as soil fertilisers: critical review of the existing regulatory framework. **Journal of Cleaner Production**, v. 214, p. 112–124, 2019.

SKLIVANITI, V. et al. Valorisation of woody biomass bottom ash in Portland cement: a characterization and hydration study. **Journal of Environmental Chemical Engineering,** v. 5, p. 205–213, 2017.

SOUSA, S. G. de. Análise temporal do comportamento da precipitação pluviométrica na Região Metropolitana do Cariri (CE), Brasil. **Revista Geográfica de América Central**, v. 2, n. 63, p. 319–340, 2019.

STEENARI, B. M.; KARLSSON, L. G.; LINDQVIST, O. Evaluation of the leaching characteristics of wood ash and the influence of ash agglomeration. **Biomass and Bioenergy,** v. 16, p. 119–136, 1999.

SUPANCIC, K.; OBERNBERGER, I. Wood ash utilisation as a stabilizer in road construction: first results of large-scale tests. In: 19th **European Biomass Conference and Exhibition**, 2011, p. 859–870.

TAN, Z.; LAGERKVIST, A. Phosphorus recovery from biomass ash: a review**. Renewable and Sustainable Energy Reviews**, v. 15, p. 3588–3602, 2011.

TARELHO, L. A. C. et al. Characteristics of distinct ash flows in a biomass thermal power plant with bubbling fluidised bed combustor. **Energy,** v. 90, p. 387–402, 2015.

TAYLOR, W. H. Jr.; ARMAN, A. Lime stabilization using preconditioned soils. **Highway Research Board Bulletin**, v. 262, p. 1–19, 1960.

THOMPSON, M. R. Lime reactivity of Illinois soils. ASCE **Journal of the Soil Mechanics and Foundations Division,** v. 92, p. 67–92, 1966.

TIWARI, M. K. et al. Suitability of leaching test methods for fly ash and slag: a review. **Journal of Radiation Research and Applied Sciences,** v. 8, n. 4, p. 523–537, 2015.

TOWNSEND, D. L.; KLYM, T. W. Durability of lime-stabilized soils. **Highway Research Record,** n. 139, p. 25–41, 1966.

TRANSPORTATION RESEARCH BOARD (TRB). **Lime stabilization: reactions, properties, design, and construction.** State of the Art Report 5. Washington, D.C.: TRB, 1987.

UNIÃO EUROPEIA. Comissão. **Decisão 2000/532/CE**, de 3 de maio de 2000. Jornal Oficial das Comunidades Europeias, L 226, 6 set. 2000, p. 3–24. Retificada pela Decisão 2002/16/CE, L 5, 9 jan. 2002, p. 5–20.

UNIÃO EUROPEIA. **Diretiva 2008/98/CE**, de 19 de novembro de 2008. Jornal Oficial da União Europeia, L 312, 22 nov. 2008, p. 3–30.

ÜNVER, S.; LAV, M.; ÇOKÇA, E. Improvement of an extremely highly plastic expansive clay with hydrated lime and fly ash. **Geotechnical and Geological Engineering,** v. 39, p. 4917–4932, 2021. doi:10.1007/s10706-021-01803-1.

UREÑA, C. et al. **Use of biomass ash as a stabilization agent for expansive marly soils** (SE Spain). In: **EGU General Assembly**, 2012, Viena. Anais…

UZAN, J. Characterization of granular material. **Transportation Research Record**, v. 1022, p. 52–59, 1985.

VAMVUKA, D.; KAKARAS, E. Ash properties and environmental impact of various biomass and coal fuels and their blends. **Fuel Processing Technology**, v. 92, n. 3, p. 570–581, 2011.

VASCONCELOS, S. D. **Avaliação das cinzas de carvão mineral produzidas em usina termelétrica para construção de camadas de pavimentos.** 2018. Dissertação (Mestrado) – Universidade Federal do Ceará, 2018.

VASKE, N. R. Estudo preliminar da viabilidade do aproveitamento da cinza proveniente de filtro multiciclone pela combustão de lenha de eucalipto em caldeira fumotubular como adição ao concreto. 2012. Tese (Doutorado) – UFRGS, 2012.

VASSILEV, S. V. et al. An overview of the composition and application of biomass ash. Part 1: phase–mineral and chemical composition and classification. **Fuel,** v. 105, p. 40–76, 2013.

VILLIBOR, D. F. **Estabilização granulométrica ou mecânica.** São Carlos, SP: Gráfica EESC USP, 1982.

VILLIBOR, D. F.; NOGAMI, J. S. **Pavimentos econômicos: tecnologia do uso dos solos finos lateríticos.** São Paulo: Arte & Ciência, 2009.

VIZCARRA, G. O. C. **Aplicabilidade de cinzas de resíduo sólido urbano para base de pavimentos.** 2010. Dissertação (Mestrado) – PUC-Rio, 2010.

WALKER, R. D.; KARABULUT, C. Effect of freezing and thawing on unconfined compressive strength of lime-stabilized soils. **Highway Research Record**, n. 92, p. 1–8, 1965.

WANG, J. W. H.; MATEOS, M.; DAVIDSON, D. T. Comparative effects of hydraulic, calcitic, and dolomitic limes and cement in soil stabilization. **Highway Research Record,** n. 29, p. 42–54, 1963.

WILES, C. C. A review of solidification/stabilization technology. **Journal of Hazardous Materials,** v. 14, p. 5–21, 1987.

WINTERKORN, H. F.; PAMUKCU, S. Soil stabilization and grouting. In: FANG, H. Y. (ed.). **Foundation Engineering Handbook**. 2. ed. New York: Springer, 1991.

WOLFE, R. E.; ALLEN, J. R. L**aboratory evaluation of lime treatment of typical Minnesota soils.** St. Paul: Minnesota Dept. of Highways, 1964. (Final Report of Investigation, n. 601).

WOODS, K. B.; YODER, E. J. Stabilization with soil, lime, or calcium chloride as an admixture. In: CONFERENCE ON SOIL STABILIZATION, 1952, Cambridge. **Proceedings…** Cambridge: MIT, 1952. p. 3–19.

XAVIER, J. M. **Estudo do comportamento geotécnico de um solo colapsível voltado para fundações superficiais.** 2018. Dissertação (Mestrado) – Universidade Federal de Pernambuco, 2018.

XING, P. et al. A comparative assessment of biomass ash preparation methods using X-ray fluorescence and wet chemical analysis. **Fuel,** v. 182, p. 161–165, 2016.

ZAGVOZDA, M. et al. Possibilities of bioash application in road building. Građevinar, v. 70, n. 5, p. 393–402, 2018.

ZAGVOZDA, M.; RUKAVINA, T.; DIMTER, S. Wood bioash effect as lime replacement in the stabilisation of different clay subgrades. **International Journal of Pavement Engineering**, v. 23, p. 2543–2553, 2020. doi:10.1080/10298436.2020.1862839.

ZAINI, M. et al. Experimental investigations on physico–mechanical properties of kaolinite clay soil stabilized at optimum silica fume content using clamshell ash and lime. Scientific Reports, v. 14, 2024. doi:10.1038/s41598-024-61854-1.

ZHANG, F. S.; YAMASAKI, S.; NANZYÔ, M. Application of waste ashes to agricultural land – effect of incineration temperature on chemical characteristics. **Science of the Total Environment**, v. 264, p. 205–214, 2001.

ZHANG, X.; LI, H.; HARVEY, J. T.; BUTT, A. A.; JIA, M.; LIU, J. A review of converting woody biomass waste into useful and eco-friendly road materials. **Transportation Safety and Environment,** v. 4, n. 1, p. tdab031, 2022.

ZHANG, Z.; TAO, M. Durability of stabilized low plasticity soils. **Journal of Geotechnical and Geoenvironmental Engineering,** v. 134, p. 203–213, 2008.

ZHOU, S.; ZHOU, D.; ZHANG, Y.; WANG, W. Study on physical–mechanical properties and microstructure of expansive soil stabilized with fly ash and lime. **Advances in Civil Engineering,** 2019. doi:10.1155/2019/4693757.

ZOLKOV, E. Influence of chlorides and hydroxides of calcium and sodium on consistency limits of a fat clay. **Highway Research Board Bulletin**, n. 309, p. 109–115, 1962.